Fuel and Chemicals from Renewable Alcohols

Part 1+2

Hansen, Jeppe Rass

Publication date:
2008

Document Version
Publisher's PDF, also known as Version of record

DOI: 10.1002/cssc.200700168

The Renewable Chemicals Industry

Claus Hviid Christensen,* Jeppe Rass-Hansen, Charlotte C. Marsden, Esben Taarning, and Kresten Egeblad[a]

The possibilities for establishing a renewable chemicals industry featuring renewable resources as the dominant feedstock rather than fossil resources are discussed in this Concept. Such use of biomass can potentially be interesting from both an economical and ecological perspective. Simple and educational tools are introduced to allow initial estimates of which chemical processes could be viable. Specifically, fossil and renewables value chains are used to indicate where renewable feedstocks can be optimally valorized. Additionally, C factors are introduced that specify the amount of CO_2 produced per kilogram of desired product to illustrate in which processes the use of renewable resources lead to the most substantial reduction of CO_2 emissions. The steps towards a renewable chemicals industry will most likely involve intimate integration of biocatalytic and conventional catalytic processes to arrive at cost-competitive and environmentally friendly processes.

Introduction

Currently, there exists an intense focus on the production of transportation fuels from biomass.[1–4] This focus can be attributed to a desire to significantly lower the emission of greenhouse gases, thereby minimizing global warming, and also to relinquish our dependence on fossil fuels. Moreover, biomass is the only accessible non-fossil source of carbon that can be processed into liquids that are easily incorporated into the existing transportation fuel infrastructure. In particular, the widespread use of bioethanol and biodiesel as fuel additives is rapidly gaining importance in many parts of the world, and significant efforts are now being devoted to develop technologies that are simultaneously more sustainable than current technologies and allow more efficient use of the available bioresources.

In some regions, it appears that bioethanol can indeed already be produced to be cost-competitive with gasoline.[5] However, it also seems that the extensive use of biomass to produce biofuels remains controversial from both an economical and an ecological perspective, and these issues clearly need to be resolved in a fully transparent manner. It is interesting that despite the ongoing efforts to widely introduce biofuels as fuel additives, all prognoses still predict the demand for fossil fuels to increase over the next decades.[6] Consequently, it is clear that there is a strong need to consider if there are other options for substituting fossil resources with bioresources.

Today, about 85% of all crude oil consumed is used for the production of transportation fuels,[6] and this is undoubtedly the reason that the production of biofuels attracts most attention when considering renewable alternatives. However, as much as 10% of crude oil is currently used for the production of industrial chemicals.[6,7] In general terms, these chemicals are significantly more economically valuable than transportation fuels and, simultaneously, their production often also involves the co-production of significant amounts of carbon dioxide. Taking this into account, it is conspicuous that relatively little attention has been given to develop the use of biomass as a raw material for the production of industrial chemicals.[8]

Herein, it is argued that the optimal use of abundant bioresources could well serve as a renewable feedstock for the chemical industry.[9] From a chemical perspective, renewable feedstocks, being highly functionalized molecules, are very different from fossil feedstocks which are generally unfunctionalized. Therefore, a huge challenge for chemists today is to provide the chemical industry with a new set of tools to convert renewables into useful chemicals in an economically viable fashion.[10,11] Here, we illustrate examples of two different approaches or strategies towards potential biomass-derived chemicals. It is proposed that the required cost-competitive and environmentally acceptable (sustainable) industrial chemical processes utilizing renewable starting materials are best achieved by the close integration of biocatalytic and heterogeneous catalytic processes.[12]

Fossil and Renewables Value Chains

Today, fossil resources are widely used to produce electricity, heat, and transportation fuels as well as the vast majority of the many chemicals that are required by contemporary society. During the 20th century, continuous scientific and technological developments led to ongoing refinements in these areas resulting in highly optimized and efficient technologies for utilizing fossil resources. Additionally, during the same period fossil resources were abundantly available at relatively low costs, and we can therefore talk of a fossil economy with re-

[a] *Prof. C. H. Christensen, J. Rass-Hansen, C. C. Marsden, E. Taarning, K. Egeblad*
Center for Sustainable and Green Chemistry
Department of Chemistry, Technical University of Denmark
Building 206, 2800 Lyngby (Denmark)
Fax: (+45) 4588 3136
E-mail: chc@kemi.dtu.dk

spect to our society today. The aforementioned factors also mean that typically existing industrial processes are very cost-competitive when compared with emerging new technologies. Accordingly, significant efforts are required to develop such new alternatives into commercially viable solutions.[13]

Herein, we explore the prospects for using renewable resources, namely biomass, as an alternative to fossil resources as a feedstock for the chemical industry. In order to attempt to start identifying promising opportunities, it is instructive to establish a simple value chain that illustrates how the petrochemical industry transforms fossil resources into desirable products by a series of chemical transformations. The value chain in Figure 1 qualitatively illustrates the value of various

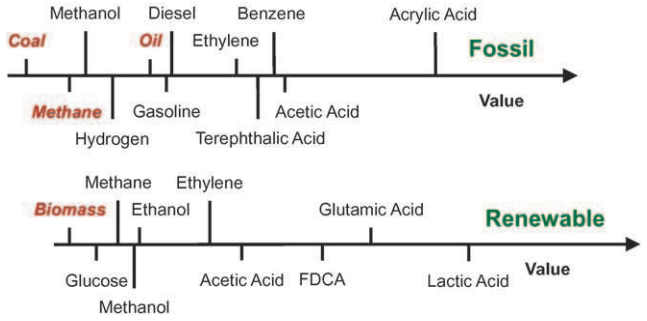

Figure 1. The fossil and renewables value chains indicate the value of different commodity chemicals relative to the feedstocks. A direct comparison between the two different value chains depends on the actual cost of the feedstocks.

important commodity chemicals relative to that of the fossil raw materials, that is, coal, natural gas, and crude oil.[14,15]

This is certainly a very simplistic illustration as the value of the fossil resources varies considerably, not only according to the geographic origin and quality but also over time for complex socio-economic reasons. Nonetheless, this fossil value chain for the chemical industry emphasizes that crude oil is transformed into transportation fuels by relatively simple, efficient, and inexpensive operations. Thus, transportation fuels are among the least expensive chemicals available.

In the petrochemical industry, fossil resources are used to produce important major chemicals; currently, the building blocks for about 95% of all the carbon-containing chemicals that are required to sustain our everyday lives. The majority of this wide range of specialized chemicals can be traced back to just seven basic building blocks. These building blocks—methanol, ethene, propene, butadiene, benzene, toluene, and xylene—can be considered as the backbone of the chemical industry.[16] The entire chemical industry is essentially constructed from these building blocks, a few of which are included in Figure 1. The fossil value chain illustrates that these building blocks are, typically, somewhat more valuable than transportation fuels and that the commodity chemicals produced from them can often be appreciably more so. The value of these bulk chemicals is essentially governed by the cost of the feedstocks and processing costs.

If we now envisage that the most important fuels and chemicals should instead be produced from biomass, then another value chain might materialize, as also depicted in Figure 1.[14] This value chain could be termed a renewables value chain for the chemical industry. As with the fossil resources chain, this is again only a qualitative evaluation for two main reasons: First, the cost and composition of the biomass feedstock will vary significantly from region to region; likewise, it will depend upon the source of biomass feedstock (e.g., food crops or waste products). In this respect, the situation differs not so greatly from that of fossil raw materials. Second, most of the chemical transformations required to establish a renewable chemicals industry are not yet developed to any major extent. In actuality, in many cases they still remain to be discovered. Thus, establishment of the renewables value chain is, to some extent, based on estimates. However, in some cases the relevant processes in this value chain can be identical to those in the fossil value chain.

In Figure 1, the fossil value chain and the renewables value chain are shown independently of one another, hence they cannot be directly compared. To directly compare the two value chains more quantitatively, it is necessary to know solely the cost of the compounds in the fossil and renewable feedstocks, assuming that the uncertainties related to the individual value chains are first handled properly as discussed. Figure 2

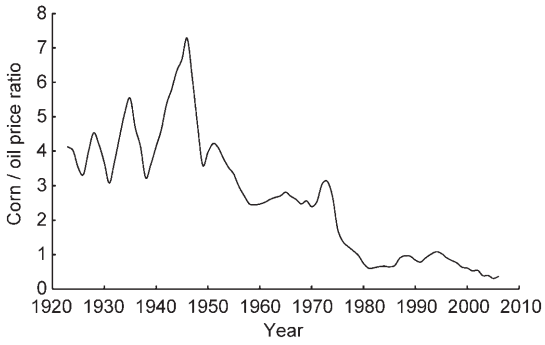

Figure 2. The plot of corn/oil price ratio during the last 80 years shows how biomass (corn) has become relatively cheaper and by that economically more interesting as an alternative to oil for the chemical industry.[14]

illustrates how the price of one specific fossil resource (crude oil) has varied relative to one specific renewable resource (corn) over time. Of special interest, during the last 80 years the corn/crude oil ratio has changed significantly but today it is at a historic low level. It is clear that if the cost of biomass feedstocks continues to decline relative to that of fossil resources, an increasing number of chemicals could be produced competitively from renewable resources.

However, it is important to be aware that the feedstock cost ratio will not change which products are the most attractive to produce from biomass; this depends exclusively on the relative values of the relevant compounds in the two different value chains. To develop an industry based on biomass is then simply a matter of developing the technologies that are best

able to compete with their fossil equivalents. Thus, from the value chains, it is possible to identify interesting first target chemicals that utilize the abundant biomass resources most efficiently, when establishing the foundation of a renewable chemicals industry. However, cost is not the only important parameter, as in many cases the potential to decrease CO_2 emissions on going from a fossil resource to a renewable resource will also hold significant importance. This is discussed briefly later, but here it is noted that this will vary significantly from one chemical on the two value chains to another. Accordingly, it would be fitting to also establish the exact amount of CO_2 produced, for instance, per kilogram of desired product (this could be termed a climate factor, or C factor, to remain consistent with the E factor introduced to indicate the overall amount of waste produced by chemical processes[17–18]). This C factor would help evaluate which renewable chemical processes are most desirable to develop under given boundary conditions.

From another perspective, the use of biomass as a sustainable resource for the production of fuels and chemicals should offer improved security in supply as biomass can be grown in most parts of the world. Conversely, oil resources are limited by being located only in a few, and in some cases, unstable areas of the world.[19] In conclusion, it appears very attractive to attempt to convert biomass into high value-added products rather than into relatively low-value fuels, in particular if this can be done in only a few and highly efficient process steps.

Prior to fossil resources becoming widely and inexpensively available, much of the chemical industry was based mostly on renewable raw materials. However, as these processes have not been continuously improved (as a result of unfavorable feedstock costs), they are generally not competitive with modern processes that rely on fossil resources. Nevertheless, in some case it has proven beneficial to explore biomass resources as raw materials and it could be even more attractive in the future.[20] This is typically the case in the production of key chemicals that have structures and functionalities which are very similar to those of the biomass feedstock.[21,22]

An economic evaluation of ethylene produced from steam-cracking of petroleum fractions and from the dehydration of bioethanol showed that the bio route was about 10–40% more expensive than the petroleum route to ethylene.[23] This study was carried out in 1988, with an oil price of about US$ 30/bbl (bbl = barrel; inflation adjusted) and a very well-established steam-cracking process. On the other hand, the production of bioethanol by fermentation of carbohydrates was not as developed as it is today. So, with today's oil prices around US$ 65–100/bbl and improved technology in the fermentation of biomass to ethanol, the route to bio-ethylene is becoming increasingly economically viable as compared to the route to petro-ethylene, and will continue to do so.

Today, all ethylene is still produced from fossil resources with the steam-cracking of naphtha as the main route. Ethylene has a price of more than US$ 1000/t[15] (metric ton = 1000 kg) and the price can only increase with the depletion of crude oil and increasing ethylene demands, in particular in China and India. Fuel-grade bioethanol has a price of less than US$ 600/t, clearly indicating that a relatively cheap dehydration process for ethanol to ethylene has good economic potential. Moreover, anhydrous ethanol is not necessary for the dehydration reaction,[23] thus the price for the bioethanol feedstock could be even lower as the expensive distillation to fuel-grade ethanol can be avoided.

A process that perhaps could be even more economically interesting is the oxidation of bioethanol to acetic acid. Acetic acid has today a value of around US$ 1400/t, which means that it is three times as expensive as fuel-grade ethanol on a molar basis. Again, it is not necessary to use anhydrous ethanol to produce acetic acid,[37] thus additionally favoring the bioprocess. These considerations lie behind the actual positions of ethylene and acetic acid in the renewables value chain (Figure 1) which we believe might be produced cheaper from renewable resources than from fossil resources.

Routes to a Renewable Chemicals Industry

In principle, it is possible to categorize the possible routes to establish a renewable chemicals industry into two distinctly different approaches, which should be pursued simultaneously. This categorization is presented in more detail here, and selected recent examples of both approaches are highlighted. It is shown how this categorization can be linked to the previously introduced value chains, and the barriers impeding the implementation of promising examples are discussed for the two different methods. In all likelihood, the future chemical industry will rely upon renewable chemicals fashioned from both approaches. In the first approach, biomass feedstocks are used to supply a proportion of the chemical building blocks that are currently produced from fossil resources, that is, the chemicals generically termed petrochemicals owing to their origin. The second approach is to target new chemicals, which have properties that make them potential substitutes for current petrochemicals.

Biomass Chemicals Identical to Current Petrochemicals

Figure 3 illustrates the current primary building blocks in the chemical industry derived from fossil resources (coal, natural gas and oil) and consequently used as building blocks for a range of significant large-scale commodity chemicals (shaded in dark gray). Syngas is produced from natural gas, along with ethylene and propylene, and is used to produce methanol on a large scale. In turn, methanol is used to produce commodity chemicals such as acetic acid and formaldehyde. Ethylene, along with other liquefied refinery gases such as propanes (propane and propylene), butanes (isobutylene and butadiene), and pentanes, is typically obtained by steam-cracking of naphtha, one of the largest industrial chemical processes today. As steam-cracking is endothermic and conducted at a very high temperature of around 750–875 °C, large amounts of fossil resources are required to heat the reaction mixture and to supply the heat of reaction. In fact, a mere 20% of the heat input to the steam-cracking process is used in the chemical conversion to olefin products; hence, there is a significant co-

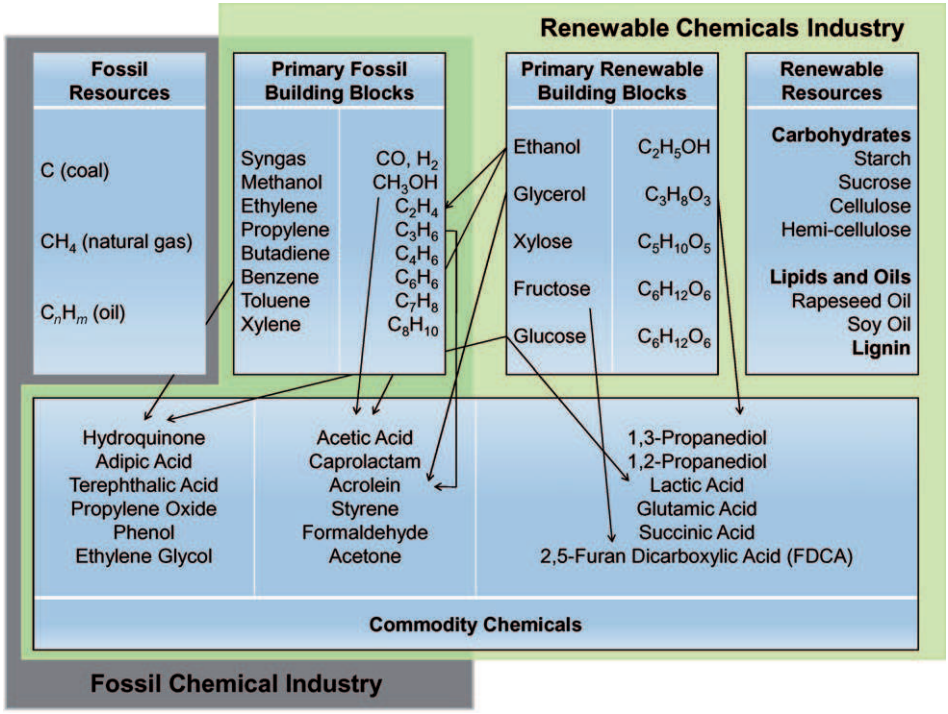

Figure 3. Strategies for producing commodity chemicals from biomass. The part set on a gray background shows some of the currently most important commodity chemicals produced from fossil resources. By strategy 1, these same chemicals are produced from renewable building blocks. Strategy 2 covers the idea of producing alternative chemicals, which potentially can substitute some of the "old" chemicals. Together strategies 1 and 2 cover the parts shown on the green background.

production of carbon dioxide. Accordingly, the C factor for the production of ethylene and propylene by steam-cracking is 0.65.[24] Ethylene is used to produce a wide range of chemicals, including ethylene glycol and styrene (with benzene via ethylbenzene), and it is also used directly as a monomer in polymers such as polyethylene and poly(ethylene terephthalate) (PET). Propylene is used to produce propylene glycol (1,2-propanediol), acrolein, acrylic acid, and acrylonitrile, and it is also used in the production of polymers. Benzene, toluene, and xylenes are derived from crude oil. Benzene is used to prepare commodity chemicals such as styrene, hydroquinone, phenol and acetone (both produced via cumene), and adipic acid and caprolactam (both produced via cyclohexane). The main outlet for xylene is in the production of terephthalic acid, which is used on a large scale for PET plastics.

Importantly, as is also illustrated in Figure 3, the primary building blocks described above can in principle also be produced from bioresources, and therefore, the commodity petrochemicals available today will also be available in the renewable chemicals industry. However, the production of these primary building blocks from bioresources will in some cases require more transformation steps as the natural primary renewable building blocks are newcomers to the commodity chemicals market. Nevertheless, biomass-derived syngas is an example of a primary fossil building block that is readily available from renewable resources by either gasification of biomass[25–27] or by aqueous-phase reforming of carbohydrate resources. However, instead of steam-reforming carbohydrates into syngas, they can also be transformed into simple sugars and fermented into building blocks such as ethanol and glycerol. Ethanol can be used to produce ethylene and butadiene (see below), and benzene, toluene, and xylenes can in turn be produced from ethylene by acid-catalyzed oligomerization.

Note that only selected chemicals are included in Figure 3, so as to focus on the synthesis strategy rather than on the exhaustive number of compounds that are produced in today's chemical industry or on the overwhelming number of possible routes to obtain these chemicals from bioresources. To outline the approach in more detail and to illustrate some recent examples of research efforts to develop new efficient routes to biomass-derived chemicals, a few selected synthesis pathways to major chemicals are highlighted with arrows. In the left part of Figure 3, the arrows connecting the fossil resources with various compounds illustrate how a given chemical is produced industrially today. On going from the top-right section of the diagram to the bottom left, the arrows indicate how it can be envisaged that the same compounds could instead be produced from renewable resources.

By way of an example, the acrylic acid family is explored in which acrolein is the key petrochemical intermediate. Acrylic acid is produced by the oxidation of propene in heterogeneously catalyzed processes, either directly or via acrolein in a two-step process. In terms of its usage, more than 90% of the acrylic acid is consumed as intermediates in the production of acrylate esters, which find widespread use as polymers, including superabsorbent polymers, detergents, adhesives, and coatings. Recently, the manufacture of acrolein from glycerol has received significant attention.[28] This is attributed to the fact that glycerol could become widely and inexpensively available as a by-product (or eventually even a waste product) from the production of biodiesel by transesterification. Indeed, it has been estimated that if the production of biodiesel grows as projected, the amount of glycerol available will rapidly be more than ten times higher than the current demand.[29] Alternatively, glycerol can be produced, for example, by the fermentation of glucose,[30] which could also develop into a cost-competitive process provided that the biodiesel market does not develop as quickly as projected. It is well known that by dehydrating glycerol, for example, with finely powdered $KHSO_4$ and K_2SO_4, it is possible to obtain acrolein in reasonable yields.[31] Through further developments, recently, several research

groups have reported that glycerol can be effectively dehydrated over solid acid catalysts to furnish acrolein in continuous processes with high yields,[32,33] and that acrolein can be oxidized to methyl acrylate in good yields even at ambient conditions.[34] Thus, the production of acrolein, and therefore also derivatives such as methyl acrylate, from glycerol obtained by fermentation will entail both biochemical as well as chemical process steps. In summary, acrolein could also be a key intermediate in the renewable chemicals industry.

Another example of integrated biochemical and chemical processes is the production of hydroquinone. Its production is currently mainly based on the oxidation of *para*-diisopropylbenzene (*p*-DIPB), which is available from Friedel–Crafts alkylation of benzene with propylene. *p*-DIPB is oxidized to the dihydroxyperoxide, which is cleaved to yield hydroquinone and acetone by an acid-catalyzed Hock rearrangement. Currently, the annual world production of hydroquinone is around 43 000 t. It has been reported that a benzene-free synthesis of hydroquinone is possible through biological pathways from glucose. The first approach proceeds by the shikimate pathway,[35] which requires 18 enzyme-catalyzed steps and one chemical step. However, a new approach to produce hydroquinone from glucose could be achieved in two enzyme-catalyzed steps and two chemical steps via 2-deoxy-*scyllo*-inosose synthase, thereby increasing the potential of the biosynthetic production of aromatic chemicals from glucose.[36]

A final example relates to the possibilities for using bioethanol as a feedstock for the chemical industry rather than, or as an alternative to, using it as a fuel additive. Ethanol can be thought of as a raw material for numerous industrially important chemicals, including ethylene, acetic acid, butadiene, and hydrogen.[14,37] As several of these transformations will be chemical processes, many of the chemicals produced from ethanol in the future will rely on integrated chemical and biochemical processes.

Originally, ethylene was manufactured primarily by the dehydration of ethanol[38] and similarly butadiene was produced from ethanol.[39,40] Today, acetic acid is still manufactured from ethanol. However, the major industrial process for the production of acetic acid is the carbonylation of methanol. Both methanol and carbon monoxide are typically produced by the steam-reforming of methane, which is a significantly endothermic reaction that takes place at temperatures above 600 °C. Approximately one quarter of the methane is directly combusted to heat the reactants and supply the heat of the reaction. Accordingly, about 0.6 kg CO_2 is produced for each kilogram of acetic acid, and the manufacture of acetic acid by this approach can therefore be said to have a C factor of about 0.6.

Alternatively, it can be conceived that acetic acid could be produced by the catalytic oxidation of ethanol. From the fossil and renewables value chains, it is observed that acetic acid is a relatively high-value commodity chemical, which is, say, twice as expensive as gasoline. In recent studies, acetic acid has been furnished in very high yields from the aerobic oxidation of ethanol in either liquid-phase[37] or gas-phase[41] processes using heterogeneous catalysts. In such new processes, it will be necessary to achieve optimal process integration so that energy-efficient handling of the large amount of water required in the fermentation is properly handled. With bioethanol available at lower prices than gasoline, a viable alternative technology for supplying acetic acid is available and could be cost-competitive and also lead to substantially lower CO_2 emissions than those reached when using bioethanol as a fuel additive.

In the manufacture of the chemicals described above, the chemical identity of the major building blocks remains unaltered when the feedstock is shifted from fossil to renewable, therefore resulting in only a modest impact on the rest of the chemical industry. As a result, the barriers presented for introducing such biomass-derived chemicals are expected to be relatively low. The focus in this approach will be on supplying the desired major chemicals at the lowest possible cost—and with the least possible environmental impact. This will require further development of efficient routes to transform biomass into useful starting materials, and here the technological developments driven by the demand for biofuels will be of appreciable importance. It appears that intimate integration of the involved biological and chemical processes is required to maximize energy efficiency, and thus this integration will be at least as important as it is in today's chemical industry.

Alternative Biomass Chemicals as Substitutes for Current Petrochemicals

The second approach towards realizing a renewable chemical industry is to produce chemicals from biomass that might potentially replace current petrochemicals. In its nature, this strategy is more visionary and will be harder to implement than the approach described above owing to the fact that such potentially new commodity chemicals are not already part of the existing markets. Therefore, cost will also become an important factor here in order for the new biomass-derived chemicals to compete with current petrochemicals and thus find an initial niche in the market. Likewise, environmental considerations need to be factored in—the new chemical should be manufacturable in a sustainable manner without the CO_2 emission problems currently encountered in the production of petrochemicals, otherwise the concept of introducing biomass as a sustainable replacement for fossil resources has little sense.

However, the concept of redesigning our chemical industry with replacement chemical commodities, designed in both process and final structure from today's know-how and technologies, is indeed an exciting one. The possibility to find biomass substitutes that are not only furnished from renewable feedstocks but involve a more efficient manufacturing process, and are maybe even more sustainable, stands as high. Examples of this approach include chemicals such as 2,5-furandicarboxylic acid (FDCA), lactic acid, and 1,2- and 1,3-propanediols, all of which are discussed here in some detail. In Figure 3, on going from the top right to the bottom right of the diagram, a pathway can be followed from renewable resources and primary building blocks to some of these potential replacement chemicals originating from biomass. Again, only a selection has been included for clarity.

Lactic acid and its polymer, poly(lactic acid) (PLA), are taken as first examples to further illustrate this approach as it is an example of a biomass chemical that has already entered the market as an alternative to fossil-derived polymers such as PET and polystyrene. The monomer, lactic acid, is produced by bacterial fermentation from cornstarch or sugar, and PLA is mostly manufactured by polymerization of its cyclic dimer lactide. The current production capacity for PLA is 450 000 tons per annum, however, this is projected to increase significantly in the coming years. PLA polymers are now used as biodegradable alternatives for packaging purposes and as fiber materials and could very well become economically competitive alternatives on a larger scale in the future. The major advantage of PLA polymers is the fact that they are fully biodegradable and compostable, and the degradation products, lactic acid and CO_2, are of course easily assimilated into biological systems. In fact, owing to the ease of absorbability, PLA polymers have been used for decades in the medical industry as, for example, resorbable implants and sutures.

FDCA is another example of a biomass chemical that could find use as a replacement monomer for making PET-type plastics. It can be produced from carbohydrates such as glucose and fructose that can undergo dehydration in the presence of acidic catalysts to form 5-hydroxymethylfurfural (HMF),[42,43] which under mild conditions can be oxidized to FDCA. This has been achieved using various strategies: notably, it has been shown that a silica-supported cobalt catalyst performs the dual task of dehydration to form HMF in situ and aerobic oxidation of HMF to furnish FDCA directly from fructose.[44] An alumina-supported platinum catalyst[45,46] as well as a titania-supported gold catalyst[47] have also been reported as effective catalysts for the oxidation reaction, although in the latter case the dimethyl ester is produced instead of the dicarboxylic acid. However, there are several obstacles to overcome for FDCA to become a viable alternative monomer in the production of PET-type plastics, namely that it remains to be demonstrated that polymers with the desired properties can indeed be made from FDCA on a large scale. Another limiting factor to the use of FDCA is the current high cost of dehydrating carbohydrates and purifying HMF.

Both isomers of propanediol are also examples of biomass chemicals that are expected to find increasing application in the future. They can both be produced from glycerol, which, as discussed above, might become an increasingly important renewable chemical in the future.[30] Although 1,2-propanediol is a petrochemical, which is typically produced in quantities exceeding 500 000 tons per annum by hydration of propylene oxide, its use for several applications is impeded by its current cost relative to ethylene glycol. However, as 1,2-propanediol can be produced in high yield by hydrogenation of glycerol,[48] it could become competitive to ethylene glycol in the future for selected applications, for example, as an antifreeze agent. Contrarily, 1,3-propanediol is not readily available from petrochemical feedstocks. However, in recent years, fermentation routes to 1,3-propanediol have been developed either from glycerol[49] or from glucose,[50] making this biomass chemical available at competitive cost. It has now found application as one of the monomers of poly(trimethylene terephthalate), a high-performance polyester material, under trade names such as Sorona 3GT (DuPont) and Corterra (Shell).

In the future, more examples of this approach will appear. Even though it can be more difficult with this approach to penetrate markets, it might be the strategy that ultimately leads to the most sustainable use of our limited bioresources.

Conclusions

Establishment of a renewable chemicals industry in which biomass is transformed into high-value-added chemicals might be the most advantageous way to secure optimal use of our abundant, but limited, bioresources from both an economical and ecological perspective. To evaluate the economical potential of new processes that transform biomass into desirable chemicals, we propose that the fossil and renewables value chains can be useful tools. Another important factor to consider in targeting the production of chemicals from renewable resources is the reduction in CO_2 emissions that might be achieved by the new technology. We put forward that the use of C factors could be a simple, convenient, and instructive method to facilitate such comparisons. Finally, it is noted that the establishment of a renewable chemicals industry appears to require an intimate integration of biocatalytic and heterogeneous catalytic processes to ensure that profuse bioresources are transformed into useful chemicals in a cost-competitive way, coupled with having minimum impact on the environment. Undoubtedly, the transition from a fossil chemical industry to a renewable chemicals industry will occur in many small steps. The rate at which these steps are taken evidently depends on the relative costs of renewable and fossil feedstocks, but also on requirements for introducing CO_2-reducing technologies. However, progress will likewise depend on our ability to focus research and development efforts on the most promising alternatives. In this aim, we hope that the present discussion might contribute to identifying suitable first targets in a more lucid manner.

Acknowledgements

The Center for Sustainable and Green Chemistry is sponsored by the Danish National Research Foundation.

Keywords: industrial chemistry · renewable resources · sustainable chemistry

[1] A. J. Ragauskas, C. K. Williams, B. H. Davison, G. Britovsek, J. Cairney, C. A. Eckert, W. J. Frederick Jr. , J. P. Hallett, D. J. Leak, C. L. Liotta, J. R. Mielenz, R. Murphy, R. Templer, T. Tschaplinski, *Science* **2006**, *311*, 484.
[2] G. W. Huber, A. Corma, *Angew. Chem.* **2007**, *119*, 7320; *Angew. Chem. Int. Ed.* **2007**, *46*, 7184.
[3] J. N. Chheda, G. W. Huber, J. A. Dumesic, *Angew. Chem.* **2007**, *119*, 7298; *Angew. Chem. Int. Ed.* **2007**, *46*, 7164.
[4] G. W. Huber, S. Iborra, A. Corma, *Chem. Rev.* **2006**, *106*, 4044.
[5] J. Goldemberg, *Science* **2007**, *315*, 808.
[6] http://www.eia.doe.gov.
[7] D. R. Dodds, R. A. Gross, *Science* **2007**, *318*, 1250.

[8] D. L. Klass, *Biomass for Renewable Energy, Fuels, and Chemicals*, Academic Press, California, **1998**, pp. 495–543.
[9] B. O. Palsson, S. Fathi-Afshar, F. F. Rudd, E. N. Lightfoot, *Science* **1981**, *213*, 513.
[10] B. Kamm, *Angew. Chem.* **2007**, *119*, 5146; *Angew. Chem. Int. Ed.* **2007**, *46*, 5056.
[11] F. W. Lichtenthaler in *Biorefineries—Industrial Processes and Products* (Eds.: B. Kamm, P. R. Gruber, M. Kamm), Wiley-VCH, Weinheim, **2006**, pp. 3–51.
[12] Y. Román-Leshkov, C. J. Barret, Z. Y. Liu, J. A. Dumesic, *Nature* **2007**, *447*, 982.
[13] M. Eissen, J. O. Metzger, E. Schmidt, U. Schneidewind, *Angew. Chem.* **2002**, *114*, 402; *Angew. Chem. Int. Ed.* **2002**, *41*, 414.
[14] J. Rass-Hansen, H. Falsig, B. Jørgensen, C. H. Christensen, *J. Chem. Technol Biotechnol.* **2007**, *82*, 329.
[15] http://www.icispricing.com.
[16] E. S. Lipinsky, *Science* **1981**, *212*, 1465.
[17] R. A. Sheldon, *Chem. Ind.* **1992**, 903.
[18] R. A. Sheldon, *Green Chem.* **2007**, *9*, 1273.
[19] E. S. Lipinsky, *Science* **1978**, *199*, 644.
[20] *Top Value-Added Chemicals From Biomass, Volume 1—Results of Screening for Potential Candidates from Sugars and Synthesis Gas* (Eds.: T. Werpy, G. Petersen), US Department of Energy, Oak Ridge, TN, August **2004**; available at http://www.eere.energy.gov/biomass/pdfs/35523.pdf.
[21] *The Key Sugars of Biomass*: F. W. Lichthenthaler in *Biorefineries—Industrial Processes and Products* (Eds.: B. Kamm, P. R. Gruber, M. Kamm), Wiley-VCH, Weinheim, **2006**.
[22] *Biomass Chemicals*: B. A. Tokay in *Ullmann's Encyclopedia of Industrial Chemistry*, Wiley-VCH, Weinheim, **2005**.
[23] R. Le Van Mao, T. M. Nguyen, G. P. McLaughlin, *Appl. Catal.* **1989**, *48*, 265.
[24] J. R. Nielson, *NATO ASI Sustainable Strategies for the Upgrading of Natural Gas: Fundamentals, Challenges, and Opportunities,* Vilamoura, July 6–18, **2003**.
[25] T. A. Milne, R. J. Evans, N. Abatzoglou, *Biomass Gasifier "Tars": Their Nature, Formation and Conversion*, NREL Technical Report (NREL/TP-570–25357), November **1998**.
[26] D. Dayton, *A Review of the Literature on Catalytic Biomass Tar Destruction*, NREL Technical Report (NREL/TP-510–32815), December **2002**.
[27] D. Sutton, B. Kelleher, J. R. H. Ross, *Fuel Process. Technol.* **2001**, *73*, 155.
[28] A. Behr, J. Eilting, K. Irawadi, J. Leschinski, F. Lindner, *Green Chem.* **2008**, *10*, 13.
[29] *Glycerol*: *Ullmann's Encyclopedia of Industrial Chemistry*, Wiley-VCH, Weinheim, **2005**.
[30] M. Pagliaro, R. Ciriminna, H. Kimura, M. Rossi, C. D. Pina, *Angew. Chem.* **2007**, *119*, 4516; *Angew. Chem. Int. Ed.* **2007**, *46*, 4434.
[31] *Organic Syntheses, Coll. Vol. 1*, **1941**, p. 15.
[32] A. Neher, T. Haas, D. Arntz, H. Klenk, W. Gierke, US Patent 5,387,720, **1995**.
[33] J. Dubois, C. Duquenne, W. Holderich, FR2882052, **2006**.
[34] C. Marsden, E. Taarning, D. Hansen, L. Johansen, S. K. Klitgaard, K. Egeblad, C. H. Christensen, *Green Chem.* **2008**, *10*, 168.
[35] N. Ran, D. R. Knop, K. M. Draths, J. W. Frost, *J. Am. Chem. Soc.* **2001**, *123*, 10927.
[36] C. A. Hansen, J. W. Frost, *J. Am. Chem. Soc.* **2002**, *124*, 5927.
[37] C. H. Christensen, B. Jørgensen, J. Rass-Hansen, K. Egeblad, R. Madsen, S. K. Klitgaard, M. R. Hansen, H. C. Andersen, A. Riisager, *Angew. Chem.* **2006**, *118*, 4764; *Angew. Chem. Int. Ed.* **2006**, *45*, 4648.
[38] Y. C. Hu, *Hydrocarbon Process.* **1983** (April issue), 113.
[39] G. S. Whitby, *Synthetic Rubber*, J. Wiley & Sons, New York, **1954**, p. 86.
[40] A. Talalay, M. Magat: *Synthetic Rubber from Alcohol*, Interscience, New York, **1945**.
[41] X. Li, E. Iglesia, *Chem. Eur. J.* **2007**, *13*, 9324.
[42] J. N. Chheda, Y. Román-Leshkov, J. A. Dumesic, *Green Chem.* **2007**, *9*, 342.
[43] H. Zhao, J. E. Holladay, H. Brown, C. Zhang, *Science* **2007**, *316*, 1597.
[44] M. L. Ribeiro, U. Schuhardt, *Catal. Commun.* **2003**, *4*, 83.
[45] P. Vinke, H. E. van Dam, H. van Bekkum, *Stud. Surf. Sci. Catal.* **1990**, *55*, 147.
[46] W. Partenheimer, V. V. Grushin, *Adv. Synth. Catal.* **2001**, *343*, 102.
[47] E. Taarning, I. S. Nielsen, K. Egeblad, R. Madsen, C. H. Christensen, *ChemSusChem* **2008**, *1*, 75.
[48] M. Dasari, P. Kiatsimkul, W. Sutterlin, G. J. Suppes, *Appl. Catal. A* **2005**, *281*, 225.
[49] M. M. Zhu, P. D. Lawman, D. C. Cameron, *Biotechnol. Prog.* **2002**, *18*, 694.
[50] A. N. Zeng, H. Biebl, *Adv. Biochem. Eng./Biotechnol.* **2002**, *74*, 239.

Received: December 21, 2007
Published online on March 25, 2008

Heterogeneous Catalysis for Production of Value-added Chemicals from Biomass

Kresten Egeblad, Jeppe Rass-Hansen, Charlotte C. Marsden, Esben Taarning, and Claus Hviid Christensen*

Center for Sustainable and Green Chemistry, Department of Chemistry, Technical University of Denmark, Building 206, DK-2800 Lyngby, Denmark. Email: chc@kemi.dtu.dk

1. Introduction

Almost everything around us is in some way a product of controlled chemical processes. That is either chemical processes conducted in Nature or chemical processes conducted in the chemical industry. In the most developed parts of the World, it is in fact products from the chemical industry that completely dominate our everyday lives. These products range from fuels and fertilizers to plastics and pharmaceuticals [1]. To make these products widely available, a huge amount of resources have been invested during the last century to develop the chemical industry to its current level where it is the largest industry worldwide, a cornerstone of contemporary society, and also a platform for further global economic growth [2,3]. It can be argued that the enormous success of the chemical industry can be attributed to the almost unlimited availability of inexpensive fossil resources, and to a continuously increasing number of catalysts and catalytic processes that make it possible to efficiently transform the fossil resources into all the required compounds and materials. Accordingly, more than 95 % of the fuels and chemicals produced worldwide are derived from fossil resources, and more than 60 % of the processes and 90 % of the products in chemical industry somehow rely on catalysis. It has been estimated that 20-30% of the production in the industrialized world is directly dependent on catalytic technology [4]. Therefore, it is not surprising

that we are continuously expanding our already vast empirical knowledge about catalysis to further improve the efficiency of existing catalysts and processes, to discover entirely new ways of valorizing available resources, and to lower the environmental impact of human activities [5]. Due to the overwhelming importance of fossil resources during the 20th century, most catalysis research efforts have, so far, concerned the conversion of these resources into value-added fuels and chemicals. There are, however, indications that the era of easy access to inexpensive fossil resources, especially crude oil, is coming to an end. The resources are certainly limited and the demand from everywhere in the world is growing rapidly. At the same time, it is becoming increasingly clear that the emission of CO_2 that follows the use of fossil resources is threatening the climate of the Earth. Together this makes the development of a chemical industry based on renewable resources one of the most important challenges of the 21th century.

This challenge has two different facets. One is the discovery and development of methods to use renewable resources to supply suitable energy currencies, i.e. fuels, in sufficient quantities at acceptable costs, and with minimal impact on the environment. The other is the discovery and development of new ways to provide all the chemicals needed to sustain a modern society. Whereas there are several possible energy scenarios that do not involve carbon-containing energy currencies, it is in fact impossible to envisage how it should be possible to provide the required chemicals and materials without relying extensively on carbon-containing compounds. Thus, to develop a chemical industry that does not depend on fossil resources, there are only two alternative carbon sources and that is CO_2 and biomass. Since transformation of CO_2 into useful chemicals always requires a significant energy input and since it is usually only available in minute concentrations, it appears attractive to instead utilize biomass as the dominant feedstock for chemical industry. In this way, it is possible to harvest the energy input from the Sun that is stored by photosynthesis in the C-C, C-H, C-O, and O-H bonds of the biomass. Clearly, a shift from fossil resources to renewable resources as the preferred feedstock in chemical industry is a formidable challenge. However, it is worth pointing out that during the early part of the 20th century, before fossil resources became widely available, biomass was the preferred feedstock for the emerging chemical industry, and today, biomass still finds use as a feedstock for a range of very

important chemicals [6]. Interestingly, these processes often rely mostly on the availability of biological catalysts whereas the processes for conversion of hydrocarbons use mostly heterogeneous catalysts. However, to explore the full potential of biomass as a feedstock in chemical industry, it appears necessary to integrate processes that rely on biological catalysts with processes that use heterogeneous or homogeneous catalysts to develop new, cost-competitive and environmentally friendly technologies [7]. Here, we will survey the possibilities for producing value-added chemicals from biomass using heterogeneous catalytic processes.

2. Setting a New Scene

Currently, there is an intense focus on the production of transportation fuels from biomass [8,9]. Clearly, this can be attributed to a desire to relinquish our dependence on fossil fuels, in particular crude oil, and also to significantly lower the emission of greenhouse gasses to minimize global warming. In some regions, it appears that production of bio-ethanol is indeed already cost-competitive with gasoline [8] and this emphasizes the potential of biomass as a renewable raw material. However, it is also clear that the extensive use of biomass to produce biofuels remains controversial from both an economical and an ecological perspective, and these issues must, of course, be resolved soon in a fully transparent way. However, it is undisputable that we will eventually need alternatives to the fossil resources for producing chemicals and materials [9,10,11]. It can be argued that if the amount of biomass available is too limited to substitute fossil resources in all its applications and if sufficiently efficient methods for transforming biomass into value-added chemical can be developed, this will represent the optimal use of biomass [7]. There are two reasons for this. First of all, most chemicals, even most of the simple petrochemical building blocks, are significantly more valuable than transportation fuels. This can be illustrated in a semi-quantitative way by comparing the value chains in a chemical industry based on fossil and renewable resources, respectively [7]. In this context, it is instructive to compare the cost of renewable resources to fossil resources over time. It is noteworthy that today, the cost of glucose is comparable to the cost of crude oil (on a mass-to-mass basis). Secondly, it is clear that by use of renewable resources as a feedstock for the chemical industry, significantly higher reductions in the emissions of green-house gases can be achieved than what is possible by production of biofuels. This can be attributed to the fact that production of many large-scale commodity chemicals from fossil resources is associated with a substantial co-production of CO_2 as expressed e.g., by the C-factor (kg CO_2 produced by kg of desirable product) [7]. This can often be attributed to the high temperature required to transform hydrocarbons. To illustrate this, the C-factor for industrial production of hydrogen from natural gas is about 9 and for ethylene from naptha it is 0.65. If hydrogen or ethylene was produced efficiently from biomass, the C-factor would approximately express the amount of CO_2 emission that would be saved compared to what would be possible by production of biofuels instead. Since ethylene

alone is currently produced in an annual amount close to 100 mill. ton, it is obvious that this would have a substantial impact on the total emission of green-house gases.

Fig. 1

There are many ways in which biomass can be envisaged to become an increasingly important feedstock for the chemical industry, and this has already been the topic of numerous studies [10-22]. The most comprehensive study was published recently by Corma et al. [10] and it contains a very detailed review of possible routes to produce chemicals from biomass. In Figure 1, we illustrate schematically how selected commodity chemicals could be produced using abundant bio-resources, i.e., carbohydrates (starch, cellulose, hemi-cellulose, sucrose), lipids and oils (rapeseed oil, soy oil, etc), and lignin as the sole raw materials. From these bio-resources, it is possible to directly obtain all the compounds classified in Figure 1 as primary renewable building blocks (of which only selected examples are given) with only one purification step. For example, ethanol can be obtained by fermentation of sucrose, glucose by hydrolysis of starch, glycerol by transesterification of triglycerides (or by fermentation of glucose), xylose by hydrolysis of hemi-cellulose, fructose by hydrolysis of sucrose (and by isomerization of glucose), and finally synthesis gas can be obtained directly by gasification of most bio-resources or by steam-reforming of the other primary renewable building blocks. From the primary renewable building blocks a wide range of possible commodity chemicals can be produced in a single step, and again examples of selected transformations are shown in Figure 1. For instance, acetic acid can be produced by fermentation of glucose or by selective oxidation of ethanol. Lactic acid is available by fermentation of glucose, and 5-hydroxymethyl furfural can be obtained by dehydration of fructose. These compounds can again be starting materials for other desirable products and so forth. Some of the commodity chemicals shown are already produced on a large scale from fossil resources, e.g., ethylene, acetic acid, acrolein and butadiene. Others are envisaged to become important large-scale commodity chemicals in the future when biomass gradually becomes a more important feedstock [14]. The different commodity chemicals are labeled using different colors to categorize them according to their number of carbon atoms. It is seen that a wide range of C_1 to C_6

compounds can be made available by quite simple means. Moreover, the chemical transformations in Figure 1 are labeled with colored arrows to illustrate specific ways to convert one building block into another. As it is apparent, the reactions all require a suitable catalyst, and this can be either a biological catalyst or a heterogeneous/homogeneous catalyst. Most of the primary renewable building blocks are produced today from bio-resources using mainly biocatalytic processes, and similarly several of the proposed commodity chemicals can also be produced from the primary renewable building blocks using biological catalysts. On the other hand, it is also clear that a very substantial number of the desirable transformations rely on the availability of suitable heterogeneous or homogeneous catalysts. Thus, it appears likely that a chemical industry based on renewable resources as the dominant feedstock will feature biological and chemical processes intimately integrated to efficiently produce all the desired chemicals and materials. Often, it appears that the possible role of heterogeneous catalysis in this scenario is not receiving sufficient attention in comparison with that of the biocatalytic methods. Therefore, in the present chapter we will highlight some of the existing possibilities for converting bio-resources, primary renewable building blocks, and commodity chemicals derived from these into value-added chemicals. We will focus on production of chemicals that can prove useful on a larger scale since they will contribute most to the valorization of significant quantities of biomass, and thereby contribute most to relinquishing the dependence on fossil fuels and to lowering the emission of green-house gases. Hopefully, this will be useful as a starting point for others to discover and develop new reactions and catalysts that can become useful in the efforts to make biomass a more useful resource for chemical industry. Our emphasis here is the catalytic reactions and the corresponding catalysts. Therefore, we have organized the literature covered in separate chapters according to five important reaction types, specifically, C-C bond breaking, hydrolysis, dehydration, oxidation, and hydrogenation. We envisage that these reaction types will be the most important for producing value-added chemicals from biomass since they can be conducted on large scale and they do not involve expensive reagents that will make them prohibitively expensive for industrial applications. Clearly, other reactions will also be important but several of those will be analogues to current methods in chemical industry. In each chapter, the presentation is organized hierarchically to first discuss the

catalytic conversion of compounds that are most closely related to the bio-resources (carbohydrates, lipids and oils, and lignin) and then successively those derived from these renewable raw materials.

3. Catalytic C-C Bond Breaking

3.1 Introduction

This section concerns catalytic processes that transform chemicals from renewables by C-C bond breaking. Among these are thermochemical processes, such as pyrolysis and also gasification, catalytic reactions, such as catalytic cracking and different reforming reactions, and decarbonylation and decarboxylation reactions. Many of these reactions occur simultaneously, particularly in the thermochemical processes. Another technically important class of C-C bond breaking reactions is the fermentation processes, however, they will not be considered in this section since they do not involve heterogeneous catalysis.

3.2 C-C Bond Breaking Reactions involving Bio-resources

3.2.1. Crude Biomass

Next to combustion, gasification is probably the easiest and most primitive method for degradation of biomass. In the simplest form, gasification involves heating of biomass (or any other carbonaceous material) to temperatures around 800-900 ºC, in an atmosphere with only little oxygen, until it thermally decomposes into smaller fragments. This partial oxidation process obviously requires a significant energy input and is not particularly selective; on the other hand, it is reasonably flexible since essentially all types of biomass can be gasified. Gasification, in particular of coal, has been known for long and was previously used to produce town gas. However, the gas resulting from gasification has a relatively low heating value of only 10-50% of that of natural gas [23-25], and this was a major reason for replacing town gas with natural gas. During World War II, biomass gasification advanced in Europe, but it was not until the oil crisis in the 1970s that new developments in the area truly took place [24]. Today, the main purpose of biomass gasification is to produce synthesis gas, with a H_2:CO ratio close to two, which is suitable for methanol synthesis or Fischer-Tropsch fuels.

There exist many different types of gasification furnaces but they generally work by having several different cracking and reforming zones. These zones are typically a pyrolysis zone, an oxidation zone and a reduction zone. Biomass is broken down either by pyrolysis (without oxygen) or by partial oxidation (with oxygen or air as oxidant) to

a mixture of CO, CO_2, H_2O, H_2, CH_4, other light hydrocarbons, some tar, char and ash, as well as some nitrogen and sulfur containing gasses such as HCN, NH_3, HCl, H_2S etc. [25]. The hydrocarbons and the char are further partially oxidized to mainly CO and H_2O (1-4) and steam reformed (5-6) or dry reformed (7-9) to CO and H_2. The heat from the exothermic oxidation reactions is used to supply the heat for the endothermic cracking reactions. Finally, the H_2:CO ratio can be adjusted by the water gas shift reaction (10). [23-26]

(1) $CH_4 + ½O_2 = CO + 2H_2$

(2) $H_2 + ½O_2 = H_2O$

(3) $C_nH_m + (n/2+m/4)O_2 = nCO + (m/2)H_2O$

(4) $C + ½O_2 = CO$

(5) $C_nH_m + nH_2O = nCO + (n+m/2)H_2$

(6) $C + H_2O = CO + H_2$

(7) $C_nH_m + nCO_2 = 2nCO + (m/2)H_2$

(8) $C + CO_2 = 2CO$

(9) $CH_4 + CO_2 = 2CO + 2H_2$

(10) $CO + H_2O = CO_2 + H_2$

The major challenge in gasification is to avoid the formation of tars, which have a tendency to clog filters and condense in end-pipelines. Tars are considered as the condensable fraction of the organic gasification products, and consist mainly of different aromatic hydrocarbons with benzene as the main species. For removal of tars three types of catalysts have been widely investigated; alkali metal salts, alkaline earth metal oxides and supported metallic oxides [24-26].

Alkali metal salts can be mixed directly with the biomass before entering the gasification furnace. They enhance the gasification reactions and lower the tar content, but recovery of the catalyst is difficult and costly making the alkali metals unattractive as catalysts for industrial use [25-26]. Another family of catalysts, which can be used effectively for gasification, is the alkaline earth metal oxides and carbonates. Of these, mainly the naturally occurring mineral dolomite ($MgCO_3 \cdot CaCO_3$) has been used [25]. It enhances the degradation of especially the tars and hydrocarbons into light gasses, though it is not active for methane reforming. When dolomite is calcined at 800 ºC, CO_2 is eliminated, yielding a far more active catalyst. These catalysts are deactivated by

carbon formation and attrition but they are inexpensive and disposable, and therefore easily replaceable. The third type of catalysts used are metals on a support, typically nickel on various oxide supports. Nickel catalysts are highly effective in tar destruction, the reforming of hydrocarbons and in adjusting the composition of the synthesis gas by the water gas shift reaction (10). They are operated as secondary catalysts in a downstream reactor, which can be operated at conditions different from those in the gasifier. Nickel catalysts primarily deactivate due to carbon formation and nickel particle sintering. Therefore, dolomite is often used in guard beds upstream of the nickel catalyst bed to remove most of the higher hydrocarbons [24-26].

Instead of gasifying biomass, it can be subjected to liquefaction in a pyrolysis process. Pyrolysis is actually one of the main processes occurring during gasification, however, in a dedicated pyrolysis plant, the desired products are liquid hydrocarbons rather than synthesis gas. In the current development of pyrolysis reactors, this is achieved by a fast pyrolysis process. Here, the biomass is heated rapidly to temperatures of around 500-600 ºC, which leads to formation of a dark brown liquid known as bio-oil along with some gasses and chars. Other types of liquefaction processes are high pressure pyrolysis (350 ºC, 20 MPa) and non-pyrolytic liquefaction (aqueous/non-aqueous) (250-425 ºC, 10-35 MPa) [27]. The liquid products from these processes are of relatively pure quality with a heating value of around half that of conventional oil. Alternatively to being used as heating oil they can be upgraded to transportation fuels or chemical feedstocks by hydrotreatment and catalytic cracking.

A possibly more sophisticated method for utilizing biomass to produce synthesis gas is by aqueous phase reforming (APR), a processing method that was developed for carbohydrates and other more readily accessible biomass oxygenates by Dumesic et al. [28-32]. Valenzuela et al. [33], however, were the first to report APR of real woody biomass. They used sawdust from pine, which was milled to an average diameter of 375 µm. The biomass was mixed with water, sulfuric acid (5%) and a catalyst (Pt/Al_2O_3) in a batch reactor. The acid catalyzed the hydrolysis of the biomass to decompose it into smaller soluble molecules, which were reformed over the platinum catalyst to yield mostly hydrogen and carbon dioxide. The process was operated at 225 ºC, with hydrogen accounting for 33% of the non-condensable product gasses.

3.2.2. Bio-oils

In the 1970s, it was shown that bio-oils from plant extracts such as rubber latex, corn oil, and peanut oil can be converted into a mixture of mainly gasoline and liquid petroleum gas over a ZSM-5 catalyst, at temperatures between 400-500 ºC [34]. These bio-oils were investigated as feedstocks for the reaction because they have high hydrogen to carbon ratios and low oxygen contents and therefore a hydrocarbon-like structure. It was suggested that such renewable plant resources, due to their siginifant content of highly reduced photosynthetic products, would be suitable for producing fuels or chemical raw materials [35]. The high hydrogen-to-carbon ratios in the biomass feed is desirable because oxygen usually must be removed and/or hydrogen must be added to achieve useful products.

Recently, several groups have investigated the catalytic conversion of bio-oils or model bio-oils over HZSM-5 catalysts [36-38], and recently a review was published describing how biomass could be converted into fuels or chemicals in a conventional petrochemical refinery in FCC or hydrotreating refinery units [39].

3.2.3. Carbohydrate Resources

Carbohydrate resources, such as hydrolyzed starch and sucrose as well as xylose and glucose, can be processed into hydrocarbons in a process similar to the one performed with bio-oils as described above (Section 3.2.2.), i.e. by using a HZSM-5 catalyst operated at around 510 ºC and ambient pressure [40]. This process is perhaps a little surprising since carbohydrates do not resemble the desired hydrocarbon product as much as the bio-oils do. However, formation of hydrocarbon compounds was found to occur as a result of oxygen removal from the carbohydrate by decarbonylation and decarboxylation reactions [40]. This process is probably one of the first attempts to conduct catalytic cracking of biomass.

Carbohydrate resources have also been processed under hydrotreating conditions, i.e. high hydrogen pressures (35-300 bar) and high temperatures (300-600 ºC) in the presence of Co-Mo or Ni-Mo-based catalysts; although other precious metals like Ru and Pt can also be used [39]. The main reaction involved under these conditions is hydrodeoxygenation (HDO), as, for example, described by Elliot et al. [41]. The important advantage of this technology is that excellent fuels and useful chemicals can

be produced in good yields, but the process is expensive and requires high hydrogen pressures.

3.3. C-C Bond Breaking Reactions involving Primary Renewable Building Blocks

3.3.1. Aqueous-phase Reforming (APR)

Aqueous phase reforming of glucose, glycerol and other biomass oxygenates, such as methanol, ethylene glycol and sorbitol, was carefully investigated by the group of Dumesic [28-32]. They showed how various biomass oxygenates can be converted into H_2, CO_2 and some light alkanes with good conversions and high selectivities over a Pt/Al_2O_3 catalyst operated at 225-265 ºC and 29-56 bar [28], as well as over a specially designed non-precious metal catalysts (Raney Ni-Sn) [29]. It was shown that this reaction could be used to supply hydrogen that could simultaneously be used for reduction of sorbitol to hexane [30]. This was achieved using a bifunctional catalyst that caused sorbitol to be partly cleaved over a metal catalyst (Pt, Pd) to form H_2 and CO_2 and at the same time sorbitol was also dehydrated over a solid acid catalyst. By carefully balancing these reaction steps, the hydrogen produced could be used directly for hydrogenation of the dehydrated sorbitol to eventually yield alkanes [30]. Alternatively, hydrogen could be co-fed, whereby the production of CO_2 was avoided and the conversion to alkanes (especially hexane) is improved [30].

3.3.2. Steam Reforming of Ethanol

Steam reforming (SR) is probably the most investigated process for breaking C-C bonds in chemicals available from biomass. Particularly, ethanol SR for production of hydrogen has been extensively examined [42-44], but also other primary renewable building blocks have received attention, such as SR of glycerol [45-46] or SR of bio-oils [47-48].

SR of methane/natural gas is one of the largest catalytic processes in the world and is by far the most important method for producing industrial hydrogen today. The process is well described in literature and it is typically carried out at 800-950 ºC over nickel-based catalysts [49]. The main reactions are methane SR (11) and water-gas-shift (WGS) (12).

(11) $CH_4 + H_2O = CO + 3H_2$

(12) $CO + H_2O = CO_2 + H_2$

SR of ethanol has mainly been conducted under similar conditions as methane SR, which means relatively high temperatures, ambient pressure, and primarily with Ni- or Rh-based catalysts [42-44]. Ideally, one mole of ethanol is converted into 6 moles of hydrogen (13). During SR, ethanol decomposes mainly through two different routes; either by dehydrogenation to acetaldehyde (14) or dehydration to ethylene (15). These two intermediates can be further catalytically reformed to a thermodynamically equilibrated reaction mixture of H_2, CO, CO_2, CH_4 and H_2O (12, 16-18) [50].

(13) $CH_3CH_2OH + 3H_2O = 2CO_2 + 6H_2$

(14) $CH_3CH_2OH = CH_3CHO + H_2$

(15) $CH_3CH_2OH = CH_2CH_2 + H_2O$

(16) $CH_3CHO = CH_4 + CO$

(17) $CH_3CHO + H_2O = 3H_2 + 2CO$

(18) $CH_2CH_2 + 2H_2O = 4H_2 + 2CO$

A substantial difficulty in ethanol SR is a too rapid catalyst deactivation due to coking. This can occur by several reactions, such as methane decomposition (19) or the Boudouard reaction (20), but primarily the polymerization of ethylene is thought to cause the problems (21). Unlike the situation for methane SR, it appears that for ethanol SR the deactivation by coke formation is lower at high temperatures.

(19) $CH_4 = 2H_2 + C$

(20) $2CO = CO_2 + C$

(21) CH_2CH_2 = polymeric deposits (coke)

SR of ethanol is an endothermic reaction and relatively high temperatures are required to convert ethanol into hydrogen and carbon monoxide and eventually carbon dioxide after equilibration by the WGS reaction (12). Thus, the drawback of this process is the energy requirements, which perhaps are not so disadvantageous. If the hydrogen is used in a high efficiency fuel cell, compared to combusting the ethanol in a motor engine with a relatively low efficiency, the overall energy output could be significantly improved [50]. Alternatively, the steam reforming reaction can be performed as a partial oxidation (22) [51]. Less hydrogen is formed in this way, but instead the reaction is

slightly exothermic, thus making hydrogen from renewable resources without the need of adding extra energy in terms of heat.

(22) $CH_3CH_2OH + 2H_2O + ½O_2 = 2CO_2 + 5H_2$

3.3.3 Decarbonylation

Furfural is easily obtained from biomass waste such as oat and rice hulls that are rich in pentosans. Further valorisation of furfural can be done by decarbonylation to produce furan, which can be further converted into tetrahydrofuran by catalytic hydrogenation.

Pure decarbonylation typically employs noble metal catalysts. Carbon supported palladium, in particular, is highly effective for furan and CO formation [52]. Typically, alkali carbonates are added as promoters for the palladium catalyst [52-53]. The decarbonylation reaction can be carried out at reflux conditions in pure furfural (165 °C), which achieves continuous removal of CO and furan from the reactor. However, a continuous flow system at 159-162 °C gave the highest activity of 36 kg furan per gram of palladium with potassium carbonate added as promoter [54]. In oxidative decarbonylation, gaseous furfural and steam is passed over a catalyst at high temperatures (300-400 °C). Typical catalysts are zinc-iron chromite or zinc-manganese chromite catalyst and furfural can be obtained in yields of around 90% at full conversion [53]. Again, addition of alkali metal carbonates promotes the reaction.

3.3.4 Deformylation

Levulinic acid is used as a starting material for the preparation of organic chemicals, dyes, polymers, pharmaceutically active compounds and flavoring agents. Acidic catalysts are required to procure levulinic acid from sugars, and/or 5-HMF. Acidic ion-exchange resins have been tested for dehydration of sucrose in pure water at 100 °C [55]. And levulinic acid could be achieved with up to 83% selectivity using all four tested ion-exchange resins (Dowex MSC-1H, Amberlyst 15, Amberlyst XN-1010 and Amberlyst XN-1005) although the overall yields were quite low (9-24%) even after 24 h reaction times [55]. Better results were achieved using zeolites as catalysts. Zeolite LZY was tested for fructose dehydration in pure water at various temperatures with the main product being levulinic acid formed in ca. 66% yield after 15 h at 140 °C [56]. Levulinic acid was also observed as one of the main products from aqueous phase dehydration of glucose using zeolite H-Y (with a SiO_2/Al_2O_3 ratio of 6.5) as well as

with acidic montmorillonite clays as catalysts [57-58], but significantly lower yields were reported. With the possibilities of levulinic acid as a renewable chemical building block, it seems interesting to develop the zeolite-catalyzed process from cellulosic feedstocks.

3.3.5 Hydrogenolysis

C-C and C-O bond breaking by hydrogenolysis of different polyols (glycerol, xylitol, erythritol and sorbitol) has been investigated by Montassier et al. [59-60]. Predominantly ruthenium and copper-based charcoal catalysts were studied at 210-260 °C and 1-6 MPa hydrogen pressures. The main products from the aqueous glycerol conversions were propylene glycol using copper catalysts and ethylene glycol along with methane using ruthenium catalysts. The hydrogenolysis of glycerol to ethylene glycol and propylene glycol using ruthenium on a range of different supports at 180 °C and 5 MPa hydrogen pressure showed the highest conversion on a TiO_2 support [61]. Blanc et al. reported the treatment of aqueous sorbitol solutions on CuO-ZnO catalysts at 180 °C 130 bar hydrogen pressure [62]. The purpose of the analysis was to achieve a high C_{4+} selectivity suitable in the synthesis of alkyd polymers, and the CuO-ZnO catalyst was superior in achieving a high C_{4+} selectivity (73 % yield) compared to Ru and Ni catalysts which mainly yielded C_1- C_3 products.

A commercial example of a hydrotreating technology is examined below. The IPCI (International Polyol Chemicals, Inc.) hydrogenolysis process is carried out at 100-300 ºC and at hydrogen pressures of 70-300 bar [63]. The hydrogenolysis process is used to cleave carbohydrates to smaller polyol fragments. Specifically, sorbitol and mannitol are reformed to propylene glycol and ethylene glycol as the main products, and to different butanediols in smaller quantities [64]. The primary product, propylene glycol, is formed by hydrocracking either of sorbitol directly (23) or, more likely, through glycerol (24,25).

(23) $C_6H_{14}O_6 + 3H_2 = 2C_3H_8O_2 + 2H_2O$

(24) $C_6H_{14}O_6 + H_2 = 2C_3H_8O_3$

(25) $C_3H_8O_3 + H_2 = C_3H_8O_2 + H_2O$

The composition of the hydrogenolysis products is very dependent on the actual process conditions and on the catalysts used in the reaction. So far, mostly supported nickel

catalysts are being applied. IPCI has constructed a 10 000 MT/y pilot plant in China in 2005, and in 2007, a commercial 200 000 MT/y plant was commissioned, also in China [63].

4. Catalytic Hydrolysis

4.1 Introduction

Hydrolysis is the process by which a compound is broken down by reaction with water, thus it can be thought of as the opposite reaction of dehydration, where water is of course removed. Hydrolysis is a key reaction type in biomass chemistry, for it is central in the depolymerisation of polysaccharides to simpler monosaccharide building blocks, such as fructose, glucose, and xylose.

4.2. Hydrolysis Reactions involving Renewable Resources

4.2.1 Sucrose, Maltose and Cellubiose

Sucrose can be hydrolyzed to give inverted sugars, i.e. a mixture of fructose and glucose (Scheme 1). For the transformation of biomass into value-added chemicals, this is a key reaction since it provides major building blocks for further chemical synthesis, fructose and glucose, from widely occurring sucrose. In the past, and on an industrial level, this reaction has been performed with the use of enzymes as the catalyst. However, due to the production of waste, low thermal stability, problems with separation of products and enzymes, and recovery, and low rate due to glucose and fructose inhibiting the reaction, a different path has been sought for.

Scheme 1

It has been established early that acids catalyze this hydrolysis reaction, thus liquid sulfuric acid has been used. Heterogeneous catalysis can potentially provide simpler and environmentally more benign processes, however, via ease of separation and recovery. Thus, solid acids, such as acidic ion-exchange resins [65-66], zeolites and heteropolyacids, can replace the homogeneous acids. Hydrolysis of sucrose is in fact already established on an industrial scale using acid ion-exchangers [67], but the main route is still via enzyme catalysis. Transfer to the heterogeneous system shows problems regarding the microenvironment of the swollen polymer, i.e. limitation of diffusion and restricted accessibility, as well as the production of many by-products [68].

In an effort to make this switch to heterogeneous catalysts viable, various acidic exchange resins have been tested, including those prepared by radiation-induced grafting to produce graft copolymers capable of hosting sulfonic groups [69-71]. A common problem with solid acids, including ion-exchange resins, is that they are subject to poisoning by water. Thus, sulfonated mesoporous silicas were investigated as a new class of solid acids, giving glucose and fructose in 90% yield after four hours at 80 °C [72]. Zeolites are also acid ion-exchangers. A conversion of sucrose of up to 90% with close to 90% selectivity and very few by-products formed was achieved using highly dealuminated zeolite Y at 70 °C [73]. Similarly, the activity of various dealuminated zeolites was compared, again showing high selectivities and few by-products, regardless of the conversion [74]. Similarly, the hydrolysis of maltose was studied by comparing the performance of acid zeolites, ion-exchange resins, amorphous silic-aluminas and also the ordered mesoporous material, MCM-41 [75]. The best results were achieved with zeolite beta (Si/Al=50) at 130 °C and 10 bar where a conversion of 85% and a selectivity of 94% was reported. Most recently, the use of organic-inorganic hybrid mesoporous silica catalysts was reported for the hydrolysis of cellubiose to yield glucose. Cellubiose was used as a model for oligosaccharides, and it was possible to achieve 100% conversion at 175 °C but significant glucose degradation was observed simultaneously [76].

It can be seen then that heterogeneous catalysis may find an opportunity for replacing the enzymatic catalysis of disaccharides to its monosaccharides, and thereby provide industry with a more efficient and benign route. However, it is also clear that more selective catalysts are required.

4.2.2 Triglycerides

Triglycerides can be hydrolyzed to give fatty acids and glycerol (Scheme 2). The fatty acids obtained have many industrial uses, mostly for the manufacture of soap. Glycerol is currently viewed as a by-product from this reaction, but maybe in the future it will be considered a commodity due to the current drive to develop it as a feedstock. Technologies in this area have often featured high temperatures and pressures because of low reaction rates. In an attempt to develop low temperature and pressure processes,

as well as methods that are easy to implement, heterogeneous catalysis has been pursued as an alternative.

Scheme 2

Similarly to the hydrolysis of sucrose, acid exchanged resins can be utilized, in one case to give 75% hydrolysis of triglycerides after six hours at 155 °C. It was shown that the Brøndsted acid sites catalyze the hydrolysis reaction, which was performed in the liquid phase with continuous steam injection [77]. The same authors reported that polystyrene sulfonic cation-exchange resin, loaded with 13 % of the superacid H_3Mo, gave 74.5% hydrolysis of palm oil at 155 °C in a batch reactor also operated with steam injection [78].

4.2.3 Polysaccharides

Before the introduction of enzymes (α-amylase and glycoamylase) to facilitate the hydrolysis of polysaccharides, this transformation was typically achieved using strong mineral acids. There have also been studies of the use of ion-exchange resins and of the zeolite mordenite to catalyze the hydrolysis of amylose and starch at 130 °C and 10 atm. With the ion-exchange resin, it was seen that the selectivity towards glucose was not lowered by lengthening the reaction time. However, this was not the case for mordenite where substantial degradation of the glucose was observed [75]. With the ion-exchange resin, it was possible to obtain 35% glucose after 24 hours reaction time. Similarly, the performance of an ion-exchange resin (Amberlyst 15), nafion-silica and sulfonated mesoporous silicas were compared for starch hydrolysis. The best yields reported were 39 % glucose and 18 % maltose obtained at 130 °C [79].

5. Catalytic Dehydrations

5.1. Introduction

There are several examples of dehydrations of chemicals derived by renewable resources by use of heteregeneous catalytic approaches in the literature. These can be categorized into three types of reactions: (a) reactions in which one (or more) molecule(s) of water is eliminated from a single substrate molecule, (b) reactions in which one (or more) molecule(s) of water is generated as the result of an esterification reaction between an alcohol and a carboxylic acid or carboxylic acid derivative and (c) reactions in which one (or more) molecule(s) of water is generated due to an etherification reaction between two alcohol functionalities.

5.2. Dehydration Reactions involving Bio-resources and Primary Renewable Building Blocks

5.2.1. Bio-oils

Transesterification of vegetable oils to produce fatty acid methyl esters (FAME) which can be used as biodiesel has been studied intensely in recent years. Mainly solid bases such as MgO and hydrotalcites are used as catalysts [80-81], however, solid acids are also studied for these reactions [81]. In a study with soybean oil as the source of fatty acids, MgO catalysts prepared in different ways, as well as a hydrotalcite catalyst, were all reported to be effective catalysts for the transesterification reactions yielding between 75 and 95% FAME after 1 h at 180 °C, whereas application of alumina resulted in less than 5% FAME [80]. At 200 °C, all the tested base catalysts (except one of the four MgO ones) resulted in a yield of FAME of 95-100%. In a similar study, experiments carried out at 180 °C showed a difference in the yields obtained using hydrotalcite and MgO catalysts [81]. Using hydrotalcite, 92% yield was obtained, whereas the yield using MgO was 75%. However, the yield obtained using these catalysts were similar (75-80%) when the reaction mixture also contained some free fatty acid. In this study, pure and metal-substituted vanadyl phosphates (MeVPO) as well as titanated silica (tetraisopropoxide titanium grafted onto silica) were also tested for the reaction [81]. The best results were obtained with GaVPO with which a yield of 82% FAME yield was obtained. The transesterification reactions have also been studied

using alumina-supported solid base catalysts at methanol reflux temperatures, e.g. using catalysts made by calcining KNO_3 adsorbed on Al_2O_3 [82]. The study showed that 35 wt% KNO_3/Al_2O_3 calcined at 500 °C was the optimum catalyst for the reaction, and this catalyst gave 87% yield after a reaction time of 7 h. Recently, KF/Al_2O_3 has also been reported as catalyst for transesterification at about 65 °C in a study using cottonseed oil as the fatty acid source [83], and even poultry fat has been transesterified recently using hydrotalcite as the catalyst [84].

5.2.2. Syngas and Methanol

Methanol is one of the top industrial chemicals today. It is produced on a very large scale from fossil-derived syngas by use of a Cu-Zn-Al-oxide catalyst, however, it can of course also be produced in a similar manner from bio-derived syngas. Methanol (and also syngas) can be used as a feedstock to produce dimethyl ether via catalytic dehydration. However, the chemistry involved in these processes is well-known, and will not be considered here, since it has been extensively dealt with in detail elsewhere [85-87].

5.2.3. Ethanol

Ethanol is the most important chemical produced by fermentation, and it has the potential to become a major feedstock for the chemical industry since many other large-scale chemicals can be produced from ethanol. In fact, ethanol can in many respects be considered a renewable alternative to ethylene, which is the largest volume carbon-containing chemical produced from fossil resources today. Via catalytic dehydration, ethanol can easily be converted into ethylene and diethyl ether, both of which are well-known acid catalyzed processes. Almost all available solid dehydration catalysts have been tested for these reactions, and a comprehensive review of this field is beyond the scope of this review. The reader is referred elsewhere for reviews on these topics [88-91].

5.2.4. Glycerol

It has long been known that glycerol can be dehydrated to produce acrolein by heating aqueous glycerol with a mixture of finely powdered $KHSO_4$ and K_2SO_4 (Scheme 3)

[92]. Recently, the reaction has received attention again, as several acidic solid oxide catalysts were tested as catalysts for the reaction [93-95]. The best results were obtained with silica-supported heteropolyacids such as silicotungstic acid with which 86% selectivity towards acrolein was obtained at 98% conversion of glycerol at 275 °C [93]. Also tungstated zirconia has been reported to be a selective catalyst for acrolein formation in a comparative study of many different catalysts; using 15 wt% WO_3/ZrO_2, 65% selectivity towards acrolein was achieved at 100% conversion at 325 °C [95].

Scheme 3

Another dehydration product from glycerol is hydroxyacetone, or acetol (Scheme 4). In one study, several catalysts were tested for this reaction [96]. Of the tested catalysts, however, only copper-chromite appeared to be effective for this transformation. Using this catalyst, 80% selectivity towards hydroxyacetone was achieved at 86% conversion in a reactive distillation experiment carried out under a slight vacuum (98 kPa) at 240 °C [96].

Scheme 4

5.2.5. Xylose

Catalytic dehydration of xylose, which is the most abundantly available pentose monomer in hemicellulose, has been known for a long time (Scheme 5). In fact, as early as 1922, an industrial process involving sulfuric acid catalyzed dehydration of xylose to produce furfural was developed by the Quaker Oats Co.

Scheme 5

Recently, several reports concerning this reaction have appeared in literature describing the use of zeolites [97], ion-exchange resins [98], sulfonic acid functionalized MCM-41 [98], immobilized heteropolyacids [99-101], niobium silicates [102] and exfoliated titanate and niobate nanosheet structures [103] as solid acid catalysts. In 1998, Moreau et al. compared zeolites H-Y and H-Mordenite in batch experiments at 170 °C with 1:3

water/toluene or water/methyl isobutylketone mixtures as the reaction media. It was found that H-Y was generally the most active catalyst whereas H-mordenite was the most selective towards furfural formation; up to 96% selectivity at 27% conversion after 30 min. using water/toluene as the reaction media [97]. Using sulfonic acid-functionalized MCM-41, 82% selectivity at 91% conversion was achieved after 24 h at 140 °C using either DMSO or toluene/water as the extraction phase [98]. Under the same conditions, application of Amberlyst-15 resulted in only 70% selectivity towards furfural at 90% conversion. Catalysts made by functionalizing MCM-41 with heteropolyacids have also been tested for the reaction. In general, however, the performances of these catalysts are not particularly good, as the highest selectivity achieved in a study of several heteropolyacids using different extraction phases were 67% at 94% conversion after 4 h at 140 °C [99]. Moreover, microporous AM-11 niobium silicate and ordered mesoporous niobium silicates have been reported as catalysts for dehydration of xylose, however, at 160 °C no more than 56% selectivity at 89% conversion was obtained using microporous AM-11 [102]. However, the study also showed that the reaction temperature could be raised to 180 °C whereby the furfural yield increased from ca. 20% after 1 h at 160 °C to ca. 45%. Very recently, exfoliated and acidified layered titanates, niobates and titanoniobates prepared by heating mixtures of TiO_2 or Nb_2O_5 with alkali carbonates followed by immersion in aqueous HCl or HNO_3 and finally exfoliating the sheets with tetrabutylammonium hydroxide [103]. Using these catalysts, furfural yields up to 55% could be obtained at 92% conversion after 4 h at 160 °C.

5.2.6. Glucose and Fructose

Sucrose is one of the largest chemicals readily available from biomass. It is produced from sugar cane or sugar beats and can be easily hydrolyzed into its constituent monomers, glucose and fructose. In general, dehydration of these carbohydrates will lead to the formation of many different products, however, some control of the dehydration products obtained can be achieved using different acid catalysts. The target chemical in most reports concerning solid acid catalyzed dehydration of hexoses is 5-hydroxymethyl furfural (Scheme 6), and to a lesser extent levulinic acid, which is formed along with formic acid from HMF by a rehydration-decomposition reaction.

HMF is sometimes referred to as a "sleeping giant" due to its enormous potential importance as a key chemical intermediate [104], and several reviews are available concerning the production as well as chemistry of HMF [105-106]. Very recently, significant achievements were made in the production of HMF by homogeneous catalytic approaches [107]. Typically, the starting material for HMF synthesis is fructose, however, there exists, of course, great interest in establishing a commercially viable process directly from glucose, since glucose is less expensive than fructose. Several types of catalysts have been applied for dehydration of fructose to produce HMF. These were categorized into five classes of catalysts (organic acids, inorganic acids, salts, Lewis acids and other) by Cottier et al. who also categorized the different methods by which the dehydration reaction was carried out into five different types (aqueous media below 100 °C, aqueous media above 100 °C, non-aqueous media, mixed-solvent systems and solvent-free/microwave processes) [105]. Most of the solid acids applied in the synthesis of HMF from fructose, zeolites, ion-exchange resins, solid inorganic phosphates, belong to the group of "other catalysts" according to the categorization of Cottier et al. Although levulinic acid can be an interesting target in itself, it is nonetheless an undesirable byproduct in processes targeting HMF, particularly, when water is used as the reaction media. Therefore, the most successful approaches to circumvent levulinic acid formation by HMF rehydration-decomposition is to carry out the reaction in a mixed water-organic solvent system, so that HMF is removed from the aqueous phase as it forms. Literature covering the synthesis of levulinic acid can be found in Section 5.3.

Scheme 6

With zeolites as the solid acid catalyst, the best results for HMF synthesis were obtained by Moreau et al. who tested acidic mordenites with different Si/Al ratios in batch experiments and reported that dealuminated H-Mordenite with Si/Al ratio of 11 exhibited the highest selectivity and even so at reasonably high fructose conversion (91% selectivity at 76% conversion after 60 min. at 165 °C using water/methyl isobutyl ketone as the reaction media) [108]. Other zeolites, H-Y, H-Beta and H-ZSM-5 were

also tested for the reaction, however, none of these catalysts were as selective as H-mordenite [109].

Also acidic ion-exchange resins were tested as catalysts for fructose dehydration. Using PK-216, a solution of water-DMSO-polyvinylpyrrolidone containing 10 wt% fructose was dehydrated to HMF after 8-16 h at 90 °C with 71% selectivity at 80% conversion using MIBK as the extraction phase [107]. Using a more concentrated fructose solution (30 wt%), 65% selectivity was achieved at 83% conversion. Working in more dilute solution (0.5 M in DMSO), also with PK-216 as the catalyst, an HMF yield of 90% was obtained after 5 h at 80 °C [110]. Even more remarkable perhaps was the observation that the reaction could be carried out in a continuous process with no signs of deactivation even after 900 h, in this case using Amberlite IR-118 as the catalyst. Recently, Amberlyst 15 was also reported as catalyst for fructose dehydration to produce HMF at 80 °C using a solvent system comprising DMSO and either a hydrophilic (BMIM-BF_4) or hydrophobic (BMIM-PF_6) ionic liquid [111]. In both cases, HMF yields of ca. 80% were achieved after 24 h, however, when the reaction was carried out without DMSO as co-solvent, a maximum yield of only ca. 50% yield could be achieved (after 3 h) using BMIM-BF_4. Very recently, ionic liquids immobilized on silica (ILIS) were used as catalysts for dehydration of fructose to HMF [112]. In the study, it was shown that both Lewis and Brøndsted acidic ILIS were effective for the transformation. 70% yield was obtained at 100% conversion after 4 min. of 200 W microwave irradiation in DMSO using Brøndsted acidic 3-allyl-1-(4-sulfobutyl)imidazolium trifluormethanesulfonate [ASBI][Tf], whereas a yield of 67% was achieved using Lewis acidic 3-allyl-1-(4-sulfurylchloride butyl)imidazolium trifluormethanesulfonate [ASCBI][Tf].

A third class of solids, which were tested as catalysts for carbohydrate dehydrations are inorganic phosphates. In a comparative study including vanadyl phosphate ($VOPO_4 \cdot 2H_2O$) and partially metal-substituted vanadyl phosphates ($M_xVO_{1-x}PO_4 \cdot 2H_2O$, M being Cr, Mn, Fe, Al and Ga), it was shown that vanadyl phosphate, which contains both Brøndsted and Lewis acid sites, is very selective towards HMF formation (80% selectivity at 50% conversion after 1 h) under mild conditions (80 °C) and in pure water

[113]. Moreover, it was shown that partial Fe-doping increased the performance quite significantly, so that even at very high fructose concentrations, a reasonable yield of HMF could be achieved (84% selectivity at 71% conversion using 30 wt% fructose as the reaction media). The study also showed that the catalyst performances are very similar when inulin is used as the carbohydrate source in stead of fructose, perhaps opening up the possibility of producing HMF from an even more inexpensive source than fructose. Overall, the performance of the vanadyl phosphate catalysts at 80 °C was quite similar to the performance of zirconium and titanium phosphate and pyrophosphate catalysts operated at 100 °C. Of the latter two types of catalysts, the best performance was achieved with cubic zirconium pyrophosphate and γ-titanium phosphate, that gave selectivities of up to 99.8% and 98.3% after 30 min., respectively [114]. Also selectivities up to ca. 100% were reported for niobium phosphate systems at 100 °C, although at low conversions of fructose [115-116]. Very recently, niobic acid and niobium phosphate catalysts were also studied under continuous flow conditions in aqueous medium. It was shown that the niobium phosphate catalyst was more active than the niobic acid catalyst due to it having a more acidic surface [117]. The use of zirconium phosphates under subcritical water conditions was also reported recently. In the study, it was shown that HMF yield of 61% at 80% fructose conversion could be achieved after only 2 min. at 240 °C [118]. Using glucose as the reactant under otherwise similar conditions, only 39% selectivity was achieved.

Dehydration of glucose and fructose was also reported using solid oxide catalysts. With anatase-TiO_2 (a-TiO_2) and a mixture of monoclinic and tetragonal ZrO_2 (m/c-ZrO_2) it was reported that fructose could be relatively selectively dehydrated to HMF after only 5 min. at 200 °C, although in quite low yields (ca. 25%) [119-120]. With the same catalysts but with glucose as the starting material, a-TiO_2 was much more selective towards HMF than m/c-ZrO_2, which gave more or less the equilibrium mixture of 1,6-anhydroglucose and HMF, which was also obtained in the absence of a catalyst. However, it should be noted that m/c-ZrO_2 presumably catalyzes the isomerization of glucose into fructose since more than 60 mol% fructose was present in the reaction mixture after experiments starting from aqueous glucose.

In 2000, Kröger et al. reported that 2,5-furan-dicarboxylic acid (FDCA) could be produced in a combined one pot dehydration-oxidation reaction starting from fructose, however, only in 25% yield [121]. Very recently, this was improved significantly, when Ribeiro and Schuchardt reported that also SiO_2-gel containing $Co(acac)_3$ could be used as catalyst for the combined dehydration-oxidation reaction of fructose to yield FDCA [122]. With pure SiO_2-gel, ca. 100% HMF selectivity could be achieved at ca. 50% conversion after 65 min. at 160 °C. However, with $Co(acac)_3$ encapsulated in SiO_2-gel, a 70% one-pot yield of 2,5-furan-dicarboxylic acid was achieved. This proves an important point, namely that an alternative strategy to improving the HMF yield by adding an extraction phase is simply to react it further in-situ to desired end-products.

5.3. Dehydration Reactions involving Commodity Chemicals

5.3.1. 1,2- and 1,3-Propanediols

Dehydration of 1,2- and 1,3-propanediols to produce allyl alcohol was studied using CeO_2 as the catalyst [123-124]. With 1,3-propanediol, the reaction is very specific towards allyl alcohol which is formed with 99% selectivity at 51% conversion at 325 °C [123]. At the same temperature and with 1,2-propanediol as the substrate, only 44% selectivity was achieved and at very low conversion. At elevated temperatures, higher conversion of 1,3-propanediol can be achieved, however, at a substantial drop in selectivity. At 425 °C, the selectivity towards allyl alcohol was 54% at 78% conversion of 1,3-propanediol.

5.3.2. Succinic Acid

Succinic acid is also available via fermentation of glucose, and has the potential to become a large-scale industrial chemical in the future. However, there are only a few reports on dehydration reactions involving succinic acids in the literature, and most of these are concerned with esterification to produce dialkyl esters. The synthesis of various dialkyl esters was reported using metal exchanged montmorillonite clays (Na^+, Mn^{2+}, Zn^{2+}, Ni^{2+}, Cr^{3+}, Fe^{3+} and Al^{3+}) as the catalysts [125-127]. For dimethyl succinate, 70% isolated yield was achieved using Fe^{3+}-exchanged montmorillonite after 4.5 h at methanol reflux temperature [127]. For dibutyl succinate, the best results were obtained with Al-montmorillonite (94% yield after 8 h, also at reflux temperature),

which also proved to be a good catalyst for other esterification reactions, e.g. for diesterification with isobutyl alcohol to produce di-(isobutyl) succinate in 98% yield [126]. Very recently, a new family of materials known as Starbons was also applied for esterification of succinic acid with ethanol in aqueous ethanol solution [128-129]. Using sulfonated Starbon-400-SO_3H as the catalyst, diethyl succinate was obtained in >99% after ca. 9 h at 80 °C [128].

5.3.3. Levulinic acid and itaconic acid

Levulinic acid could also become an important intermediate chemical in the future since it can be produced by acid catalyzed dehydration-decomposition of fructose. The synthesis of diethyl levulinate was recently reported using sulfonated Starbon-400-SO_3H. The selectivity towards the diester was >99% at 85% conversion after 6 h at 80 °C [128]. In the paper esterification of itaconic acid was also reported. However, this reaction is much slower and less selective, as ethyl itaconate was achieved with 75% selectivity at 81% conversion after 24 h [128].

5.3.4. Sorbitol

Sorbitol is the sugar alcohol obtained by reduction of glucose and it can be dehydrated to either isosorbide or to 1,4- and 2,5-sorbitan in acid or base catalyzed processes, respectively. Using sulfonic acid functionalized MCM-41 type materials lauric acid esters of isosorbide can be achieved quite selectively starting from sorbitol (>95% selectivity towards isosorbide dilaurate at 33% lauric acid conversion) in a dehydration-esterification reaction [130].

6. Catalytic Oxidations

6.1. Introduction

Oxidation as a process to transform biomass into value-added chemicals is a key one. Here, we focus on oxidations using molecular oxygen as the oxidant, with the aim of illustrating selected interesting reactions that could be important in the efforts to develop sustainable chemistry since they only require abundant bio-resources as reactants and have water as the only, or at least the main, byproduct.

6.2. Oxidation Reactions involving Primary Renewable Building Blocks

6.2.1. Ethanol

Acetic acid, an important chemical reagent and industrial chemical with a global demand of around 10 million tonnes per year, can be produced from the oxidation of bioethanol. It has a very large number of industrial applications e.g., in the production of cellulose acetate for photographic films and in polyvinyl acetate for wood glue. Moreover, it also finds use in the food industry as an acidity regulator, as the additive E260.

The oxidation of ethanol to acetic acid was among the first heterogeneous catalyzed reactions to be reported, but it has not attracted continued interest. During the 1990ies, however, 100% conversion of ethanol coupled with 100% selectivity to acetic acid was reported in a gas-phase reaction using molybdenum oxide catalytic systems on various supports, at temperatures below 250 °C [131]. Similarly, a tin oxide and molybdenum oxide catalyst was used with a feed consisting of 80% aqueous ethanol to produce acetic acid at 320 °C [132]. Recently, it was reported that a mixed Mo-V-Nb oxide also catalyzes the selective oxidation of ethanol to acetic acid with oxygen in a gas phase reaction at about 235 °C with 95 % selectivity at full conversion at about 235 °C [133].

At even milder conditions, gold nanoparticles were found to be effective heterogeneous catalysts for this reaction in aqueous phase. A yield of acetic acid of 92% after eight hours and at the considerably lower temperature of 180 °C and 3.5 MPa air pressure was achieved, employing $Au/MgAl_2O_4$ as the catalyst, and starting from ethanol concentrations comparable to those obtained by fermentation (ca. 5 wt% aqueous

ethanol). Platinum and palladium, as traditional catalysts in this area, were compared to gold to show that a superior selectivity and conversion can be achieved using gold catalysis. At 180 °C, 3 MPa air pressure and after four hours, gold yielded 83% acetic acid, platinum 16% and palladium 60%. Moreover, gold catalysts exhibited a selectivity of 97%, whereas platinum and palladium gave only 82% and 93% respectively [134]. At higher ethanol concentrations (above 60%), the same catalytic reaction leads primarily to formation of ethyl acetate [135] and the reaction was shown to proceed via acetalaldehyde as intermediate.

6.2.2. Glycerol

Recently, the possibilities for oxidizing glycerol into valuable chemicals have received significant attention, and there are several recent reviews with entire sections devoted to this particular topic [136-138]. The market for glycerol oxidation products is not yet developed due to the current catalytic routes providing too low selectivities and yields. However, since many expect that glycerol will be widely (and inexpensively) available as a result of glycerol being a major waste product in the production of biodiesel by transesterification [136], there is a significant drive to develop new catalytic technologies. Glycerol possesses two (identical) primary alcohol functionalities and one secondary. Consequently, there exist a multitude of possible products from the oxidation reaction. Catalytic selectivity is therefore a central factor to consider in developing this chemistry. In fact, the nature of the metal, as well as the pH, largely controls the selectivity for converting either type of alcohol. The main products possible from glycerol oxidation are glyceric acid or glycerate depending on pH, dihydroxyacetone (DHA), and glyceraldehyde. Under acidic conditions, oxidation of glycerol usually leads to the formation of DHA (Scheme 7). In initial experiments performed at pH of 2-4, platinum on charcoal showed low catalytic activity for oxidation of the secondary hydroxy group of glycerol with a dihydroxyacetone yield of only 4% at a glycerol conversion of 37%. Several promoters were tried, including bismuth, tellurium, lead, tin, and selenium. On addition of bismuth (mass ratio of bismuth/platinum = 0.2), a drastic increase was seen in the DHA selectivity, which increased from 10% to 80% [139]. The bismuth addition decreases the conversion slightly, but the yield still increased from 4% to 20%.

Scheme 7

The selective oxidation of a 50% aqueous solution of glycerol was performed at 50 °C with an oxygen/glycerol ratio of 2, in a continuous fixed bed process using a Pt-Bi catalyst supported on charcoal. Here, a DHA selectivity of 80% at a conversion of 80% was obtained [140].
Under basic conditions, oxidation of glycerol mainly leads to the formation of glycerate (Scheme 8). By employing a 5 wt% Pd/C catalyst, the selectivity to glycerate can be as high as 70% at 100% conversion at pH=11 [141-142].

Scheme 8

During the last few years, significant attention has been devoted to the aerobic oxidation of glycerol using heterogeneous gold catalysts. Glycerol was oxidized to glycerate in the presence of NaOH with 100 % selectivity at 60 °C using water as the solvent, and at an oxygen pressure of 0.3 MPa. The catalysts used were either 1% Au/charcoal or 1% Au/graphite both giving around 55 % conversion [143]. A range of different supports for the gold nanoparticles catalysts were investigated, TiO_2, MgO, and Al_2O_3, but all showed low activity compared to Au/C. Depending on the base concentration and the reaction time, the selectivity of the Au/C catalyzed liquid phase glycerol oxidation could be controlled [144]. Most recently, it was shown that hydrogen peroxide is formed during oxidation of glycerol using gold catalysts [145] and that this leads to C-C bond breakage and a resulting loss of selectivity. This was independently supported by the fact the Au-Pd catalysts showed higher selectivity to glycerate than the monometallic Au catalyst, which was shown to be related to the higher efficiency of Pd to catalytically decompose the produced hydrogen peroxide in situ [146]. By employing a reaction temperature of 100 °C and an air pressure of 21 bar with methanol as the solvent, it is possible to obtain dimethyl mesoxalate in yields as high as 89% [147] and this clearly illustrates the effect of temperature on the degree of oxidation of the glycerol feedstock.

6.2.3. Glucose

Glucose can be selectively oxidized to a number of products. Currently, gluconic acid, glucuronic acid, glucaric acid and 2-keto-gluconic acid can be formed from such catalytic transformations. All these oxidations can be performed with air or oxygen, in an aqueous medium, under mild conditions and using a supported noble metal catalyst. Owing to the multifunctionality of glucose, the possibility of controlling the catalytic selectivity is again highly important. By use of Pt/C as the catalyst, the anomeric carbon atom of glucose is oxidized most readily, followed by the terminal primary alcohol moiety. The least oxidizable group is found to be the equatorial alcohol moieties [148-150]. A plausible mechanism of the reaction is that a dehydrogenation of glucose takes place to form gluconic acid and adsorbed hydrogen on the platinum surface. The hydrogen is then subsequently oxidized by oxygen to form water. This mechanism is supported by the observation that gluconic acid is formed even in the absence of oxygen in strongly basic solution and in the presence of the Pt catalyst [148-149]. The main product from the reaction of glucose is gluconic acid (Scheme 9). This represents one of the first examples where oxidation occurs solely by dehydrogenation, and thus it is clearly an attractive option with the only reagents required being simply water and hydroxide ions [151-152].

Scheme 9

Gluconic acid is found naturally in many fruits, in tea and in wine. Gluconic acid is also used as an additive, to regulate pH in food (E574). Currently, gluconic acid is produced industrially from glucose, using glucose oxidase enzymes. The market of gluconic acid is in the range of 60.000 t/year [153]. However, heterogeneous catalytic oxidation is also a viable method, and one under currently intense investigation. It has been debated whether the currently best heterogeneously catalyzed process is possibly better than the industrial biocatalytic process [154].

Oxidation is usually selective for the anomeric position, as mentioned previously. Thus when glucose is oxidized in the presence of supported metal catalysts, specifically Pd and Pt, gluconic acid is achieved in high yields, for example with 5% Pt/C, a 70% yield is obtained [155], or, also reported, complete conversion is seen with Pd/C after six hours [156]. However, when using palladium catalysts deactivation is observed at high

conversions. This problem can be alleviated using a modified palladium catalyst. Thus, a Pd-Bi/C catalyst was found to be capable of oxidizing glucose to gluconic acid with excellent selectivity (95-100%) at rates up to 20 times greater than that of the Pd/C catalyst [157-158]. An oxidative dehydrogenation mechanism is also proposed here [159].

The use of gold as a catalyst in the oxidation of glucose to gluconic acid has also been reported, on supports such as activated carbon, CeO_2, TiO_2, Fe_2O_3. Gold exhibits somewhat lower selectivity than the Pd-Bi/C catalyst, though. However, the activity of gold is strongly dependent on particle size, and it is less sensitive to low pH, being active even under acidic conditions [160-164]. In the aerobic oxidation of glucose over gold catalysts, hydrogen peroxide has been observed to be a reaction product, just as it was the case in the oxidation of glycerol [165]. Most recently, it has proved possible to achieve long-term stability (recycled 17 times without noticeable loss of activity) of an Au/TiO_2 catalyst in the oxidation of glucose at pH=9, and at temperature between 40 and 60 °C [166].

6.3. Oxidation Reactions involving Commodity Chemicals

6.3.1. 1,2-Propanediol and 1,3-Propanediol

1,2-propanediol and 1,3-propanediol can be obtained as hydrogenation products of glycerol. The first example of gold catalysts being able conduct aerobic oxidations of alcohols was provided by Prati and Rossi, who showed that 1,2-propanediol can be oxidized at about 80 °C in alkaline aqueous solution to yield lactate with a selectivity of 90-100% at 80-94% conversion using an Au/C catalyst [167]. Later, it was shown that similar results can be achieved using Au nanosols stabilized with poly(vinylalcohol) [168]. If the reaction is instead performed in methanol, it is only necessary to add a catalytic amount of base, and under these conditions 1,2-propanediol and 1,3-propanediol are oxidized to yield methyl lactate and methyl-3-hydroxypropionate, respectively. Methyl lactate can be formed with 71% selectivity at 99% conversion in the presence of 2 wt% Au/TiO_2. The reaction requires about 20 hours at 100 °C and with 2.5 MPa air pressure [147]. Similarly, methyl 3-hydroxypropionate can be produced with a somewhat higher selectivity of 85% at 99% conversion [147].

6.3.2 Acrolein

Acrylic acid and acrylate esters constitute an important group of chemicals in today's chemical indstry, for example, they are used to make water-based paints, solvent-based coatings and acrylic coatings. Typically, acrolein is obtained by catalytic oxidation of propene. However, acrolein can also be obtained from glycerol, and in this way it can be thought considered a renewable feedstock. Industrially, acrolein is oxidized to acrylic acid in a gas-phase process operated at temperatures above 350 °C employing mixed oxide catalysts [169]. Therefore, it is noteworthy that methyl acrylate can be produced from acrolein with 87% selectivity at 97% conversion in the presence of catalytic amounts of Au/ZnO, suspended in methanol, at room temperature and ambient pressure [170].

6.3.3. Glyceric Acid

The selectivity for the catalytic oxidation of glyceric acid, and the calcium salt, can be controlled by the nature of the catalyst, and the pH, in a similar way to that of glycerol as discussed above. In this way, it is possible to obtain products corresponding to the oxidation of the primary and secondary alcohol moieties, i.e., tartronic acid and hydroxypyruvic acid, respectively. As reported by Fordham et al., oxidation of glyceric acid under basic conditions leads to the formation of tartronic acid whereas hydroxypuric is afforded under acidic conditions [171]. The catalyst was suspended in glyceric acid, a calcium salt added, and oxygen gas bubbled through. NaOH was added to keep the pH constant. Two catalytic systems were tested; 5 wt% Pt/C at pH 10-11 yields tartronic acid with a selectivity of 60% at a conversion of 94%; when 2% of bismuth is added, the same product is obtained but with a selectivity of 83% at 90% conversion [171]. Hydroxypyruvic acid was obtained by aerobic oxidation of glyceric acid using a bismuth-promoted platinum catalyst under acidic conditions (pH 3–4) to give a 64% yield at 75% conversion [171]. After prolonged contact with the catalyst, tartronic acid was oxidized to oxalate whereas hydroxypyruvic acid was oxidised even more rapidly to glycolic acid.

6.3.3. Lactic Acid

Pyruvic acid and its derivatives are in increasing demand due to their use as precursors in the synthesis of drugs and agrochemicals [10]. It has proved difficult to obtain pyruvic acid directly from lactic acid via heterogeneous catalysis, because the major part of lactic acid is converted to form acetaldehyde and CO_2 by the oxidative C-C bond cleavage over most catalysts, e.g. V_2O_5- or MoO_3- based mixed oxide catalysts [172].
The vapor-phase oxidation of lactic acid with air was executed using an iron phosphate catalyst with a P/Fe atomic ratio of 1.2. It was found that lactic acid is selectively converted to form pyruvic acid by oxidative dehydrogenation. The one-pass yield reached 50 mol%; however, acetaldehyde, acetic acid, and CO_2 was still formed, and the pyruvic acid produced decomposes over time to give acetic acid and CO_2 [173].

Oxidation has also been tried over iron phosphates with a P/Fe atomic ratios of 1.2, including $FePO_4$, $Fe_2P_2O_7$ and $Fe_3(P_2O_7)_2$, at 230 °C. The catalysts containing both Fe^{2+} and Fe^{3+} performed better than those with just one oxidation state present. The best results were 62% selectivity at 60% conversion [174].

6.3.4. Furfural

Furfural is a commodity chemical that is readily available from dehydration of pentoses, and it can be produced in a very large scale if necessary. Furfural finds limited use today, though, which is reflected in its pricing being similar to the cheapest fossil bulk chemicals such as benzene and toluene [10]. In this way then, it can be seen that furfural could become a key feedstock in the future, especially given the new turn towards using bio-resources as a feedstock for chemicals when oil supplies become more and more insecure and/or expensive. Furoic acid is used as a feedstock in organic syntheses, and as an intermediate in the synthesis of perfumes and medicines. The oxidation of furfural to furoic acid is mainly described in patents, which discloses the use of various different catalysts including Ag_2O and Ag_2O/CuO mixtures. However, during the 1990s, the use of PbPt/C catalysts was also investigated [175]. Very recently, methyl furoate was synthesized using gold catalysis. Au/TiO_2 was suspended in a solution of furfural in methanol, a catalytic amount of sodium methoxide was added, and methyl furoate could be produced with 90% selectivity at more than 90% conversion [176].

6.3.5. 5-Hydroxymethyl Furfural

2,5-diformylfuran (DFF) is a furan derivative that has many uses, including use as a polymer building block [177-178]. By utilizing a platinum catalyst supported on carbon, and running the reaction in water at high temperatures, DFF is produced as the major product in neutral solution. If low temperatures and high pH are employed, 2,5-furandicarboxylic acid results [179].

2,5-furandicarboxylic acid (FDCA) is another furan derivative available from oxidation of HMF (Scheme 10). It holds a great promise in the polymers industry because it can potentially replace terephthalic acid, which is produced in a massive scale for making PET plastics [179-180]. HMF is converted to FDCA under strongly alkaline conditions, pH 12 or above, with oxygen gas bubbled through the alkaline system. Platinum, or platinum and a mixture of silver and copper oxides, preferably supported on carbon, were employed as catalysts.

Scheme 10

Oxidation of HMF was also attempted in situ directly from fructose, using a membrane reactor or encapsulating PtBi/C into a polymeric silicone matrix, and again, with air as the oxidant. However, the yield was never more than 25% [181]. A further attempt to obtain FDCA directly from fructose involved a one pot reaction in the presence of cobalt acetylacetonate encapsulated in sol–gel silica, at 155 °C and with 2 MPa of air pressure giving FDCA with 99% selectivity directly from fructose at a conversion of 72% [122].

HMMF can be obtained from HMF by oxidation with Au/TiO_2 (Scheme 11), under very mild conditions – 25 °C, 1 bar O_2 and 8 % NaOMe – in near quantitative yields. This is an intermediate on the route to FDMC, but the reaction can be stopped at this stage [176].

Scheme 11

Similarly to above, but at a higher temperature and pressure – 130 °C and 4 bar O_2 – 2,5-furan dimethyl furoate (FDMC), a direct analogue of FDMA, can be obtained in near quantitative yields from HMF [176]. It is possible that the formation of a diester directly, rather than a diacid, could save a further synthesis step on the route to polymerization.

6.3.6. Gluconic Acid

Glucaric acid can be furnished by the selective oxidation of the primary alcohol of gluconic acid with Pt-based catalysts [182]. Platinum is preferred over palladium due its greater selectivity for the oxidation of primary alcohols [183]. Low rates of oxidation of primary the alcohols is usually a complication, since products and byproducts bind more strongly to the platinum surface than the primary alcohol moiety and in effect poison the catalyst. Oxidation of secondary alcohols can also occur, leading to the formation of highly oxidized species such as oxalic acid, resulting in a poor selectivity towards gluraric acid. Gluconic acid was oxidized to glucaric acid with 55% selecticity at 97.2 % conversion, using a Pt/C catalyst [182,184].

When modifying the Pt catalyst by addition of bismuth or lead, a significant change in selectivity occurs. Oxidation of the primary terminal alcohol moiety in gluconic acid is no longer the dominating reaction. Instead oxidation of the α-hydroxy group, next to the carboxylic acid takes place, resulting in the formation of 2-keto gluconic acid with a 98% selectivity under slightly acidic conditions [184-185]. It has been proposed that the carboxylic acid coordinates to the promoter, as does the α-alcohol group, thus promoting the oxidation of the α-alcohol group [184]. This is supported by the reaction proceeding in a weakly acidic medium; when run in a basic medium, other products form and this is thought to be due to further coordination with the remaining alcohol groups [186].

7. Catalytic Hydrogenations

7.1. Introduction

Catalytic hydrogenation represents a set of reactions that will be extremely important in the production of value-added chemicals from biomass. Already now, they play a significant role in today's industry, and holds great promise for further developments. Here, selected examples of heterogeneously catalyzed hydrogenations of chemicals available from renewables resources are presented.

7.2. Hydrogenation Reactions involving Bio-resources and Primary Renewable Building Blocks

7.2.1. Cellulose

The hydrolysis of polysaccharides, e.g. starch, inulin, can also be combined with hydrogenation processes to yield polyols directly, in a one step process. A one-pot process was previously reported using a homogenous catalyst based on $Ru(TPPTS)_3$ [187], however, heterogeneous catalysis would be preferential in terms of the ease of recovery and re-use of the catalyst. In this way, a heterogeneous system was developed whereby ruthenium is supported on carbon, which is made acidic by treatment with different oxidizing agents, thereby catalyzing the hydrolysis part of the reaction. Selectivities to mannitol of 37-40% were achieved, which is in line with the yields from the non-coupled hydrolysis reaction, i.e. simply the hydrogenation reaction, from fructose to mannitol [188]. Cellulose, making up around 40-50% of biomass by weight makes it the largest component of biomass. Cellulose is a linear polysaccharide consisting of many thousands of glucose subunits. The glucose monomers are adjoined by 1-4-β glycosidic bonds, which can be hydrolysed by strong acids at high temperature. Direct hydrogenation of cellulose to sorbitol would be a highly desirable way to valorize biomass. The major complication in this strategy is the insolubility of cellulose in water. However, hydrogenation of cellulose to sorbitol has been achieved in superheated water (190 °C) using platinum and ruthenium on acidic supports [189]. The highest activity can be achieved using a 2.5% $Pt/\gamma\text{-}Al_2O_3$ catalyst which affords sorbitol in 25% yield and mannitol, resulting from epimerisation, is formed in 6% yield. The catalyst is reported to remain active after several runs. However, the maximum overall

yield is limited to 31%, which is attributed to the complex structure of cellulose that does not allow it to undergo complete hydrolysis under these conditions.

In a different study, the 1-4-β glucose dimer cellubiose was used as a model substrate for cellulose. Using a polymer supported ruthenium nanocluster catalyst; cellubiose was converted to sorbitol in a one-pot hydrolysis-hydrogenation reaction in 100% yield under acidic conditions using an ionic liquid solvent [190]. This procedure was found to result in a complicated separation of the sorbitol from the ionic liquid and catalyst. A modification to the procedure was reported recently, in which cellulose is hydrolyzed in superheated water (200-250 °C) and reduced using a carbon-supported ruthenium catalyst [191]. Cellulose conversion of 85% and 39% selectivity towards hexitols (sorbitol and mannitol) was achieved with a hydrogen pressure of 60 bar using this procedure.

7.2.2. Glycerol

Hydrogenation of glycerol to 1,2-propanediol or 1,3-propanediol has been reported using different metal catalysts including nickel, copper, copper-chromite, ruthenium, rhodium palladium and platinum [192-195]. For these reactions, the difficulties lie in achieving either diol with high selectivity. One method that has proven useful for producing 1,2-propanediol selectively is to carry out the hydrogenation reaction in the presence of an ion-exchange resin in addition to a hydrogenation catalyst containing Ru [193-196]. In this approach, the ion-exchange resins functions as a dehydration catalyst which presumably facilitates the dehydration of glycerol to hydroxyacetone, that is subsequently hydrogenated into 1,2-propanediol.

7.2.3. Glucose

Catalytic hydrogenation of glucose leads to the formation of sorbitol (Scheme 12). Typically, Raney nickel is used to catalyze the reaction [197], however, several other catalysts including platinum and ruthenium have been reported to be active for the reaction, and in many cases these catalysts are more effective than standard Raney nickel, which can be problematic due to leaching of nickel [197-200]. Very recently, an impressive yield of more than 99.5% sorbitol was obtained using Pt supported on

microporous activated carbon cloth [198]. The experiments were conducted at 100 °C using a 40 wt% aqueous solution of glucose in a 300 ml stirred autoclave pressurized to a hydrogen pressure of 80 bar. The high selectivity towards sorbitol exhibited by the catalyst was attributed to fast desorption of sorbitol from the catalyst surface, which effectively lowers sorbitol epimerization and thus suppresses the formation of mannitol.

Scheme 12

7.2.4. Xylose and Fructose

Xylose can be hydrogenated into xylitol (Scheme 13). This reaction was reported using hydrogenation catalysts such as Raney nickel as well as platinum group metal catalysts [201-202].

Scheme 13

Raney nickel, copper and platinum group metal catalysts have also been used as catalysts for transforming fructose into mannitol via catalytic hydrogenation (Scheme 14) [197-199,203-204]. Ruthenium supported on carbon is among the most studied catalysts for this reaction [205], and it is, in fact, also effective for the combined hydrolysis-hydrogenation of inulin to mannitol when the carbon support has been made acidic prior to the catalytic experiments [188]. The bifunctional catalyst applied in the study was made by pre-oxidizing activated carbon (SX1G) with various oxidants such as nitric acid and ammonium persulfate and then introducing Ru onto this support by incipient wetness impregnation followed by reduction with $NaBH_4$. The oxidized carbon catalyzes the hydrolysis of inulin to a mixture of glucose and fructose which is subsequently hydrogenated to a mixture of glucitol and mannitol. Increasing the hydrogen pressure (up to 100 bar) apparently also increases the rate of hydrolysis dramatically.

Scheme 14

7.3. Hydrogenation Reactions involving Commodity Chemicals

7.3.1 3-Hydroxypropanal

3-Hydroxypropanal can be formed by fermentation of glucose and is thus an attractive starting material for production of 1,3-propanediol, which can be polymerized with *tere*-phthalic acid to produce polytrimethylene terephthalate (PTT). PTT is used in the fibers industry in the production of stain resistant carpets etc.

Aqueous solutions of 3-hydroxypropanal were reduced using TiO_2 supported ruthenium catalysts at 40-60 °C using 40 bar of hydrogen [206]. The most stable catalysts were found to be ruthenium catalysts supported on low surface area macroporous rutile.

7.3.2 Lactic acid

Propylene glycol (1,2-propanediol) can be employed as a de-icing agent replacing ethylene glycol, which is currently produced from fossil resources. Furthermore, propylene glycol is a safe alternative to ethylene glycol, which is toxic to humans due to its metabolism to oxalic acid.

Hydrogenation of lactic acid represents a simple route from a biomass chemical to propylene glycol. Lactic acid has been hydrogenated in the vapor phase using a Cu/SiO_2 catalyst at 140-220 °C with a hydrogen pressure of 0.1-0.72 MPa. The selectivity of 1,2-propanediol was 88% at full conversion, with 2-hydroxypropionaldehyde and propionic acid formed as the major by-products [207]. In a different study, aqueous phase hydrogenation of lactic acid was achieved using a carbon supported ruthenium catalyst. The hydrogenation is operated at temperatures from 100-170 °C with a hydrogen pressure of 7-14 MPa resulting in the formation of 1,2-propanediol in 90% selectivity at 95% conversion [208]. Disappointingly though, hydrogenation of salts of lactic acid did not result in the formation of 1,2-propandiol. Hydrogenation has also been carried out using a magnesia supported poly-γ-aminopropysiloxane-ruthenium complex in aqueous solution at 240 °C and 5 MPa hydrogen pressure for 18 hours, giving 100% yield of 1,2-propandiol, with no apparent deactivation of the catalyst [209].

7.3.3. Furfural

Furfural is readily obtainable from dehydration of pentoses. Reduction of furfural can lead to a variety of products that are more volatile, more stable and possibly also more useful than furfural itself. Selective reduction of the aldehyde moiety leads to furfuryl

alcohol (Scheme 15), whereas further reduction of the furan core will lead to tetrahydrofurfuryl alcohol. Reductive deoxygenation can result in the formation of either 2-methylfuran or 2-methyltetrahydrofuran, which can be used as liquid fuels or solvents.

Scheme 15

Furfuryl alcohol has traditionally been obtained from furfural by hydrogenation with copper containing catalysts, e.g. copper-barium-chromium oxide, copper oxide supported on silica or alumina, copper-chromium oxide and copper-cobalt oxide on silica yields furfuryl alcohol as the major product [210]. Due to its toxicity, attempts have been made to eliminate chromium from such catalytic systems, especially due to new restrictions that prevent used copper chromite catalysts from being deposited in landfill sites [211]. In recent years, several new catalytic systems have been demonstrated to successfully catalyze the hydrogenation of furfural to furfuryl alcohol. Copper has been investigated as a catalyst for this reaction on its own. Furfural hydrogenation over copper dispersed on three forms of carbon – activated carbon, diamond and graphitized fibers – was studied. Similar to other copper-containing catalysts, only products corresponding to hydrogenation of the carbonyl bond were detected, and the selectivity to furfuryl alcohol was comparable to that obtained with commercial copper chromite catalysts [212]. Copper supported on magnesium oxide has also been prepared, via the coprecipitation method, giving a 98% selectivity of furfuryl alcohol at 98% conversion of furfural. This is attributed to the higher number of surface copper sites and the defective sites at the copper and magnesium oxide interfacial region. Similarly, Cu-Ca/SiO_2 catalysts revealed a selectivity of 98% in the gas phase hydrogenation of furfural to furfuryl alcohol at a conversion of 98% and a temperature of 130 °C [213]. Various other catalytic systems have recently been used to promote hydrogenation, including a molybdenum doped cobalt-boron amorphous catalyst exhibiting excellent activity and nearly 100% selectivity to furfuryl alcohol during liquid phase hydrogenation of furfural, at 100 °C and 1 MPa hydrogen pressure [214].
Reduction of the alcohol group to produce 2-methyl furan can be achieved using a commercial Cu/Zn/Al/Ca/Na catalyst with the atomic ratio 59:33:6:1:1. This catalyst

was found to achieve 99.7% conversion with 87.0% selectivity to 2-methyl fural at 250 °C. Hydrogenation from furfuryl alcohol yields a slightly higher selectivity of 92.7% at 98.1% conversion under similar conditions [215].

7.3.5. Levulinic acid

Hydrogenation of levulinic acid resulting in the reduction of the ketone moiety leads to 4-hydroxy pentanoic acid. This acid can cyclize to form γ-valerolactone (GVL) which is a useful industrial solvent. A 94% yield of GVL was obtained with a Raney nickel catalyst, and a hydrogen pressure of 5 MPa at a temperature of 100-150 °C [216].

1,4-Pentanediol (PDO) holds promise for being used in the synthesis of polyesters. It has been synthesized from GVL in the presence of a copper chromite catalyst. At 150 °C and 20.3–30.4 MPa hydrogen pressure, 78.5% PDO was produced together with 8.1% 1-pentanol [217].

7.3.6. 5-Hydroxymethylfurfural

2,5-di(hydroxymethyl)furan can be synthesized from 5-HMF via hydrogenation (Scheme 16). Under a hydrogen pressure of 7 MPa at 140 °C in the presence of platinum or copper catalysts, practically quantitative yields of 2,5-di(hydroxymethyl)furan can be obtained [218]. However, under similar conditions but with palladium or nickel as catalyst, hydrogenation of the ring system occurs so that 2,5-di(hydroxymethyl)-tetrahydrofuran is obtained as the predominant product.

Scheme 16

8. Summary and Outlook

From a chemical perspective, renewable feedstocks being highly functionalized molecules are very different from fossil feedstocks that are generally unfunctionalized. Therefore, the challenge in converting fossil resources, in particular crude oil, into useful products has been to develop methods that allow *controlled addition* of desirable chemical functionality to the hydrocarbon feedstock. Due to the quite low reactivity of the hydrocarbons; it has been possible to develop efficient catalytic processes that operate satisfactorily at relatively high temperatures and pressures. Here, heterogeneous catalysis has proven most successful and therefore played a dominant role in chemical industry. The challenge of converting renewable feedstocks into useful chemicals is very different. Still the desirable transformations are entirely dependent on catalysis, but now it is often a question of *controlled removal* of superfluous chemical functionality under sufficiently mild conditions to prevent uncontrolled degradation of the renewable feedstock. So far, most emphasis has been on using biocatalytic processes to facilitate these transformations but it appears likely that heterogeneous catalysis could also play a significant role in the future valorization of renewables. Since the conversion of bio-resources into the primary renewable building blocks is typically achieved using biocatalytic processes operating in water as the natural solvent, it seems likely that there will be a significant drive to develop heterogeneous catalysts that also operate in water, and preferably at low temperatures. In this way, it will be possible to achieve maximum process integration between the biocatalytic processes and the heterogeneously catalyzed processes. This integration will lead to lower costs of the resulting products since the need for expensive unit operations, especially separations, will be minimized. Clearly, it represents a significant challenge to discover and develop heterogeneous catalysts that exhibit sufficient activity and selectivity under these conditions but it seems likely that this will be one of the new directions that heterogeneous catalysis will take during the next decade. The progress made in this endeavor will obviously determine how large a role heterogeneous catalysis will eventually play in the production of value-added chemicals from biomass. Here, we have shown that there are several reaction types where heterogeneous catalysis already offers some very promising opportunities but that there clearly exists a great need for further discoveries and developments in this emerging field.

References

[1] C. H. Christensen, J. K., Nørskov, J. Chem. Phys. **2008**, in press

[2] S. Shaik, *Angew. Chem. Int. Ed.* **2003**, *42*, 3208

[3] S. Senkan, *Angew. Chem. Int. Ed*. **2001**, *40*, 312

[4] I. Maxwell, *Stud. Surf. Sci. Catal.* **1996,** *101*, 1

[5] Handbook of Heterogeneous Catalysis (Eds. G. Ertl, H. Knözinger, F. Schüth, J. Weitkamp), Wiley-VCH, Weinheim, **2008**.

[6] B. A. Tokay, *Biomass Chemicals*, in Ullmann's Encyclopedia of Industrial Chemistry, Wiley-VCH, Weinheim, **2005**.

[7] C. H. Christensen, J. Rass-Hansen, C. C. Marsden, E. Taarning, K. Egeblad, ChemSusChem. **2008**, in press.

[8] J. Goldemberg, *Science* **2007**, *315*, 808

[9] G. W. Huber, S. Iborra, A. Corma, *Chem. Rev.* **2006**, *106*, 4044

[10] A. Corma, S. Iborra, A. Velty, *Chem. Rev.* **2007**, *107*, 2411

[11] A. J. Ragauskas, C. K. Williams, B. H. Davison, G. Britovsek, J. Cairney, C. A. Eckert, W. J. Frederick Jr., J. P. Hallett, D. J. Leak, C. L. Liotta, J. R. Mielenz, R. Murphy, R. Templer, T. Tschaplinski, *Science* **2006**, *311*, 484

[12] D. R. Dodds, R. A. Gross, *Science* **2007**, *318*, 1250.

[13] P. Mäki-Arbela, B. Holmbom, T. Salmi, D. Y. Murzin, *Catal. Rev. Sci. Eng.* **2007**, *49*, 197.

[14] T. Werpy, G. Petersen, Eds., Top Value Added Chemicals From Biomass, Volume 1—Results of Screening for Potential Candidates from Sugars and Synthesis Gas (U.S. Department of Energy, Oak Ridge, TN, August 2004; available at www.eere.energy.gov/biomass/pdfs/35523.pdf).

[15] Biorefineries – Industrial Processes and Products (Eds. B. Kamm, P. R. Gruber, M. Kamm), Wiley-VCH, Weinheim, **2005**.

[16] B. O. Palsson, S. Fathi-Afshar, F. F. Rudd, E. N. Lightfoot, *Science* **1980**, *213*, 513.

[17] E. S. Lipinsky, *Science* **1981**, *212*, 1465.

[18] B. Kamm, *Angew. Chem. Int. Ed.* **2007**, *46*, 5056.

[19] J. Rass-Hansen, H. Falsig, B. Jørgensen, C.H. Christensen, *J. Chem. Technol. Biotechnol.* **2007**, *82*, 329.

[20] F. W. Lichtenhaler, S. Peters, *C. R. Chimia* **2004**, *7*, 65.

[21] P. Gallezot, *Catal. Today* **2007**, *121*, 76

[22] P. Gallezot, *Green Chem.* **2007**, *9*, 295

[23] M. A. Paisley, *Biomass Energy*, in Kirk-Othmer Encyclopedia of Chemical Technology, Wiley VCH, Weinheim, **2003**

[24] Milne et al 1998 _ NREL/TP-570-25357

[25] Dayton 2002_Nrel/TP-510-32815

[26] D. Sutton, B. Kelleher, J.R.H. Ross, *Fuel Process. Technol.* **2001**, *73*, 155

[27] D. L. Klass, *Biomass for Renewable Energy, Fuels, and Chemicals*, Academic Press. San Diego, **1998**

[28] R. D. Cortright, R. R. Davda, J. A. Dumesic, *Nature* **2002**, *418*, 964

[29] G. W. Huber, J. W. Shabaker, J. A. Dumesic, *Science* **2003**, *300*, 2075

[30] G. W. Huber, R. D. Cortright, J. A. Dumesic, *Angew. Chem. Int. Ed.* **2004**, *43*, 1549

[31] R. R. Davda, J. W. Shabaker, G. W. Huber, R. D. Cortright, J.A. Dumesic, *Appl. Catal. B*, **2005**, *56*, 171

[32] G. W. Huber, J. N. Chheda, C. J. Barrett, J. A. Dumesic, *Science* **2005**, *308*, 1446

[33] M. B. Valenzuela, C. W. Jones, P. K. Agrawal, *Energy Fuels* **2006**, *20*, 1744

[34] P. B. Weisz, W. O. Haag, P. G. Rodewald, *Science* **1979**, *206*, 57

[35] P. E. Nielsen, H. Nishimura, J. W. Otvos, M. Calvin, *Science* **1977**, *198*, 942

[36] R. K. Sharma, N. N. Bakhshi, *Biomass Bioenergy* **1993**, *5(6)*, 445

[37] A. G. Gayubo, A. T. Aguayo, A. Atutxa, R. Aguado, J. Bilbao, *Ind. Eng. Chem. Res.*, **2004**, *43*, 2610

[38] A. Corma, G. W. Huber, L. Sauvanaud, P. O'Connor, *J. Catal.*, **2007**, *247*, 307

[39] G. W. Huber, A. Corma, *Angew. Chem. Int. Ed.*, **2007**, *46*, 7184

[40] N.Y. Chen, T.F. Degnan Jr., L.R. Koenig. *Chemtech* **1986**, *August*, 506

[41] D. C. Elliott, D. Beckman, A. V. Bridgwater, J. P. Diebold, S. B. Gevert, Y. Solantausta, *Energy Fuels* **1991**, *5*, 399

[42] A. Haryanto, S. Fernando, N. Murali, S. Adhikari, *Energy Fuels* **2005**, *19*, 2098

[43] P. D. Vaidya, A. E. Rodrigues, *Chem. Eng. J.* **2006**, *117*, 39

[44] M. Ni, D. Y. C. Leung, M. K. H. Leung, *Int. J. Hydrogen Energy* **2007**, *32*, 3238

[45] A. Behr, J. Eilting, K. Irawadi, J. Leschinski, F. Lindner, *Green Chem.* **2008**, *10*, 13

[46] S. Adhikari, S. Fernando, A. Haryanto, *Energy Fuels* **2007**, *21*, 2306

[47] D. Wang, S. Czernik, D. Montané, M. Mann, E. Chornet, *Ind. Eng. Chem. Res.* **1997**, *36*, 1507

[48] S. Czernik, R. Evans, R. French, *Catal. Today* **2007**, *129*, 265

[49] J. R. Rostrup-Nielsen, J. Sehested, J. K. Nørskov, *Adv. Catal.* **2002**, *47*, 65

[50] J. Rass-Hansen, C. H. Christensen, J. Sehested, S. Helveg, J. R. Rostrup-Nielsen, S. Dahl, *Green Chem.* **2007**, *9*, 1016

[51] G. A. Deluga, J. R. Salge, L. D. Schmidt, X. E. Verykios, *Science* **2004**, *303*, 993

[52] P. Lejemble, A. Gaset, P. Kalck, *Biomass* **1984**, *4*, 263

[53] H. E. Hoydonckx, W. M. Van Rhijn, W. Van Rihjn, D. E. De Vos, P. A. Jacobs, *Furfural and Derivatives*, in Ullmann's Encyclopedia of Industrial Chemistry, Wiley-VCH, Weinheim, **2007**.

[54] K. J. Jung, A. Gaset, *Biomass* **1988**, *16*, 89

[55] R. A.. Schraufnagel, H. F. Rase, *Ind. Eng. Chem. Prod. Res. Dev.* **1975**, *14*, 40

[56] J. Jow, G. L. Rorrer, M. C. Hawley, D. T. A. Lamport, *Biomass* **1987**, *14*, 185.

[57] K. Lourvanij, G. L. Rorrer, *Ind. Eng. Chem. Res.* **1993**, *32*, 11.

[58] K. Lourvanij, G. L. Rorrer, *Appl. Catal. A* **1994**, *109*, 147.

[59] C. Montassier, J. C. Ménézo, L. C. Hoang, C. Renaud, J. Barbier, *J. Mol. Catal.*, **1991**, *70*, 99

[60] C. Montassier, J. M. Dumas, P. Granger, J. Barbier, *Appl. Catal. A* **1995**, *121*, 231

[61] J. Feng, H. Fu, J. Wang, R. Li, H. Chen, X. Li, *Catal. Comm.* **2008**, *9*, 1458

[62] B. Blanc, A. Bourrel, P. Gallezot, T. Haas, P. Taylor, *Green Chem.* **2000**, *2*, 89

[63] www.polyolchem.com

[64] T. Brix, BBI Conference, Portland, 9-11 October, 2007

[65] B. Satyanarayana, Y. B. G. Varma, *Indian J. Technol.* **1970**, *8*, 58

[66] A. Masroua, A. Revillon, J. C. Martin, A. Guyot, G. Descotes, *Bull. Soc. Chim.* **1988**, 561

[67] G. Siegers, F. Martinola, *Int. Sugar. J.* **1985**, *87*, 23

[68] C. Buttersack, *React. Polymers* **1989**, *10*, 143

[69] T. Mizota, S. Tsuneda, K. Saito, T. Sugo, *Ind. Eng. Chem. Res.* **1994**, *33*, 2215

[70] T. Yoshioka, M. Shimamura, *Bull. Chem. Soc. Jpn.* **1984**, *57*, 334

[71] M. M. Nasef, H. Saidi, M. M. Senna, *Chem. Eng. J.*, **2005**, *108*, 13

[72] P. L. Dhepe, M. Ohashi, S. Inagaki, M. Ichikawa, A. Fukuoka, *Catal. Lett.* **2005**, *102*, 163

[73] C. Buttersack, D. Laketic, *J. Mol. Catal.* **1994**, L283

[74] C. Moreau, R. Durand, F. Aliès, M. Cotillon, T. Frutz, M. Théoleyre, *Ind. Crops Prod.* **2000**, *11*, 237

[75] A. Abbadi, K. F. Gotlieb, H. van Bekkum, *Starch/Stärke* **1998**, *50*, 23

[76] J. A. Bootsma, B. H. Shanks, *Appl. Catal. A* **2007**, *327*, 44

[77] C. J. Yow, K. Y. Liew, *J. Am. Oil Chem. Soc.* **1999**, *76*, 529

[78] C. J. Yow, K. Y. Liew, *J. Am. Oil Chem. Soc.* **2002**, *79*, 357

[79] P. L. Dhepe, M. Ohashi, S. Inagaki, M. Ichikawa, A. Fukuoka, *Catal. Lett.* **2005**, *102*, 163

[80] M. D. Serio, M. Ledda, M. Cozzolino, G. Minutillo, R. Tesser, E. Santacesaria, *Ind. Eng. Chem. Res.* **2006**, *45*, 3009

[81] M. D. Serio, M. Cozzolino, M. Giodano, R. Tesser, P. Patrono, E. Santacesaria, *Ind. Eng. Chem. Res.* **2007** *46*, 6379

[82] W. Xe, H. Pong, L. Chen, *Appl. Catal. A* **2006**, *300*, 67

[83] C. Lingfeng, X. Guomin, X. Bo, T. Guangyuan, *Energy Fuels* **2007**, *21*, 3740

[84] Y. Liu, E. Lotero, J. G. Goodwin Jr., X. Mo, *Appl. Catal. A* **2007**, *331*, 138

[85] S. Lee, A. Sardesai. *Top. Catal.* **2005**, *32*, 197.

[86] J. Rostrup-Nielsen, *Proceedings of the World Petroleum Congress* **1998**, *2*, 767.

[87] J. J. Spivey, *Chem. Eng. Commun.* **1991**, *110*, 123.

[88] Y.C. Hu, Hydrocarbon Processing **1983**, april issue, 113.

[89] Y.C. Hu, Hydrocarbon Processing **1983**, may issue, 88.

[90] J. Schulz, F. Bandermann. *Chem. Eng. Technol.* **1994**, *17*, 179.

[91] W.J. Toussaint, J.T. Dunn, D.R. Jackson, *Ind. Eng. Chem.* **1947**, february issue, 121.

[92] Organic Syntheses **1941**, Coll. Vol. 1, p.15

[93] E. Tsukuda, S. Sato, R. Takahashi, T. Sodesawa, *Catal. Comm.* **2007**, *8*, 1349

[94] S.-H. Chai, H.-P. Wang, Y. Liang, B.-Q. Xu, *J. Catal.* **2007**, *250*, 342

[95] S.-H. Chai, H.-P. Wang, Y. Liang, B.-Q. Xu, *Green Chem.* **2007**, *9*, 1130

[96] C.-W. Chiu, M. A. Dasari, G. J. Suppes, *AIChE Journal* **2006**, *52*, 3543

[97] C. Moreau, R. Durand, D. Peyron, J. Duhamet, P. Rivalier, *Ind. Crops Prod.* **1998**, *7*, 95

[98] A. S. Dias, M. Pillinger, A. A. Valente, *J. Catal.* **2005**, *229*, 414

[99] A. S. Dias, M. Pillinger, A. A. Valente, *Appl. Catal. A* **2005**, *285*, 126

[100] A. S. Dias, S. Lima, M. Pillinger, A. A. Valente, *Carbohydrate Res.* **2006**, *341*, 2946

[101] A. S. Dias, M. Pillinger, A. A. Valente, *Micropor. Mesopor. Mater.* **2006**, *94*, 214

[102] A. S. Dias, S. Lima, P. Brandao, M. Pillinger, J. Rocha, A. A. Valente, *Catal. Lett.* **2006**, *108*, 179.

[103] A. S. Dias, S. Lima, D. Carriazo, V. Rives, M. Pillinger, *J. Catal.* **2006**, *244*, 230

[104] M. Bicker, J. Hirth, H. Vogel, *Green Chem.* **2003**, *5*, 280.

[105] L. Cottier, G. Descotes, *Trends Heterocycl. Chem* **1991**, *2*, 233.

[106] J. Lewkowski, *Arkivoc* **2001**, *i*, 17.

[107] Y. Román-Leshkov, J. N. Chheda, J. A. Dumesic, *Science* **2006**, *312*, 1933.

[108] C. Moreau, R. Durand, S. Razigade, J. Duhamet, P. Faugeras, P. Rivalier, P. Ros, G. Avignon, *Appl. Catal. A-General* **1996**, *145*, 211

[109] P. Rivalier, J. Duhamet, C. Moreau, R. Durand, *Catal. Today* **1995**, *24*, 165.

[110] Y. Nakamura, S. Morikawa, *Bull. Chem. Soc. Jpn.* **1980**, *53*, 3705.

[111] C. Lansalot-Matras, C. Moreau, *Catal. Commun.* **2003**, *4*, 517.

[112] Q. Bao, K. Qiao, D. Tomida, C. Yokoyama, *Catal. Comm.* **2008**, *9*, 1383

[113] C. Carlini, P. Patrono, P. Raspolli, A. M. Galletti, G. Sbrana, *Appl. Catal. A* **2004**, *275*, 111

[114] F. Benvenuti, C. Carlini, P. Patrono, P. Raspolli, A. M. Galletti, G. Sbrana, M. A. Massucci, P. Galli, *Appl. Catal. A* **2000**, *193*, 147

[115] C. Carlini, M. Giuttari, A. M. R. Galletti, G. Sbrana, T. Armaroli, G. Busca, *Appl. Catal. A-General* **1999**, *183*, 295.

[116] T. Armaroli, G. Busca, C. Carlini, M Giuttari, A. M. R. Galletti, G. Sbrana, *J. Mol. Catal. A* **2000**, *151*, 233

[117] P. Carniti, A. Gervasini, S. Biella, A. Auroux, *Catal. Today* **2006**, *118*, 373

[118] F. S. Ashgari, H. Yoshida, *Carbohydrate Res.* **2006**, *341*, 2379

[119] M. Watanabe, Y. Aizawa, T. Iida, R. Nishimura, H. Inomata, *Appl. Catal. A* **2005**, *295*, 150.

[120] M. Watanabe, Y. Aizawa, T. Iida, T.M. Aida, C. Levy, K. Sue, H. Inomata, *Carbohydrate Research* **2005**, *340*, 1925

[121] M. Kröger, U. Prüsse, K.-D. Vorlop, *Top. Catal.* **2000**, *13*, 237

[122] M. L. Ribeiro, U. Schuchardt, *Catal. Commun.* **2003**, *4*, 83

[123] S. Sato, R. Takahashi, T. Sodesawa, N. Honda, H. Shimizu, *Catal. Comm.* **2003**, *4*, 77

[124] S. Sato, R. Takahashi, T. Sodesawa, N. Honda, *J. Mol. Catal. A* **2004**, *221*, 177

[125] C. R. Reddy, P. Iyengar, G. Nagendrappa, B. S. J. Prakasha, *J. Mol. Catal. A* **2005**, *229*, 31

[126] C. R. Reddy, P. Iyengar, G. Nagendrappa, B. S. J. Prakash, *Catal. Lett.* **2005**, *101*, 87.

[127] M. L. Kantam, V. Bhaskar, B. M. Choudary, *Catal. Lett.* **2002**, *78*, 185.

[128] V. L. Budarin, J. H. Clark, R. Luque, D. J. Macquarrie, *Chem. Commun.* **2007**, 634

[129] V. Budarin, R. Luque, D. J. Macquarrie, J. H. Clark, *Chem. Eur. J.* **2007**, *13*, 6914

[130] W. M. Van Rhijn, D.E. De Vos, B.F. Sels, W.D. Bossaert, P.A. Jacobs, *Chem. Commun.* **1998**, 317.

[131] E. C. Alyea, K. F. Brown, L. Durham, I. Svazic, *Stud. Surf. Sci. Catal.* **1992**, *73*, 309

[132] P. A. Awasarkar, A. Y. Sonsale, A. K. Chatterjee, *React. Kinet. Catal. Lett.* **1988**, *36*, 301

[133] X. Li, E. Iglesia, *Chem. Eur. J.* **2007**, *13*, 9324

[134] C. H. Christensen, B. Jørgensen, J. Rass-Hansen, K. Egeblad, Kresten, R. Madsen, S. K. Klitgaard, S. M. Hansen, M. R. Hansen, H. C. Andersen, A. Riisager, *Angew. Chem. Int. Ed.* **2006**, *45*, 4648

[135] B. Jørgensen, S. E. Christiansen, M. L. D. Thomsen, C. H. Christensen, *J. Catal.* **2007**, *251*, 332

[136] C.-H. Zhou, J. N. Beltramini, Y.-X. Fan, G. Q. Lu, *Chem. Soc. Rev.* **2008**, *37*, 527

[137] D. T. Johnson, K. A. Taconi, *Environmental Progress* **2007**, *26*, 338

[138] M. Pagliaro, R. Ciriminna, H. Kimura, M. Rossi, C. D. Pina, *Angew. Chem. Int. Ed.* **2007**, *46*, 4434

[139] H. Kimura, K. Tsuto, T. Wakisaka, Y. Kazumi, Y. Inaya, *Appl. Catal. A* **1993**, *96*, 217

[140] H. Kimura, *Appl. Catal. A* **1993**, *105*, 147

[141] R. Garcia,M. Besson, P. Gallezot, *Appl. Catal. A* **1995**, *127*, 165

[142] N. Dimitratos, J. A. Lopez-Sanchez, D. Lennon, F. Porta, L. Prati, A. Villa, *Catal. Lett.* **2006**, *108*, 147

[143] S. Carrettin, P. McMorn, P. Johnston, K. Griffin, G. J. Hutchings, G. J. *Chem. Commun.* **2002**, 696

[144] S. Demirel-Guelen, M. Lucas, P. Claus, *Catal. Today* **2005**, *102*, 166

[145] W. C. Ketchie, M. Murayama, R. J. Davis, *Top. Catal.* **2007**, *44*, 307

[146] W. C. Ketchie, M. Murayama, R. J. Davis, *J. Catal.* **2007**, *250*, 264

[147] E. Taarning, R. Madsen, J. M. Marchetti, K. Egeblad, C. H. Christensen, *Green Chem.* **2008**, *10*, 408

[148] K. Heyns, H. Paulsen, *Angew. Chem.* **1957**, *69*, 600

[149] K. Heyns, H. Paulsen, *Adv. Carbohydr. Chem.* **1962**, *17*, 169

[150] K. Heyns, W. D. Soldat, P. Koll, *Chem. Ber.* **1975**, *108*, 3619

[151] G. Dewit, J. J. Devlieger, A. C. Kockvandalen, R. Heus, R. Laroy, A. J. Vanhengstum, A. P. G. Kieboom, H. Van Bekkum, *Carbohydr. Res.* **1981**, *91*, 125

[152] G. D. Wit, J. J. D. Vlieger, A. C. Kockvandalen, A. P. G. Kieboom, H. Van Bekkum, *Tetrahedron Lett.* **1978**, 1327

[153] F. W. Lichtenthaler, *Acc. Chem. Res.* **2002**, *35*, 728

[154] M. Comotti, C. D. Pina, E. Falletta, M. Rossi, *J. Catal.* **2006**, *244*, 122

[155] P. Gallezot, *Catal. Today* **1997**, *37*, 405

[156] M. Besson, P. Gallezot, F. Lahmer, G. Fleche, P. Fuertes, In *Catalysis of Organic Reactions*; Kosak, J. R., Johnson, T. A., Eds.; Marcel Dekker: New York, 1993; Vol. 53, pp 169-180

[157] A. Abbadi, H. Van Bekkum, *J. Mol. Catal. A* **1995**, *97*, 111

[158] S. Karski, I. Witonska, J. Goluchowska, *J. Mol. Catal. A* **2005**, *245*, 225

[159] M. Besson, F. Lahmer, P. Gallezot, P. Fuertes, G. Fleche, *J. Catal.* **1995**, *152*, 116

[160] A. Abbadi, M. Makkee, W. Visscher, J. A. R. Vanveen, H. Van Bekkum, *J. Carbohydr. Chem.* **1993**, *12*, 573

[161] A. Abad, P. Concepcion, A. Corma, H. Garcia, *Angew. Chem. Int. Ed.* **2005**, *44*, 4066

[162] A. Corma, P. Serna, *Science* **2006**, *313*, 332

[163] A. Mirescu, U. Prusse, *Catal. Commun.* **2006**, *7*, 11

[164] S. Biella, L. Prati and M. Rossi, *J. Catal.*, **2002**, 206, 242

[165] M. Comotti, C. D. Pina, E. Falletta, M. Rossi, *Adv. Synth. Catal.* **2006**, *348*, 313

[166] A. Mirescu, H. Berndt, A. Martin, U. Prüsse, *Appl. Catal. A* **2007**, *317*, 204

[167] L. Prati, M. Rossi, *J. Catal.* **1998**, *176*, 552

[168] P. G. N. Mertens, M. Bulut, L. E. M. Gevers, I. F. J. Vankelecom, P. A. Jacobs, D. E. De Vos, *Catal. Lett.* **2005**, *102*, 57

[169] T. V. Andrushkevich, *Catal. Rev. Sci. Eng.* **1993**, *35*, 213

[170] C. Marsden, E. Taarning, D. Hansen, L. Johansen, S. K. Klitgaard, K. Egeblad, C. H. Christensen, *Green Chem.*, **2008**, *10*, 168.

[171] P. Fordham, M. Besson, P. Gallezot, *Appl. Catal. A* **1995**, *133*, L179

[172] S. Sugiyama, N. Shigemoto, N. Masaoka, S. Suetoh, H. Kawami, K. Miyaura and H. Hayashi, *Bull. Chem. Soc. Jpn.*, **1993**, *66*, 1542

[173] M. Ai, K. Ohdan, *Appl. Catal. A* **1997**, *150*, 13

[174] M. Ai, K. Ohdan, *Appl. Catal.* **1997**, *165*, 461

[175] P. Verdegeur, N. Merat, A. Gaset, *Appl. Catal. A* **1994**, *112*, 1

[176] E. Taarning, I. Nielsen, K. Egeblad, R. Madsen, C. H. Christensen, *ChemSusChem* **2008**, *1*, 75

[177] A. Gandini, M. N. Belgacem, *Prog. Polym. Sci.* **1997**, *22*, 1203

[178] F. W. Lichtenthaler, S. Nishiyama, T. Weiner, *Liebigs Ann.* **1989**, 1163

[179] F. W. Lichtenthaler, U. Kraska, *Carbohydr. Res.* **1977**, *58*, 363

[180] C. Moreau, M. N. Belgacem, A. Gandini, *Top. Catal.* **2004**, *27*, 11

[181] M. Kroger, U. Prusse,K. D. Vorlop, *Top. Catal.* **2000**, *13*, 237

[182] M. Besson, G. Fleche, P. Fuertes, P. Gallezot, F. Lahmer, *Recl. Tra*v. *Chim. Pays-Bas* **1996**, *115*, 217

[183] A. W. Heinen, J. A. Peters, H. Van Bekkum, *Carbohydr. Res.* **1997**, *304*, 155

[184] P. C. C. Smits, B. F. M. Kuster, K. Van der Wiele, H. Van der Baan, H. S. *Appl. Catal.* **1987**, *33*, 83

[185] P. C. C. Smits, B. F. M. Kuster, K. Van der Wiele, H. S. Van der Baan, *Carbohydr. Res.* **1986**, *153*, 227

[186] A. Abbadi, H. Van Bekkum, *Appl. Catal. A* **1995**, *124*, 409

[187] A. W. Heinen, G. Papadogianakis, R. A. Sheldon, J. A. Peters, H. van Bekkum, *J. Mol. Catal. A* **1999**, *142*, 17.

[188] A. W. Heinen, J. A. Peters, H. van Bekkum, *Carbohydrate Res.* **2001**, *330*, 381

[189] A. Fukuoka, L. Dhepe, *Angew. Chem. Int. Ed.* **2006**, *45*, 5161

[190] N. Yan, C. Zhao, C. Luo, P.J. Dyson, H. Liu, Y. Kou, *J. Am. Chem. Soc.* **2006**, *128*, 8714-8715.

[191] C. Luo, S. Wang, H. Liu, *Angew. Chem. Int. Ed.*, **2007**, *46*, 7637

[192] M. A. Dasari, P. P. Kiatsimkul, W. R. Sutterlin, G. J. Suppes, *Appl. Catal. A* **2005**, *281*, 225

[193] D. G. Lahr, B. Shanks, *J. Catal.* **2005**, *232*, 386

[194] T. Miyazawa, Y. Kusunoki, K. Kunimori, K. Tomishige, *J. Catal.* **2006**, *240*, 213

[195] J. Chaminand, L. Djakovitch, P. Gallezot, P. Marion, C. Pinel, C. Rosier, *Green Chem.* **2004**, *6*, 359

[196] T. Miyazawa, S. Koso, K. Kunimori, K. Tomishige, *Appl. Catal. A* **2007**, *329*, 30.

[197] B.W. Hoffer, E. Crezee, P.R.M. Mooijman, A.D. van Langeveld, F. Kapteijn, J.A. Moulijn, *Catal. Today*, **2003**, *79-80*, 35-41.

[198] A. Perrard, P. Gallezot, J.-P. Joly, R. Durand, C. Baljou, B. Coq, P. Trens, *Appl. Catal. A* **2007**, *331*, 100

[199] H. C. M. Pijnenburg, B. F. M. Kuster, H. S. Van der Baan, *Staerke* **1978**, *30*, 352

[200] J. Wisniak, R. Simon, *Ind. Eng. Chem. Prod. Res. Dev.* **1979**, *18*, 50

[201] J. Wisniak, M. Hershkowitz, S. Stein, *Ind. Eng. Chem. Prod. Res. Dev.* **1974**, *13*, 232.

[202] J. Wisniak, M. Hershkowitz, R. Leibowitz, S. Stein, *Ind. Eng. Chem. Prod. Res. Dev.* **1974**, *13*, 75.

[203] M. Makkee, A. P. G. Kieboom, H. Van Bekkum, *Carbohydrate Res.* **1985**, *138*, 225

[204] J. Wisniak, R. Simon, *Ind. Eng. Chem. Prod. Res. Dev.* **1979**, *18*, 50

[205] A. W. Heinen, J. A. Peters, H. van Bekkum, *Carbohydrate Res.* **2000**, *328*, 449

[206] M. Besson, P. Gallezot, A. Pigamo, S. Reifsnyder, *Appl. Catal. A* **2003**, 117-124.

[207] R.D. Cortright, M. Sanchez-Castillo, J.A. Dumesic, *Appl. Catal. B* **2002**, *39*, 353-359.

[208] Z. Zhang, J.E. Jackson, D.J. Miller, *Appl. Catal. A* **2001**, *219*, 89-98.

[209] B. W. Mao, Z. Z. Cai, M. Y. Huang, Y. Y. Jiang, *Polym. Adv. Technol.* **2003**, *14*, 278

[210] G. Seo, H. Chon, *J. Catal.* **1981**, *67*, 424

[211] R. Rao, R. Dandekar, R. T. K. Baker, Vannice, M. A. *J. Catal.*, **1997**, *171*, 406

[212] R. S. Rao, R. T. Baker, M. A. Vannice, *Catal. Lett.* **1999**, *60*, 51

[213] J. Wu, Y. Shen, C. Liu, H. Wang, C. Geng, Z. Zhang, *Catal. Commun.* **2005**, *6*, 633

[214] X. Chen, H. Li, H. Luo, M. Qiao, *Appl. Catal. A* **2002**, *233*, 13

[215] H. Y. Zheng, Y. L. Zhua, B. T. Teng, Z. Q. Bai, C. H. Zhang, H. W. Xiang, Y. W. Li, *J. Mol. Catal. A* **2006**, *246*, 18

[216] R. V. Christian, H. D. Brown, R. M. Hixon, *J. Am. Chem. Soc.* **1947**, *69*, 1961

[217] K. Folkers, H. Adkins, *J. Am. Chem. Soc.* **1932**, *54*, 1145

[218] V. Schiavo, G. Descotes, J. Mentech, *Bull. Soc. Chim. Fr.* **1991**, 704

Fig. 1. Overview of how selected commodity chemicals could be produced from primary renewable building blocks.

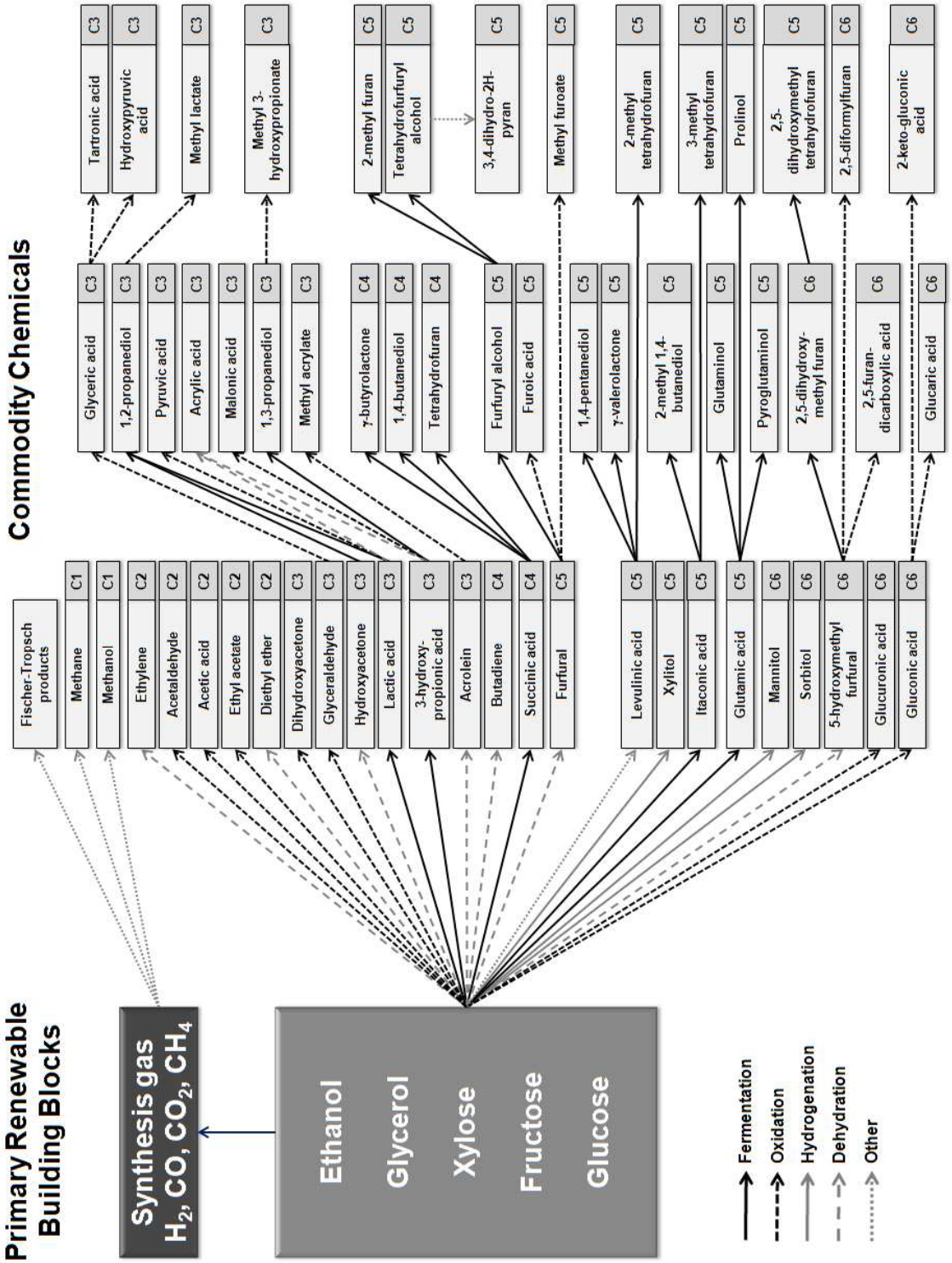

Scheme 1. Sucrose is hydrolyzed into a mixture of glucose and fructose when exposed to an acid catalyst. Sulfuric acid has been used for this, but also heterogeneous solid acid catalysts have found use, especially acidic ion exchange resins.

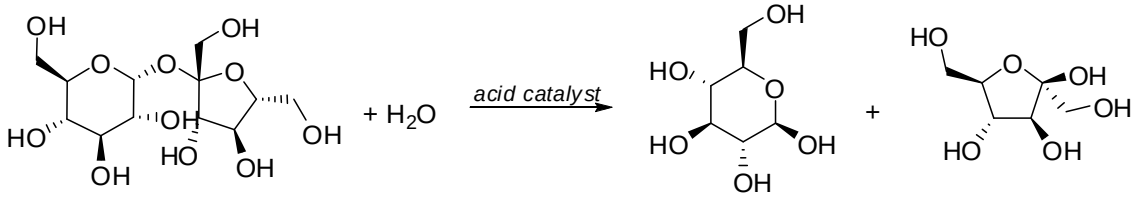

sucrose glucose fructose

Scheme 2. Triglycerides can be hydrolyzed to give fatty acids and glycerol. This can be catalyzed by solid acid catalysts like zeolites or acid exchanged resins.

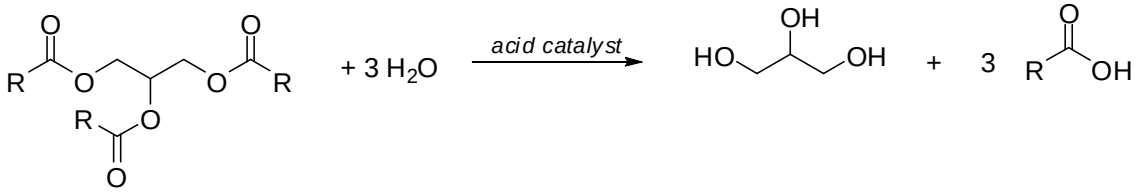

triglyceride glycerol fatty acid

Scheme 3. Acrolein can be obtained by dehydration of glycerol. The reaction was reported many years ago using powdered $KHSO_4/K_2SO_4$ as catalyst. Recently, the use of silica-supported heteropolyacids has also been described, notably with silicotungstic acid as catalyst.

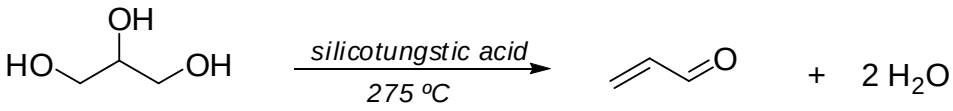

Glycerol Acrolein

Scheme 4. Hydroxyacetone can be obtained from glycerol by dehydration. The reaction has been reported using copper-chromite as catalyst.

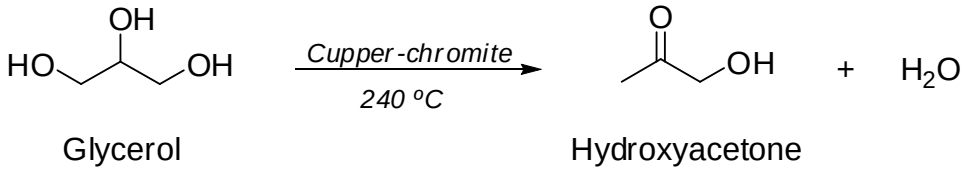

Glycerol Hydroxyacetone

Scheme 5. Xylose can be dehydrated to produce furfural. The reaction has been reported using several different catalysts including zeolites, sulfonic acid functionalized MCM-41 and immobilized heteropolyacids. The best selectivity towards furfural was achieved using zeolite H-mordenite, although at low conversion of xylose [88]. Overall, the best yield of furfural was obtained using sulfonic acid functionalized MCM-41.

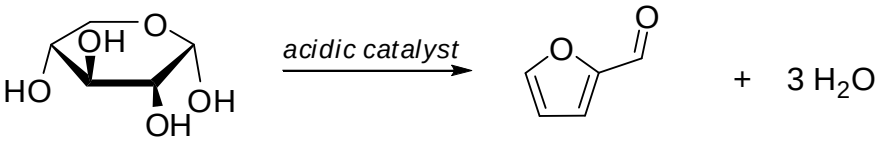

Xylose Furfural

Scheme 6. Fructose can be transformed into 5-hydroxymethyl furfural (HMF) via acid-catalyzed dehydration. Solid acid catalysts applied to facilitate the reaction are zeolites, ion-exchange resins and solid inorganic phosphates. With sporadic success, notably with inorganic phosphates, other carbohydrate sources such as inulin can also be transformed into HMF.

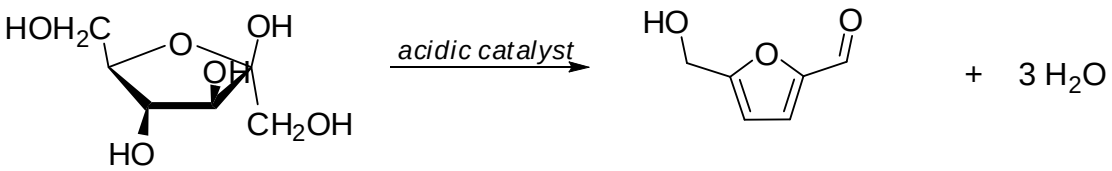

Fructose 5-hydroxymethyl furfural

Scheme 7. Oxidation of glycerol in acid media leads to dihydroxyacetone, using Pt-Bi/C as catalyst.

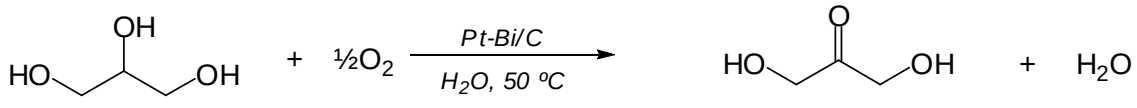

glycerol dihydroxy acetone

Scheme 8. Oxidation of glycerol in basic media leads to glyceric acid, using Pd/C or Au/C as catalyst.

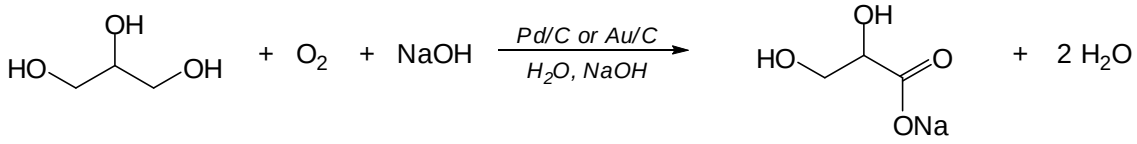

glycerol sodium glycerate

Scheme 9. Oxidation of glucose to gluconic acid has been reported using oxidation catalysts such as Pt/C, Pd/C, Pd-Bi/C and Au/C.

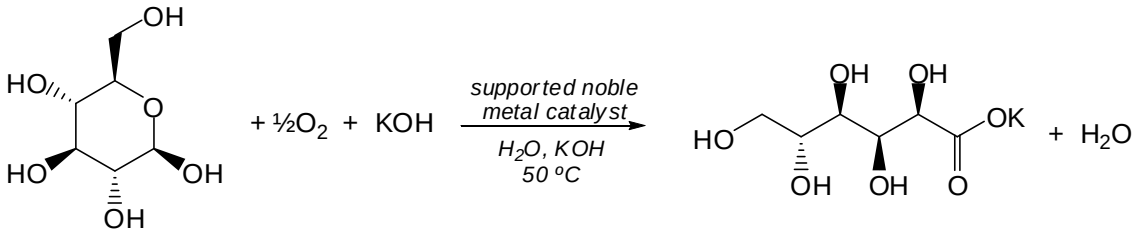

glucose gluconic acid

Scheme 10. Oxidation of both the aldehyde and alcohol moieties of HMF leads to formation of 2,5-furandicarboxylic acid. The oxidation reaction is catalyzed by Pt.

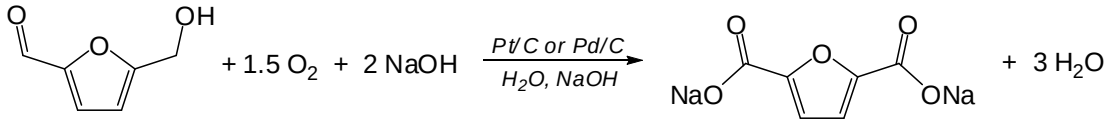

hydroxymethyl furfural 2,5-furandicarboxylic acid

Scheme 11. Under mild conditions, oxidation of HMF in methanol can be tuned to yield methyl (5-hydroxymethyl)-furoate via oxidation of the aldehyde moiety.

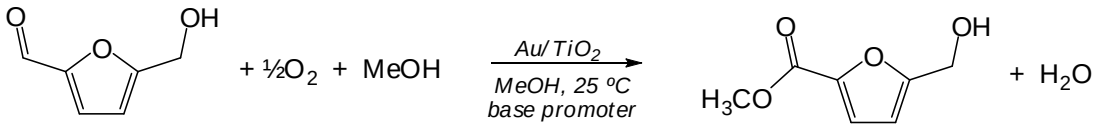

hydroxymethyl furfural methyl (5-hydroxymethyl)-furoate

Scheme 12. Various catalysts have been applied to facilitate the catalytic hydrogenation of glucose to sorbitol, notably Pt supported on activated carbon cloth using which 99.5% yield of sorbitol can be obtained.

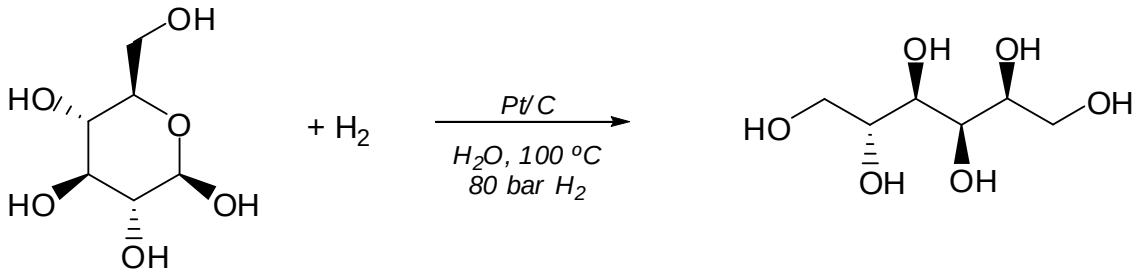

glucose sorbitol

Scheme 13. Hydrogenation of xylose to produce xylitol can be achieved with 95% selectivity using Raney nickel or Ru/C as catalyst.

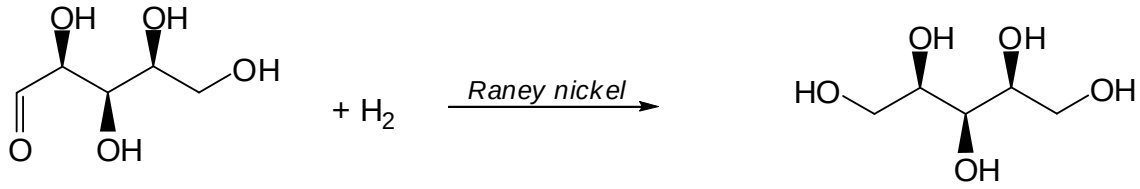

xylose xylitol

Scheme 14. Hydrogenation of fructose to mannitol is catalyzed by hydrogenation catalysts such as Raney nickel and Ru/C.

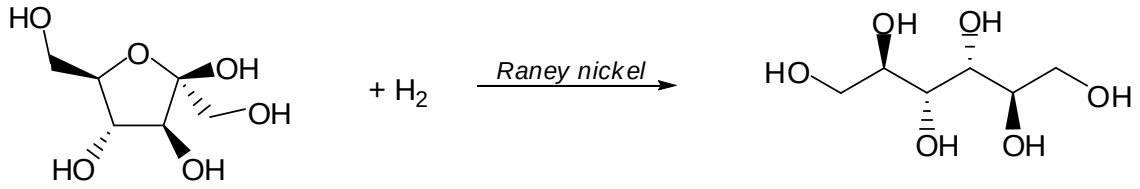

fructose mannitol

Scheme 15. Hydrogenation of furfural to furfuryl alcohol is catalyzed by Cu-containing catalysts.

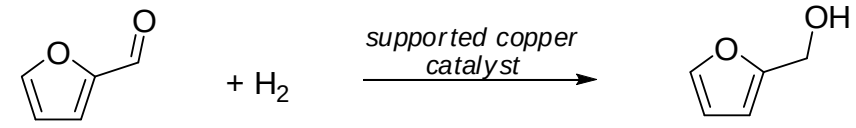

furfural furfuryl alcohol

Scheme 16. Hydrogenation of HMF to 2,5-di(hydroxymethyl)furan is catalyzed by Pt and Cu.

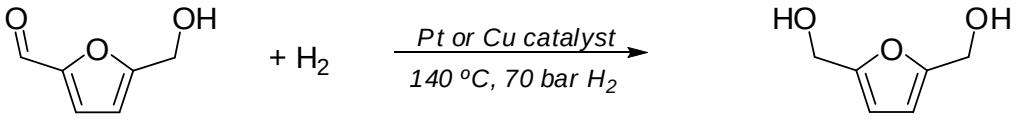

5-hydroxymethyl furfural

2,5-dihydroxymethyl furan

Perspective
Bioethanol: fuel or feedstock?

Jeppe Rass-Hansen, Hanne Falsig, Betina Jørgensen and Claus H Christensen*
Center for Sustainable and Green Chemistry, Department of Chemistry, NanoDTU, Technical University of Denmark, DK-2800 Kgs. Lyngby, Denmark

Abstract: Increasing amounts of bioethanol are being produced from fermentation of biomass, mainly to counteract the continuing depletion of fossil resources and the consequential escalation of oil prices. Today, bioethanol is mainly utilized as a fuel or fuel additive in motor vehicles, but it could also be used as a versatile feedstock in the chemical industry. Currently the production of carbon-containing commodity chemicals is dependent on fossil resources, and more than 95% of these chemicals are produced from non-renewable carbon resources. The question is: what will be the optimal use of bioethanol in a longer perspective?

Keywords: bioethanol; fuel; feedstock

SETTING A NEW SCENE

Growing demands for CO_2-neutral transportation fuels and the desire to achieve a reduced dependence on fossil resources have been the major driving forces for the substantial increase in the amounts of bioethanol produced by fermentation of biomass. An interesting question is whether the optimal use of bioethanol is as a fuel, or as a feedstock for producing higher-value chemical products.

The vast majority of all fuels and carbon-containing chemicals are produced from fossil resources. Studies predict that most kinds of fossil resources will be depleted within the next century.[1] Furthermore the combustion of fossil fuels causes elevated levels of greenhouse gases (GHG) in the atmosphere, which could possibly lead to global warming.[2,3] As a consequence, society must gradually change from an economy based on fossil resources to one based on sustainable resources. Here, biomass could have a significant role to play. In Fig. 1, the price for a range of selected fuels and chemicals produced from fossil or renewable resources are indicated. Obviously, the costs of the raw materials, both fossil and renewable, depend on many factors and therefore the scale is only approximate. From these raw materials it is possible to produce all the chemicals needed in society. The relevant transformations are typically catalytic reactions, and the cost of the various fuels and chemicals is largely governed by the cost of the raw material and the efficiency of the involved processes. It is noteworthy that with the proper technology it is possible to convert biomass to essentially all the high-value commodity chemicals and fuels currently available from fossil resources. There could even be some advantages using biomass compared to fossil fuels as a feedstock, e.g., for production of certain oxygenated chemicals since introduction of oxygen functionalities into hydrocarbons can be rather difficult, whereas many products derived from biomass already contain some oxygen.[4] However, this also entails an increase in production costs for some of the non-oxygen-containing products, such as gasoline.

Figure 1 illustrates that, in relative terms, it is possible to produce some chemicals more easily and in fewer steps from biomass than from fossil resources, whereas others are less readily available.[5] Thus, fossil and renewable resources are not necessarily equally useful starting materials for all possible products. In this context, it is particularly important to note that

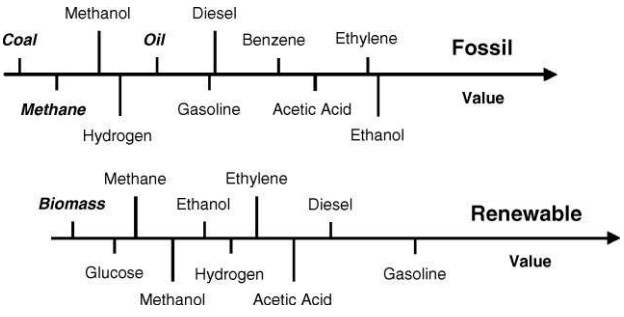

Figure 1. Indication of relative prices for a range of selected chemicals produced from either renewable or fossil resources. The raw materials are shown in italics and the remaining fuels and chemicals are typically produced in one or more process steps starting from fossil or renewable resources.

* Correspondence to: Claus H Christensen, Center for Sustainable and Green Chemistry, Department of Chemistry, NanoDTU, Technical University of Denmark, DK-2800 Kgs. Lyngby, Denmark
E-mail: chc@kemi.dtu.dk
(*Received 9 October 2006; revised version received 18 November 2006; accepted 23 November 2006*)
DOI: 10.1002/jctb.1665

 J Chem Technol Biotechnol 0268–2575/2007/$30.00

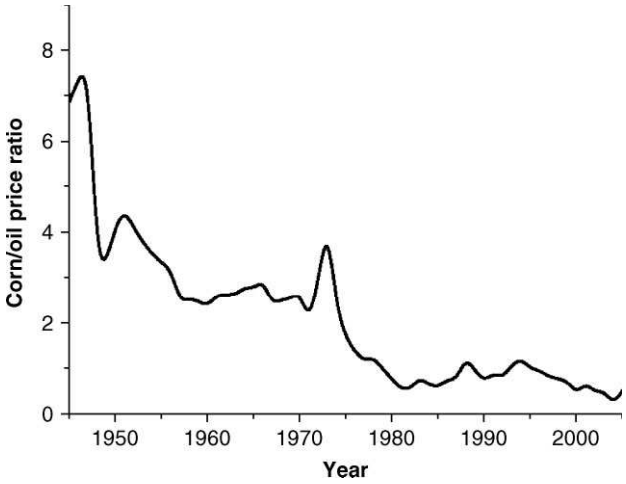

Figure 2. Corn/oil price ratio during in the last part of the 20th century (data from www.eia.doe.gov or www.lefflercom.com).

the figure does not show the amount of each chemical produced. For instance, it is not currently possible to produce the world's need for ethylene from biomass, because the production of ethylene is about three times as high as the production of bioethanol, which would be the most likely feedstock for ethylene production in a renewable economy.

In an evaluation of the usefulness of renewable resources compared to fossil resources as possible sources of fuels and chemicals, the cost of the feedstocks plays a central role. Therefore, it is very interesting to note that the price of biomass relative to oil has decreased more than 10 times over the last 60 years, as shown in Fig. 2 (data from www.eia.doe.gov or www.lefflercom.com). The prices of the products derived from renewable resources are sensitive to technological improvements of the production process, probably more so than those in the fossil economy, since here the involved processes have been improved through significant efforts over many years. One key improvement would be to find more efficient routes for conversion of biomass to fuels or chemicals. If the decrease in the corn/oil price ratio continues and the technology improves, the relative cost for biomass-derived chemicals and fuels will decrease, making it more feasible to switch to biomass.

In addition, it could be important that the use of biomass as a sustainable resource for production of fuels and commodity chemicals should offer improved security in supply, since biomass can be grown in most parts of the world. This is in contrast to oil resources, which are limited by being located in few and, for some, unstable areas of the world.

Ethanol is one chemical that can be readily obtained from biomass by fermentation. The total world production of bioethanol is constantly increasing and was estimated to reach more than 46 billion liters per year in 2005.[6]

RENEWABLE FUELS

In many countries, ethanol is used as an additive to gasoline. In particular, Brazil and the United States have invested significant resources in using blends of ethanol and gasoline as a fuel for motor vehicles (with internal combustion engines). Today, around 2% of the total transportation fuels are covered by bioethanol in the United States.[7] The US Department of Energy has set a goal of replacing 30% of transportation fuels with bioethanol and biodiesel by 2025.[7] Many other countries are also producing or planning to produce ethanol from biomass for use as a motor fuel. The European Union has established a goal of 5.75% biomass-derived transportation fuels by December 2010.[7] The use of fuel ethanol has been quite successful in Brazil, where it is produced at a very low cost by fermentation of sugarcane. In the United States corn is the dominant biomass feedstock for production of ethanol, and in the EU straw and other agricultural wastes are the preferred types of biomass for ethanol production. It is, however, somewhat more difficult to obtain a high conversion to ethanol from these types of biomass, resulting in much higher production costs of bioethanol in Europe.

The renewable energy content for production of bioethanol from corn with current technology was recently estimated to be between 5% and 26%, where the non-renewable energy used in the production was mainly contributed by coal and natural gas.[8] However, currently the energy balance for bioethanol production is quite controversial. Anyhow, an increase in the renewable energy content and a significant reduction in GHG emissions can be expected by use of gene-modified starch-rich non-food biomass and/or second-generation fermentation plants with improved conversion of lignocellulose. First-generation plants use only the sugar and the starch in the biomass material and are therefore only highly effective with starch-rich materials like sugarcane. On the other hand, second-generation fermentation plants can also convert most of the lignocellulose (cellulose, hemicellulose and lignin) to useful chemicals, which is necessary when, for instance, straw is the biomass feedstock.[9] Thus these new improved technologies for biomass conversion uses less non-renewable energy and give both a higher CO_2 reduction and a higher ethanol yield than first-generation plants due to a higher utilization of the feedstock.[10,11] Moreover, the feedstocks for second-generation plants are cheaper (agricultural waste etc.) and do not give the same ethical concerns when using potential food resources for energy production. In the second-generation biorefinery, the highest CO_2 reduction is reached by co-producing other valuable products. In the Danish bioenergy concept this is achieved by co-producing methane and hydrogen.[12] Another significant issue is that abundant coal resources are the primary source of non-renewable energy in conversion of biomass into ethanol. In that way, a premium liquid transportation fuel is produced from a less valuable

J Chem Technol Biotechnol **82**:329–333 (2007)
DOI: 10.1002/jctb

energy resource, which further reduces the need for import of petroleum.[13]

The environmental impact of using blends of ethanol–gasoline depends on the actual fraction of ethanol in the blend. A recent review by Niven questions whether the use of ethanol as a fuel additive has any environmental advantage compared to using pure gasoline.[15] A fuel blend of 10 vol% ethanol offers little reduction in GHG emissions or improvement in energy efficiency, with the drawback of increasing risk and severity of soil and groundwater contamination. Increasing the ethanol fraction to 85 vol% decreases emissions of GHG, but may cause significant air pollution in the form of NO_x and organic compounds.[14] However, if 85 vol% ethanol is the goal, alterations to existing combustion engines are necessary, and different car exhaust catalysts could probably reduce the emissions of NO_x and organic compounds. When 10 vol% mixtures are used, ethanol works as an octane enhancer and improves combustion, which reduces CO and ground-level ozone emissions.[13] Ethanol is also less poisonous to the environment than other octane boosters such as lead and methyl *tert*-butyl ether (MTBE).

Another possible future use of bioethanol to supply a sustainable/green transportation fuel is catalytic steam reforming for production of H_2. Many consider hydrogen to be a future energy source, especially for the transportation sector and mobile devices.[15] Today most hydrogen is produced from steam reforming of natural gas. However, this is not a solution to substantially decrease emissions of GHG to the atmosphere. There are two primary reasons as to why conversion of bioethanol to hydrogen is promising. First, direct combustion of ethanol used for transportation is estimated to have an energy efficiency of approximately 20%, whereas utilizing hydrogen in a fuel cell has an energy efficiency of up to 60%.[16] Therefore, even though the conversion of ethanol to hydrogen requires some energy input, it may be possible to capture more than 50% of the energy from photosynthesis as electricity from autothermal reforming of ethanol.[17] Secondly, the most expensive step in using bioethanol directly as a fuel is removal of the water. With steam reforming of ethanol to hydrogen, it is not necessary to remove water, making the process considerably cheaper. Ethanol can also be used directly in a fuel cell. However, the efficiency of the current direct ethanol fuel cell is quite inadequate.[18] The catalytic chemical reactions for steam reforming of bioresources are very complex. Specific information about the intermediates can, however, be provided by computational methods and thereby help pinpoint where to set in catalytic modifications to improve this viable route to large-scale hydrogen production.[19]

FEEDSTOCK

More than 95% of all carbonaceous chemicals are produced from fossil resources. The only existing alternative to produce these chemicals is to use biomass and biomass-derived molecules as feedstocks. The chemical industry is enormous, and a significant reduction in GHG emissions could therefore be achieved by a change to renewable CO_2-neutral resources. Bioethanol production is already implemented in many places around the world and in progress in many other places. This means that the amount of bioethanol available most likely will keep increasing for several years. Studies suggest a yearly increase of approximately 6.5% until 2020, leading to an annual production of more than 120 billion liters in 2020.[20] With this amount of bioethanol available, there is great promise in partly converting the chemical industry to one based on renewable resources.

Instead of using bioethanol for transportation fuel purposes where it has a relatively low value, it could instead be used as feedstock for other important chemical products with a much higher value. Figure 3 illustrates some possible uses of biomass-derived ethanol. Besides its use for hydrogen production by steam reforming or the direct use as a fuel or fuel additive, it could be utilized for producing acetaldehyde, ethylene, butadiene and acetic acid, among others. The annual amount of these chemicals produced worldwide is around 1.4, 120, 7.5 and 8.5 million tons, respectively.[21] Today, the annual production of bioethanol is around 45 million tons, which means that it could replace a significant amount of these petrochemical products. For this to be economically viable, the products produced from bioethanol must obviously be more valuable than the bioethanol itself. Moreover, it is necessary to keep the conversion processes inexpensive.

The production costs for bioethanol is on average around 250 US $ per ton, for ethylene it is around 700 US $ per ton, and for acetic acid it is around 650 US $ per ton.[5] Looking into the amounts and production costs of the respective chemicals, it seems realistic to produce, for example, acetic acid from bioethanol with the proper catalytic reaction pathway. Such a reaction was recently proposed, where ethanol is oxidized with air in an aqueous-phase reaction over a gold catalyst.[22] Moreover, analysis of the reaction indicates that it is competitive both economically and environmentally to the conventional petrochemical production of acetic acid by the Monsanto process. With regard to CO_2 emission, the Monsanto process produces around 0.7

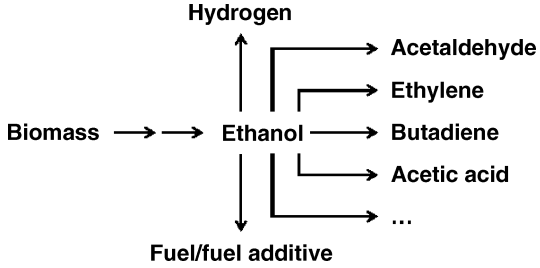

Figure 3. Possible uses of bioethanol as a fuel or as a feedstock for important bulk chemicals.

tons of CO_2 for every ton of acetic acid, whereas production from bioethanol is almost CO_2 neutral. Thus, production of chemicals from bioethanol can actually lead to higher CO_2 savings than by using it as a fuel. At the moment, it is not possible to produce all the required ethylene from bioethanol, because ethylene is produced in much greater amounts than bioethanol. This, though, is likely to change in the future with increasing production capacity of bioethanol and eventually with increasing oil prices. However, in the foreseeable future, the production of bioethanol will most likely be smaller than the production of the most important carbon-containing commodity chemicals, and therefore it could easily be an important feedstock for several of these.

THE FUTURE

During the previous century, petroleum became an essential source for energy and commodity chemicals. One future goal is to convert biomass into products that can compete with corresponding products derived from fossil resources with a focus on sustainability, resource availability and supply reliability. The aim for the US Department of Energy is to replace 25% of carbonaceous chemicals with biomass-derived chemicals by 2025.[7] To achieve this goal, there is a need for some manageable oxygenated molecules. With its large-scale production ethanol is an obvious choice for such a molecule, but other easily available molecules from biomass, like glucose and fructose, could also be very important for attaining this and further ambitions.

The most energy-efficient utilization of dry biomass is to use it in a combined heat and power plant, where it directly substitutes fossil fuels on a 1:1 basis, and yields energy efficiencies above 90%. Furthermore, a 50% increased CO_2 reduction can be achieved if biomass is used for combined heat and power production instead of production of bioethanol using first-generation technologies.[23]

Recently, it was estimated for the European Union that around 20% of the total energy consumption in the future could be covered from the use of biomass, without compromising the need for food. Thus, biomass cannot alone cover the energy demands.[24]

The main motivation for producing ethanol has so far been the need for transportation fuels. The consumption of transportation fuels alone in the United States is over 530 billion liters per year, whereas US bioethanol production was only about 15 billion liters in 2005.[25] Bioethanol will most certainly have some positive influence on CO_2 emissions from the transportation sector, but it might prove possible to achieve an even better environmental effect by using it as a feedstock for the chemical industry. Finding effective catalytic reaction pathways for producing commodity or specialty chemicals from bioethanol rather than using it to substitute the least expensive fossil products, such as the fuels, will most likely hold the greatest economic promise. Thus, the optimal use of bioethanol, in terms of efficiency, could well be to incorporate it into high-value materials otherwise produced from fossil resources and eventually burn the resulting waste in a thermal power station for heat generation.

The central point is that all available resources, both fossil and renewable, are limited and it is essential that we carefully consider how each is best used. This is a future key challenge for chemical research and development.

REFERENCES

1 *BP Statistical Review of World Energy*, June 2005 (www.bp.com).
2 Huybrechts P, Kuhn M, Lambeck K, Nhuan MT, Qin D, Woodworth PL, Changes in sea level, in *Climate Change 2001: The Scientific Basis*, ed. by Douglas BC and Ramirez A. Cambridge University Press, Cambridge, UK, pp. 639–693 (2001).
3 Wigley TML, The climate change commitment. *Science* **307**:1766–1769 (2005).
4 Dale BE, 'Greening' the chemical industry: research and development priorities for biobased industrial products. *J Chem Technol Biotechnol* **78**:1093–1103 (2003).
5 Kosaric N, Duvnjak Z, Farkas A, Sahm H, Bringer-Meyer S, Goebel O, *et al.*, Ethanol in *Ullmann's Encyclopedia of Industrial Chemistry* (7th edn). Wiley, Chichester (2006.). Additional data from www.icispricing.com, www.eia.doe.gov and www.dft.gov.uk.
6 *Biofuels Strategy: Key Facts and Figures*. MEMO/06/05 European Commission, Brussels (2005).
7 Ragauskas AJ, Williams CK, Davison BH, Britovsek G, Cairney J, Eckert CA, *et al.*, The path forward for biofuels and biomaterials. *Science* **311**:484–489 (2006).
8 Farrell AE, Plevin RJ, Turner BT, Jones AD, O'Hare M and Kammen DM, Ethanol can contribute to energy and environmental goals. *Science* **311**:506–508 (2006).
9 Haagesen F, Torry-Smith M and Ahring BK, Fermentation of biomass to alcohols, in *Biofuels for Fuel Cells: Renewable Energy from Biomass Fermentation*, ed. by Lens P, Westermann P, Haberbauer M and Moreno A. IWA Publishing, London, pp. 169–190 (2005).
10 *Biofuels for Transport: An International Perspective*. International Energy Agency, Paris (2004). (www.iea.org).
11 Hammerschlag R, Ethanol's energy return on investment: a survey of the literature 1990–present. *Environ Sci Technol* **40**:1744–1750 (2006).
12 Westermann P and Ahring B, The biorefinery for production of multiple biofuels, in *Biofuels for Fuel Cells: Renewable Energy from Biomass Fermentation*, ed. by Lens P, Westermann P, Haberbauer M and Moreno A. IWA Publishing, London, pp. 194–205 (2005).
13 Shapouri H, Duffield JA and Wang M, The energy balance of corn ethanol revisited. *Trans ASAE* **46**:959–968 (2003).
14 Niven RK, Ethanol in gasoline: environmental impacts and sustainability review article. *Renew Sust Energ Rev* **9**:535–555 (2005).
15 Jacobson MZ, Colella WG and Golden DM, Cleaning the air and improving health with hydrogen fuel-cell vehicles. *Science* **308**:1901–1905 (2005).
16 Larminie J and Dicks A, *Fuel Cell Systems Explained* (2nd edn). Wiley, Chichester (2005).
17 Deluga GA, Salge JR, Schmidt LD and Verykios XE, Renewable hydrogen from ethanol by autothermal reforming. *Science* **303**:993–997 (2004).
18 Lamy C, Belgsir EM and Léger J-M, Electrocatalytic oxidation of aliphatic alcohols: application to the direct alcohol fuel cell (DAFC). *J Appl Electrochem* **31**:799–809 (2001).

19 Nørskov JK and Christensen CH, Toward efficient hydrogen production at surfaces. *Science* **312**:1322–1323 (2006).
20 *Biofuel Market Worldwide (2006)*, RNCOS, 1 July (2006). (www.rncos.com).
21 Weissermel K and Arpe H-J, *Industrial Organic Chemistry* (4th edn). Wiley-VCH, Weinheim (2003).
22 Christensen CH, Jørgensen B, Rass-Hansen J, Egeblad K, Madsen R, Klitgaard SK, *et al*, Formation of acetic acid by aqueous-phase oxidation of ethanol with air in the presence of a heterogeneous gold catalyst. *Angew Chem Int Ed* **45**:4648–4651 (2006).
23 Nielsen PH and Wenzel H, Environmental assessment of ethanol produced from corn starch and used as an alternative to conventional gasoline for car driving. IPU Pruduktion (2005). (http://www.ipu.dk/IPU-Produktion/Publikationer/bio-ethanol-report,-d-,pdf.aspx.).
24 Ericsson K and Nilsson LJ, Assessment of the potential biomass supply in Europe using a resource-focused approach. *Biomass Bioenerg* **30**:1–15 (2006).
25 Editorial, Bioethanol needs biotech now. *Nature Biotechnol* **24**:725 (2006).

Renewable hydrogen: carbon formation on Ni and Ru catalysts during ethanol steam-reforming

Jeppe Rass-Hansen,[a] Claus Hviid Christensen,*[a] Jens Sehested,[b] Stig Helveg,[b] Jens R. Rostrup-Nielsen[b] and Søren Dahl*[b]

Received 26th February 2007, Accepted 3rd May 2007
First published as an Advance Article on the web 29th May 2007
DOI: 10.1039/b702890c

Biomass is probably the only realistic green and sustainable carbonaceous alternative to fossil fuels. By degradation and fermentation, it can be converted into bioethanol, which is a chemical with a range of possible applications. In this study, the catalytic steam-reforming of ethanol for the production of hydrogen is investigated, along with quantitative and qualitative determinations of carbon formation on the catalysts by TPO and TEM experiments. A $Ru/MgAl_2O_4$ catalyst, a $Ni/MgAl_2O_4$ catalyst as well as Ag- and K-promoted $Ni/MgAl_2O_4$ catalysts were studied. The operating temperature was between 673 and 873 K, and a 25 vol% ethanol–water mixture was employed. Deactivation of the catalysts by carbon formation is the main obstacle for industrial use of this process. Carbon formation was found to be highly affected by the operating temperature and the choice of catalyst. The effect of Ag addition was a rapid deactivation of the catalyst due to an enhanced gum carbon formation on the Ni crystals. Contrary to this, the effect of K addition was a prolonged resistance against carbon formation and therefore against deactivation. The Ru catalyst operates better than all the Ni catalysts, especially at lower temperatures.

Introduction

The continuously increasing oil prices and the need for a CO_2-neutral energy production have in recent years increased the interest in different bio-fuels. Lately, bioethanol in particular has achieved significant attention for several reasons. First of all, it can be produced in large amounts from biomass by a relatively simple fermentation, it is considered CO_2-neutral, it is easy to handle, and it is non-toxic.[1,2]

Here, the catalytic steam-reforming (SR) of ethanol for hydrogen production is investigated. In particular, the objectives of this paper are to quantitatively determine the effect of temperature and the role of the catalytic metal on the formation rate for coke on the technical catalysts during the SR. This is important to eventually implement ethanol SR in stationary and/or mobile units.

It is well known[3] that highly pure ethanol in small quantities can be mixed with gasoline to increase the octane number. Additionally, it is possible to run cars on any mixture of ethanol and gasoline with an engine adjustment. These cars are called flexible fuel vehicles (FFVs). The production of highly pure ethanol is, however, still quite expensive and generally not cost-competitive with gasoline.[3,4] But the world ethanol production has more than doubled from 2000 to 2005 and is expected to increase significantly.[5] Together with technological improvements and lack of oil this will continue to favor ethanol prices compared to gasoline prices.

When ethanol is burned in a combustion engine, the energy efficiency of the fuel is limited by the Carnot efficiency and can reach only about 25%.[6] This fuel efficiency can be significantly increased when ethanol is first converted to hydrogen and then used in a fuel cell with an efficiency of more than 50%.[6–8] Besides that, it will not be necessary to first produce the highly pure ethanol required for fuel in combustion engines by expensive distillation since the reaction of ethanol SR [eqn (1)] requires at least three moles of water for every mole of ethanol:

$$CH_3CH_2OH + 3H_2O \rightarrow 2CO_2 + 6H_2 \quad (1)$$

The use of agricultural feedstocks for a form of CO_2-neutral energy production relies on the photosynthesis of carbohydrates with high energy contents. These can, by degradation and fermentation, be converted into ethanol and CO_2. Especially in Brazil and the USA this is done on large scales (around 16 billion L in each country)[9] by fermentation of sugar-cane and corn, respectively. Further catalytic conversion of ethanol into hydrogen requires energy, but the higher efficiency from using hydrogen in fuel cells, probably, makes the effort worthwhile. Fig. 1 shows in an energy level diagram the idea and potential of using biohydrogen *versus* bioethanol for energy applications. Theoretically, the total efficiency could be raised by about 70% with the given energy efficiencies, or even higher when considering distillation issues and the efficient use of waste heat.

The catalytic SR of ethanol has recently been reviewed by Haryanto *et al.*[10] The conversion of ethanol to hydrogen and CO_2 is possible with many different catalysts, but in particular Rh and Ni catalysts have shown promising results.[10–14] One major problem is, however, the formation of coke on the less noble catalysts and the resulting deactivation.[10]

[a]*Center for Sustainable and Green Chemistry, Department of Chemistry, Technical University of Denmark, DK-2800 Kgs. Lyngby, Denmark. E-mail: chc@kemi.dtu.dk; Tel: +45 45252402*
[b]*Haldor Topsøe A/S, Nymøllevej 55, DK-2800 Kgs. Lyngby, Denmark. E-mail: sda@topsoe.dk; Tel: +45 45272487*

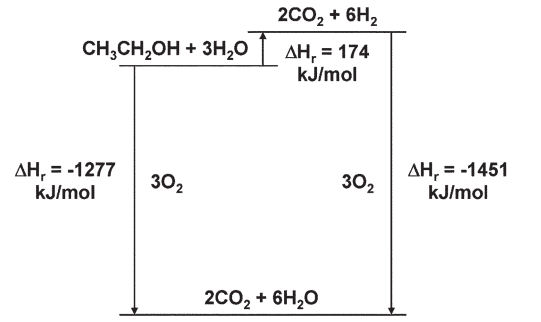

Energy output for ethanol combustion with an energy efficiency of 25 %:
0.25·1277 kJ/mol = **319 kJ/mol**

Energy output for hydrogen utilization in fuel cells with an energy efficiency of 50 %: 0.50·1451 kJ/mol – 174 kJ/mol = **552 kJ/mol**

Total energy efficiency could potentially be raised by **73 %**

Fig. 1 Energy level diagram comparing the combustion of ethanol with the transformation of ethanol to hydrogen and use in a fuel cell.

Fierro *et al.*[11] found that Rh and Ru catalysts gave the highest hydrogen selectivity among different noble metals for oxidative SR. Moreover, they found that addition of Cu to Ni catalysts enhanced the lifetime of the catalyst by lowering the coke depositions. Auprêtre *et al.*[12] showed that Ni and Rh catalysts were very active for non-oxidative SR, and later that a combination with Rh on a $Ni_{1-x}Mg_xAl_2O_4$ support gave particularly promising results.[13] Frusteri *et al.*[14] reported that Ni catalysts have the highest selectivity towards hydrogen, and Rh catalysts to be almost as selective but far more resistant to carbon formation. They also describe how doping a Ni catalyst with an alkali metal can improve the catalyst performance with regard to ethanol conversion.[15] Furthermore, they suggested that carbon formation is significantly lowered by using a basic rather than an acidic support.[15] Similarly, Liguras *et al.*[16] described how the acidity of the support influences the carbon formation on the catalyst, mainly because acidic supports lead to the formation of ethylene, which is known to be a carbon-forming species in SR reactions.[17,18]

Here, a Ru- and a Ni-catalyst was prepared on a non-acidic support ($MgAl_2O_4$) and tested for the SR of ethanol. Moreover, nickel catalysts doped with small amounts of potassium and silver were prepared to analyze the effect on carbon formation on the catalysts.

Experimental

Catalyst synthesis

Pure Ni, and Ag- and K-doped 10 wt% Ni/$MgAl_2O_4$ catalysts were prepared by the *incipient wetness impregnation technique*. A high surface area spinel ($MgAl_2O_4$) with a pore volume of 427 mL kg^{-1} and a specific surface area of 72 m^2 g^{-1} was used as support material. This support was chosen due to its stability at high water pressures and temperatures, and because it does not contain acidic sites. The spinel tablets were crushed to a fraction of 300–710 μm and dried for 1 h at 373 K. The solution for the impregnation was prepared by dissolving the desired amount of the different metal compounds, as nitrate salts, in water under moderate heating. After impregnation, the catalysts were dried for 2 h at 373 K and finally calcined at 773 K for 4 h.

A 2 wt% Ru/$MgAl_2O_4$ catalyst was prepared similarly from a nitrosyl nitrate aqueous solution [$Ru(NO)(NO_3)_3$] but without the calcination step. The different catalysts are listed in Table 1.

Table 1 List of pure and promoted catalysts

Sample	Composition
Ni	10 wt% Ni/$MgAl_2O_4$
Ag/Ni	1 wt% Ag–10 wt% Ni/$MgAl_2O_4$
K/Ni	1 wt% K–10 wt% Ni/$MgAl_2O_4$
Ru	2 wt% Ru/$MgAl_2O_4$

Catalytic measurements

The catalytic experiments were performed in a tubular fixed-bed quartz reactor with an inner diameter of 6 mm. For each test, 200 mg of catalyst material was loaded into the reactor and secured by quartz wool. The reactor was placed in an electrically heated oven. Before each run, the loaded catalyst was reduced and activated by heating at 5 K min^{-1} to 773 K for 2 h in a gas flow of 100 mL min^{-1} of equal amounts of hydrogen and nitrogen (the Ru catalyst was reduced at 873 K).

After reduction, SR experiments were conducted with a nitrogen gas flow of 80 mL min^{-1} and an ethanol–water liquid flow of 40 μL min^{-1}. The liquid was pumped by a Gynkotek 480 high precision pump and vaporized by heating tape at 493 K. The ethanol–water mixture consisted of 25 vol% ethanol, which gave a total molar gas flow ratio to the catalyst bed of ethanol–water–nitrogen of about 1 : 10 : 20.

A Leybold-Heraeus BINOS was used for analyzing the reaction stream by continuously measuring the CO and CO_2 contents in the exit gas after condensation of any liquids in an ice bath. The condensate was mainly water and occasionally a minor amount of unreacted ethanol, and trace amounts of other liquid species. Some experiments were further analyzed by GC measurements on a HP 5890A gas chromatograph (both FID and TCD).

Temperature programmed oxidation (TPO)

The same experimental setup was used for analyzing the amount of coke formed on the catalysts during SR. The TPO experiments were carried out by heating the oven to 873 K at 10 K min^{-1} in a gas flow of 20 mL min^{-1} consisting of a mixture of 91.5% nitrogen and 8.5% oxygen. By this method, the coke was completely oxidized to CO and CO_2, which was very convenient for making accurate measurements on the BINOS.

Transmission electron microscopy (TEM)

High resolution TEM images were obtained from selected catalysts after reaction in order to characterize the morphology and structure of the carbon deposits. The pictures were recorded with a Philips CM200 FEG transmission electron microscope operating with a primary electron energy of 200 kV and a point resolution of 1.9Å. About 30 pictures were taken for each catalyst at varying magnifications to identify reasonable trends.

Results

Steam-reforming experiments

During SR, ethanol decomposes mainly *via* two different routes: either by dehydration forming ethylene, or by dehydrogenation forming acetaldehyde.[10,14,19] These two intermediate products can be further catalytically decomposed and steam-reformed to an equilibrated mixture of methane, carbon dioxide, carbon monoxide, hydrogen and water (*cf.* Fig. 2). Experiments performed under the chosen conditions (200 mg catalyst material, a molar mixture of ethanol–water–nitrogen of 1 : 10 : 20, temperatures from 673 to 873 K and a gas flow to the catalyst bed of 120 mL min^{-1}) all reached equilibrium[20] as fresh catalysts, meaning that equilibrium was always reached during the first 6 h of run time. Hereafter, carbon formation and the resulting catalyst deactivation influenced the ethanol conversion and product distribution for some of the catalysts. At equilibrium conditions, all ethanol is converted to the products shown in Fig. 2, and the amount of hydrogen produced is determined by the operating temperature. The BINOS was used to continuously identify the CO and CO_2 concentrations in the exit gas, and together with occasional GC measurements, a total carbon balance was achieved.

The BINOS signals from SR experiments performed at 673 K are shown in Fig. 3 and 4. After a 16 h run time, the Ni-based catalysts all showed large amounts of coke depositions on the catalyst pellets. There were, however, significant differences in the deactivation patterns for the different catalysts. Deactivation can obviously be seen by unconverted ethanol in the exit gas, but more conveniently (in this setup) by a drop in the CO_2 concentration, and a rise in the CO concentration. Fig. 3 illustrates these patterns and how the Ag-promoted nickel catalyst shows a rapid deactivation after *ca.* 7 h, and the pure Ni catalyst deactivates more slowly after *ca.* 10 h, whereas the K/Ni catalyst barely deactivates during the first 16 h. The Ru catalyst does not seem to deactivate at all (*cf.* Fig. 4). These time indications are only suitable for a fast comparison between the different nickel catalysts, and they are very dependent on the dimensions of the catalyst bed. The deactivation appears as a profile that develops down through the entire catalyst bed. At the start of a run, the gas is equilibrated in the first part of the bed and this is also where the carbon is deposited. Along with carbon depositions formed on the catalyst, the equilibration part is shifted down through the bed. This proceeds until all of the catalyst is eventually partly covered with coke, and equilibration of the gas stream is

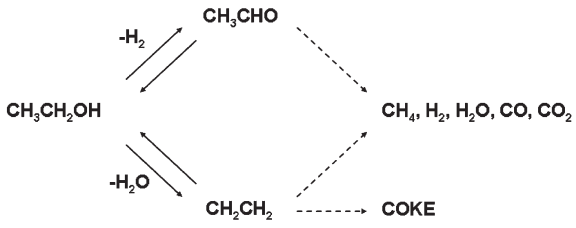

Fig. 2 Ethanol reaction pathways. Ethanol can be directly dehydrogenated to acetaldehyde or dehydrated to ethylene. Both of these species can in multiple steps be further converted to a synthesis-gas mixture, equilibrated by ordinary SR and WGS reactions.

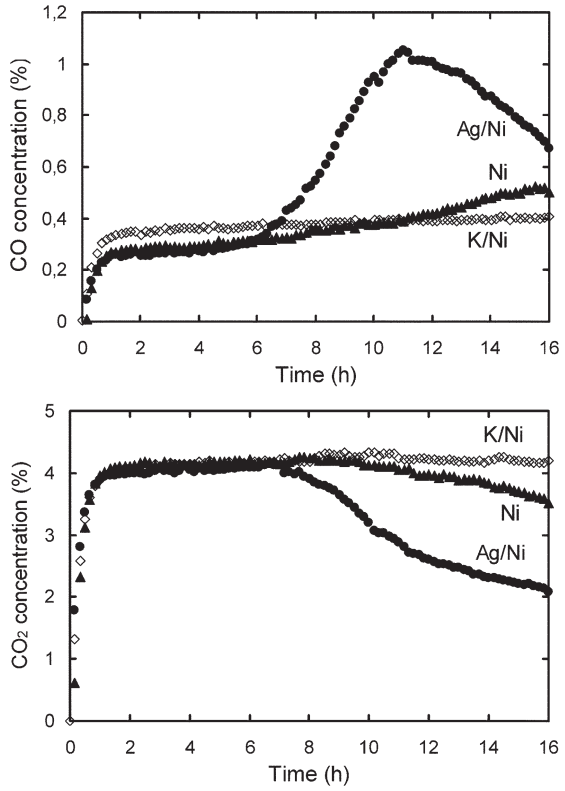

Fig. 3 CO and CO_2 signals from the BINOS in experiments performed at 673 K.

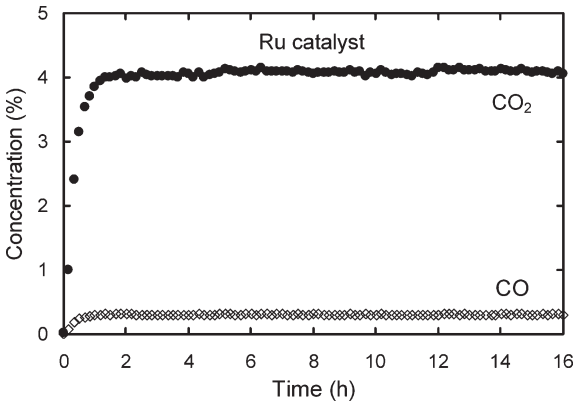

Fig. 4 CO and CO_2 signals from the BINOS for the Ru catalyst operated at 673 K.

therefore no longer possible, or until the top part of the reactor is totally clogged by carbon.

The combined analytical experiments show for the silver-promoted nickel catalyst that the first thing that happens during deactivation is a decrease in the CO_2 concentration and a simultaneous increase in the CO concentration. Then, the ethanol conversion starts decreasing and so does the production of methane whereas acetaldehyde and small amounts of ethylene start to appear in the gas stream. It is around this point that the highest CO concentration is reached, as seen in Fig. 3. Following this, acetaldehyde and ethylene reach a maximum before going towards zero. Since acetaldehyde is much more abundant than ethylene in the gas stream during

Table 2 TPO experiments for catalysts operated at 673 K for 16 h

Catalyst	TPO/mg C	TPO/(mg C) h^{-1}	Comment
Ni	73.5	4.6	Deactivation
Ag/Ni	66.2	4.1	Rapid deactivation
K/Ni	26.9	1.7	Slow deactivation
Ru	1.70	0.1	No deactivation

the deactivation, it seems likely that the main reaction path for ethanol is through acetaldehyde. However, both reaction paths are possible and less ethylene is expected in the exit gas due to the higher coke-forming potential of ethylene, *cf.* Fig. 2.

At 873 K, all catalysts established an equilibrium and none of them seemed to deactivate. Even after a run time of six days, there was no deactivation of the $Ni/MgAl_2O_4$ catalyst.

TPO experiments

Table 2 shows the results from the TPO experiments following the SR experiments illustrated in Fig. 3 and 4. From these experiments it is seen that less carbon depositions are formed on the Ag/Ni catalyst than on the pure Ni catalyst, even though the Ag/Ni catalyst deactivates more rapidly. The K/Ni catalyst has only about one-third of the amount of carbon formed on the Ni catalyst, but still more than 15 times the amount of carbon formed on the Ru catalyst. In general, the rate of coke formation was between 0.01 and 5 mg h^{-1}, which is an almost negligible amount in the total carbon balance, where around 240 mg carbon is reacted per hour.

Discussion

Formation of carbon and deactivation

One of the main challenges for industrial use of ethanol SR is carbon depositions on the catalysts formed during the SR.[10,19] Carbon is formed through several well known reactions, but, in particular, ethylene is an important precursor for carbon formation, as illustrated in Fig. 2.[10] Rostrup-Nielsen *et al.*[17,18] have previously described the different reaction paths for coke formation and the types of coke formed on the catalysts during the SR of hydrocarbons, as summarized in Table 3. From the table, it is clear that a lot of different parameters influence the carbon formation. Some of the most important are temperature and steam/carbon ratio, but the catalytic metal, the support material, the exact process conditions, the surface structure of the catalytic metal, the presence of promoters, *etc.*, are also critical parameters for the formation of carbon on the catalysts.

One approach to lower the rate of carbon formation on nickel catalysts is to promote them with another metal that blocks the most reactive sites (the step sites).[21] Blocking of these sites on the nickel crystals can have a far more pronounced effect on the rate of coke formation than on the rate of reforming.[11,18] Besenbacher *et al.*[22] designed a Au/Ni surface alloy catalyst for SR with gold blocking the most reactive sites. Hereby, a slightly less active but far more robust catalyst was achieved compared to an unpromoted nickel catalyst.[22] Thus, the nickel catalysts doped with potassium and silver were prepared. In addition to step-site blocking, potassium is also expected to increase the steam adsorption and thereby lower the formation of coke on the catalyst.[17] A high steam pressure is known to decrease carbon formation,[17] and therefore a high water to ethanol ratio will also decrease coking problems.

The above considerations and the results from the TPO and SR experiments suggest that different types of carbon are formed on the catalysts, but only some types are leading to rapid deactivation. Therefore, the carbon deposits on selected catalysts were studied by TEM. It was apparent that on all the Ni-based catalysts various types of carbon formations were observed. However, the four TEM images in Fig. 5 exemplify the most abundant or archetypal carbon structures formed on each catalyst.

On Fig. 5, it is seen that the nickel crystals are generally around 10 nm in diameter. A mixture of amorphous carbon, whisker carbon and gum was formed on all the nickel catalysts. Apparently, the gum formation is more predominant on the Ag/Ni catalyst than on any of the other catalysts where whisker carbon formation seems to dominate. According to Rostrup-Nielsen *et al.*,[17,18] gum formation leads to rapid catalyst deactivation caused by carbon encapsulation of the metal on the catalyst pellets (*cf.* Table 3). This can perhaps explain why the Ag/Ni catalyst deactivates more rapidly than the other catalysts. The Ag particles are expected to block the most reactive sites on the Ni crystals, the step-sites, and thereby significantly lower the ethanol SR reaction rate. This will cause a much higher ethanol concentration on the surface and therefore a higher carbon formation rate.

On the other Ni catalysts, where whisker carbon dominates, less deactivation should be observed due to the fact that whisker carbon does not immediately lead to deactivation of the catalyst.[18] Whisker carbon or carbon nanotubes is a result

Table 3 Carbon-forming reactions and nature of the coke deposits

Reaction		Carbon type	Phenomena	Critical parameters
$2CO \leftrightarrow C + 2CO_2$	(2)	Whisker carbon	Break-up of catalyst pellets	Low H_2O/C ratio, high temperature, presence of olefins and aromatics
$CO + H_2 \leftrightarrow C + H_2O$	(3)			
$CH_4 \leftrightarrow C + 2H_2$	(4)			
$C_nH_m \rightarrow nC + m/2H_2$	(5)			
$C_nH_m \rightarrow$ olefins $\rightarrow$ coke	(6)	Pyrolytic coke	Encapsulation of catalyst pellet, deposits on tube wall	High temperature, residence time, presence of olefins
$C_nH_m \rightarrow (CH_2)_n \rightarrow$ gum	(7)	Gum	Blocking of metal surface	Low H_2O/C ratio, low temperature, presence of olefins and aromatics, absence of H_2

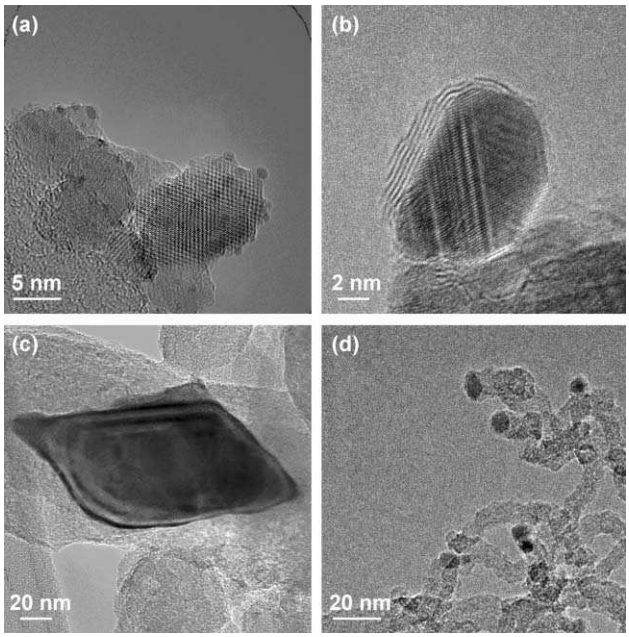

Fig. 5 TEM images of typical carbon formations on the different catalysts: (a) Ru catalyst, the image shows an ensemble of supported Ru particles without carbon deposits; (b) Ag/Ni catalyst, the image shows a Ni particle encapsulated by gum (graphitic layers); (c) K/Ni catalyst, the image shows an 'octopus' carbon nanofiber formed around a Ni particle; (d) Ni catalyst, the image shows numerous carbon nanofibers with Ni particles located at their tip apexes.

of adsorbed carbon atoms, which forms on a Ni particle, diffuses and nucleates into a carbon fiber. In this process, most of the nickel crystal remains open for catalysis and only part of it is blocked by the growing carbon fiber. However, eventually the catalyst particle will be completely destroyed as described in Table 3.[18]

The K/Ni catalyst was very special in the way that among the small Ni crystals several relatively large particles (around 100 nm) were also present resulting in carbon formed in the so-called 'octopus' structure, where several fibers are growing from one nickel crystal (*cf.* Fig. 5).[23] These large particles create a kind of whisker carbon formation, which perhaps partly can explain the almost complete lack of deactivation observed with the K-promoted catalyst. Another important observation is, of course, that far less carbon is formed on the K/Ni catalyst, which could also be the reason for the very slow deactivation. The reason why less carbon is formed on the K/Ni catalyst can probably be ascribed to a better steam adsorption as discussed.[17]

Essentially no carbon was observed on the ruthenium catalyst, which is in agreement with earlier published work on methane SR.[24] As seen in Fig. 5, the Ru particles are distributed quite uniformly on the spinel with a crystal size of *ca.* 1–2 nm.

Fig. 6 clearly illustrates the effect of temperature on the amount of carbon formed on the catalysts. Experiments performed at high temperatures *e.g.* 873 K show no catalyst deactivation and almost no carbon formations on any of the catalysts, even after running for a week. These results are somewhat surprising since methane decomposition on

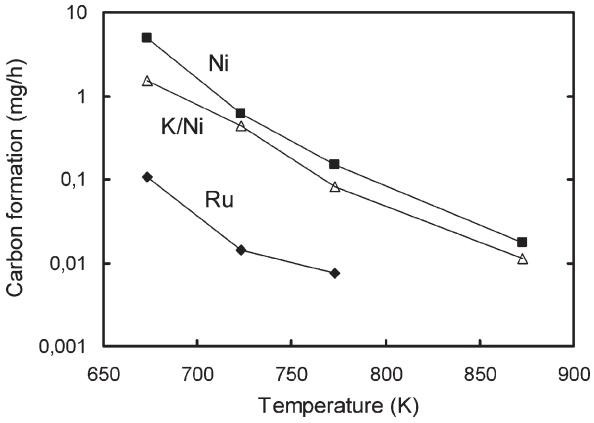

Fig. 6 Carbon formation as a function of temperature.

supported nickel catalysts usually leads to increasing carbon formation with increasing temperature.[18] This might be explained by diffusion limitations at high temperatures resulting in a very low ethanol concentration at the catalyst surface and therefore in a very low rate of carbon formation. It is clear that promotion by potassium has a positive effect on the nickel catalyst because it significantly lowers the coking rate. The silver-promoted catalyst is not included in this diagram because the rapid deactivation gives incomparable results regarding the hourly normalized carbon formation. The Ru catalyst is by far the best of the tested catalysts, especially at lower temperatures around 673 K.

Applications

Ethanol SR can be implemented either in mobile or stationary units. For 'on-board' SR in vehicles, relatively low temperatures should be applied in order to meet the requirements of the polymer electrolyte membrane fuel cell (PEMFC). This type of FC is probably the most convenient to use in cars, because of its high power density and its ability to vary the output very fast, which, for example, is required to reach the power demands for a quick start-up. To run the SR 'on-board' it will be necessary to burn some of the ethanol to make the required heat for the endothermic SR reaction. Cavallaro *et al.*[14,25] suggest instead to use a molten carbonate FC (MCFC). MCFCs, as well as solid oxide FCs (SOFCs), are convenient when running due to their operating temperature of around 900–1200 K, which provides the system with the necessary heat for the SR reaction, improves the hydrogen production and lowers the coking rate. Moreover, the MCFC and SOFC can use a less clean hydrogen fuel than the PEMFC. However, the high temperatures needed for the MCFC or SOFC are also the main disadvantage of the system for use in vehicles where they cannot meet the flexibility requirements.[26] They are more likely to be used in a stationary system. The optimal hydrogen production is, however, according to equilibrium calculations[20] at high temperatures. Therefore a better alternative might be to integrate a SR and water gas shift (WGS) reactor in extension to the bio-refinery producing the ethanol. Westermann and Ahring[27] describe a new type of bio-refinery in which bio-material rich in lignocelluloses (*e.g.* straw) can be used in combination with

manure for a combined ethanol and methane production. In this bio-refinery the methane produced could be used directly as a fuel for the endothermic SR process. Another possibility is to add a SOFC or a MCFC to the system to produce electricity, and then use the generated heat at 900–1200 K to run the endothermic SR reaction.

Moreover, for implementation of 'on-board' ethanol SR in vehicles, no carbon formations are allowed on the catalyst during the lifetime of the vehicle. It will be far too inconvenient if the catalyst is something that has to be replaced over time. For stationary applications the requirements for the catalyst could perhaps be a little less strict concerning the carbon formations. It might be acceptable, after a certain period of time, that the catalyst should be replaced, or at least oxidized to get rid of possible carbon depositions. Nevertheless, carbon depositions should by all means be minimized.

An alternative to lower the coke depositions and the costs for the endothermic SR, which has gained a lot of interest,[11,28] is to do oxidative SR [eqn (8)]. For this exothermic reaction no external heat is necessary to do the SR. Moreover, the oxygen decreases the coke depositions by oxidizing the solid carbon to CO and CO_2. However, the total amount of hydrogen produced by oxidative SR is significantly less than from non-oxidative SR.

$$CH_3CH_2OH + 2H_2O + \tfrac{1}{2}O_2 \rightarrow 2CO_2 + 5H_2 \qquad (8)$$

Conclusions

Bioethanol is a fast growing industrial chemical, whose main use is as an additive to gasoline for fueling automobiles. However, simple calculations indicate that this is an inefficient use of the chemical. Instead, bioethanol could be converted to hydrogen and used in fuel cells, which have much higher energy efficiencies.

Catalytic conversion of bioethanol by SR has turned out to be a very promising route to hydrogen. But severe difficulties with catalyst deactivation caused by coke depositions exist.

In this paper it is clarified how important the temperature is on the rate of carbon formation on the catalysts. It is shown that at 873 K both Ru- and Ni-based catalysts perform without any deactivation under the chosen conditions. Below 773 K, however, a noble metal like Ru is needed to avoid coke depositions.

It is illustrated how the addition of other metals to the $Ni/MgAl_2O_4$ catalyst influence the type of carbon deposition formed on the catalysts. Doping with K prolonged the lifetime of the catalyst by lowering the rate of carbon formation, whereas Ag promotion lowered the lifetime of the catalyst probably, due to a more pronounced gum carbon formation.

Both the $Ru/MgAl_2O_4$ catalyst and the $Ni/MgAl_2O_4$-based catalysts had high selectivity towards hydrogen since the reaction mixture was equilibrated. This also meant the total conversion of ethanol.

The $K–Ni/MgAl_2O_4$ catalyst is very cheap and a promising candidate for high temperature SR in stationary systems. However, low temperature SR could be even more interesting regarding its use in mobile units, and here the $Ru/MgAl_2O_4$ catalyst shows great potential. The challenges for the implementation in mobile units are, on the other hand, probably much more difficult than in stationary systems.

Acknowledgements

The Center for Sustainable and Green Chemistry is sponsored by the National Danish Research Foundation.

References

1 E. C. Wanat, K. Venkataraman and L. D. Smith, *Appl. Catal., A*, 2004, **276**, 155–162.
2 L. F. Brown, *Int. J. Hydrogen Energy*, 2001, **26**, 381–397.
3 H. Bayraktar, *Renewable Energy*, 2005, **30**, 1733–1747.
4 *Bio-methane & Bio-hydrogen: status and perspectives of biological methane and hydrogen production*, ed. J. H. Reith, R. H. Wijffels and H. Barten, Dutch Biological Hydrogen Foundation, ZG Petten, Netherlands, 2003.
5 RNCOS, *Biofuel Market Worldwide (2006)*, July 1, 2006, 85 pp., pub. ID: CICQ1316286, http://www.rncos.com.
6 L. Schlapbach and A. Züttel, *Nature*, 2001, **414**, 353–358.
7 I. Chorkendorf and J. W. Niemantsverdriet, in *Concepts of Modern Catalysis and Kinetics*, Wiley-VCH, Weinheim, 2003.
8 J. R. Rostrup-Nielsen, *Phys. Chem. Chem. Phys.*, 2001, **3**, 283–288.
9 F. O. Licht, *World Ethanol and Biofuels Report*, vol. 4, no. 17 (9 May 2006), Table: 'Ethanol: World Production, by Country', p. 395.
10 A. Haryanto, S. Fernando, N. Murali and S. Adhikari, *Energy Fuels*, 2005, **19**, 2098–2106.
11 V. Fierro, O. Akdim and C. Mirodatos, *Green Chem.*, 2003, **5**, 20–24.
12 F. Auprêtre, C. Descorme and D. Duprez, *Catal. Commun.*, 2002, **3**, 263–267.
13 F. Auprêtre, C. Descorme, D. Duprez, D. Casanave and D. Uzio, *J. Catal.*, 2005, **233**, 464–477.
14 F. Frusteri, S. Freni, L. Spadaro, V. Chiodo, G. Bonura, S. Donato and S. Cavallaro, *Catal. Commun.*, 2004, **5**, 611–615.
15 F. Frusteri, S. Freni, V. Chiodo, L. Spadaro, O. Di Blasi, G. Bonura and S. Cavallaro, *Appl. Catal., A*, 2004, **270**, 1–7.
16 D. K. Liguras, D. I. Kondarides and X. E. Verykios, *Appl. Catal., B*, 2003, **43**, 345–354.
17 J. R. Rostrup-Nielsen, *Steam Reforming Catalysts*, Teknisk Forlag, Copenhagen, 1975.
18 J. R. Rostrup-Nielsen, J. Sehested and J. K. Nørskov, *Adv. Catal.*, 2002, **47**, 65–139.
19 P. D. Vaidya and A. E. Rodrigues, *Chem. Eng. J.*, 2006, **117**, 39–49.
20 Equilibrium calculations are performed with the program Outokumpu HSC Chemistry 5.1.
21 R. T. Vang, K. Honkala, S. Dahl, E. K. Vestergaard, J. Schnadt, E. Lægsgaard, B. S. Clausen, J. K. Nørskov and F. Besenbacher, *Nat. Mater.*, 2005, **4**, 160–162.
22 F. Besenbacher, I. Chorkendorff, B. S. Clausen, B. Hammer, A. M. Molenbroek, J. K. Nørskov and I. Stensgaard, *Science*, 1998, **279**, 1913–1915.
23 C. A. Bernardo, I. Alstrup and J. R. Rostrup-Nielsen, *J. Catal.*, 1985, **96**, 517–534.
24 J. R. Rostrup-Nielsen and J.-H. B. Hansen, *J. Catal.*, 1992, **144**, 38–49.
25 S. Cavallaro, *Energy Fuels*, 2000, **14**, 1195–1199.
26 N. M. Sammes, Y. Du and R. Bove, in *Biofuels for Fuel Cells*, ed. P. Lens, P. Westermann, M. Haberbauer and A. Moreno, IWA, London, UK, 2005, ch. 14, pp. 235–247.
27 P. Westermann and B. Ahring, in *Biofuels for Fuel Cells*, ed. P. Lens, P. Westermann, M. Haberbauer and A. Moreno, IWA, London, UK, 2005, ch. 11, pp. 194–205.
28 G. A. Deluga, J. R. Salge, L. D. Schmidt and X. E. Verykios, *Science*, 2004, **303**, 993–997.

INTERNATIONAL JOURNAL OF HYDROGEN ENERGY 33 (2008) 4547–4554

Available at www.sciencedirect.com

ScienceDirect

journal homepage: www.elsevier.com/locate/he

Steam reforming of technical bioethanol for hydrogen production

Jeppe Rass-Hansen[a], *Roger Johansson*[a], *Martin Møller*[b], *Claus Hviid Christensen*[a,*]

[a]*Center for Sustainable and Green Chemistry, Department of Chemistry, Technical University of Denmark, Building 206, DK-2800 Kgs. Lyngby, Denmark*

[b]*DONG Energy, DK-7000 Fredericia, Denmark*

ARTICLE INFO

Article history:
Received 8 May 2008
Received in revised form
13 June 2008
Accepted 14 June 2008
Available online 19 August 2008

Keywords:
Bioethanol
Steam reforming
Carbon depositions
Hydrogen production

ABSTRACT

Essentially all work on ethanol steam reforming so far has been carried out using simulated bioethanol feedstocks, which means pure ethanol mixed with water. However, technical bioethanol consists of a lot of different components including sugars, which cannot be easily vaporized and steam reformed. For ethanol steam reforming to be of practical interest, it is important to avoid the energy-intensive purification steps to fuel grade ethanol. Therefore, it is imperative to analyze how technical bioethanol, with the relevant impurities, reacts during the steam reforming process. We show how three different distillation fractions of technical 2nd generation bioethanol, produced in a pilot plant, influence the performance of nickel- and ruthenium-based catalysts during steam reforming, and we discuss what is required to obtain high activity and long catalyst lifetime. We conclude that the use of technical bioethanol will result in a faster catalyst deactivation than what is observed when using pure ethanol–water mixtures because of contaminants remaining in the feed. However, the initial activity of the catalysts are not affected by this, hence it is important to not only focus on catalyst activity but rather on the lifetime of the catalyst.

1. Introduction

Recent reviews [1–3] show how steam reforming (SR) of ethanol has received significant attention in the literature as a promising way to produce hydrogen from renewable resources. However, so far essentially all reported investigations have been performed with pure ethanol/water mixtures, i.e. by mixing distilled ethanol and water. Here, we present results on catalytic steam reforming of technical 2nd generation bioethanol produced from straw. To our knowledge, this is the first investigation using 2nd generation bioethanol feedstock although there do exist a few previous papers on the topic using 1st generation bioethanol [4–6]. The difference between 1st and 2nd generation bioethanol is the source of feedstock. 1st generation feedstocks are for instance corn, sugarcane and crops, whereas 2nd generation feedstocks could be agricultural waste, wood or household waste. Typically, 1st generation feedstocks are based on sucrose or starch whereas 2nd generation feedstocks are based on lignocellulose. Ethanol is produced by fermentation of glucose, which is readily achieved from the first group of feedstocks through simple hydrolysis. 2nd generation feedstocks typically consist of cellulose, hemicelluloses and lignin with the glucose bound in complex structures and more energy is required to release the glucose for fermentation [7]. It is important to realize that the 1st generation feedstocks are also used as food for humans and animals, which is usually not the case for the 2nd generation feedstocks. The use of 1st generation

* *Corresponding author.*
E-mail address: chc@kemi.dtu.dk (C.H. Christensen).
0360-3199/$ – see front matter
doi:10.1016/j.ijhydene.2008.06.020

bioethanol has led to a vehement debate about the ethical issues of using food for fuels, see for example reference [8]. Contrary to 1st generation bioethanol, 2nd generation bioethanol significantly reduce greenhouse gas emissions from fuels [9], thus the use of 2nd generation plants are expected to increase at the expense of 1st generation bioethanol plants. Also, the use of diverse feedstocks for the production of ethanol can pose different challenges in a subsequent steam reforming process, due to the variety of contaminants, and hence it is vital to have good experimental data with different feeds. We have analyzed three different distillation fractions of a technical 2nd generation bioethanol produced from wheat straw and we will give a discussion about the hurdles in using technical bioethanol in steam reforming.

The two largest producers of bioethanol in the world are Brazil and the USA, each producing approximately 13 million tons annually (2005) [10] from sugarcane and corn, respectively. With regard to the Brazilian situation, the price of ethanol is comparable to, if not lower than, the equivalent amount of fossil fuel, and the amount of sugarcane available exceeds the need as an edible resource, leading to a situation that might be sustainable [11]. In the US, bioethanol is mainly produced by fermentation of corn. With a corn/oil price ratio that has decreased more than 10 times in the last 60 years [12], bioethanol is continuously gaining importance as a fuel for combustion engines in vehicles. The efficiency of a combustion engine is, however, relatively low and only 20–25% [13] of the energy in the fuel is converted into useful power. Fuel cells, on the other hand, potentially have energy efficiencies of 50–60% [13–15] when operating on pure hydrogen. Fuel cells connected to an onboard ethanol reformer could potentially be used in the automotive sector or to produce heat and power in household micro combined heat and power plants (CHP's). Therefore, a process allowing inexpensive and energy-efficient conversion of bioethanol to hydrogen could increase the value of the fuel considerably [16].

Important factors to consider when evaluating the use of bioethanol as fuel or feedstock is the overall economy of the processes involved as well as the energy-efficiency from biomass to wheel. Fuel grade bioethanol needs to be water-free, thus the production requires distillation beyond the azeotrope point, and this is one of the major production costs of fuel-ethanol [17–19]. On the other hand, the ethanol SR process requires a significant amount of water (Eq. (1)), which makes the expensive distillation superfluous. Only a simple flash distillation to some 50–70% is necessary thereby considerably lowering the production costs of bioethanol.

$$CH_3CH_2OH + 3H_2O \rightarrow 2CO_2 + 6H_2 \quad (1)$$

The use of 1st generation bioethanol, like that obtained in Brazil and in the US from sugarcane and corn is, as mentioned above, continuously questioned due to the use of food for fuels [20]; and there have also been concerns over the amount of fossil fuels used in the production of the bioethanol [18] but the topic is still controversial [8,21]. In most places of the world, it will only be reasonable to produce bioethanol from non-food resources like household waste, straw, cornstower and wood. These resources are often considered to be waste materials and are thus significantly less valuable than edible ones; not only will the use of these resources not interfere with food production it will also greatly reduce the greenhouse gas emissions and feedstock costs from the ethanol production [9]. Therefore, there is globally an intense research on developing so-called 2nd generation bioethanol, however only a few companies have reached the point of demonstrating the process in a pilot plant. The Danish company Inbicon, a subsidiary of DONG Energy A/S, has for the last 4 years operated a pilot plant, able to convert straw into ethanol using the so-called IBUS process. The demonstration plant is located in Skærbæk, Denmark, and has a capacity up to 1000 kg of straw per hour. The bioethanol examined in this paper was received from this pilot plant.

2. Experimental

2.1. *Production and characterization of technical bioethanol*

The bioethanol received from Inbicon, was delivered in three different purities. The produced fractions were based on a run of 50 kg/hr of Danish wheat straw. The straw was heated with steam for 5–15 min between 180 and 220 °C. The dry-matter concentration of the pretreated straw was approximately 26%. To the pretreated straw was added yeast and enzymes supplied by Novozymes AS, no other chemicals are added in the process. The mixture of heated straw, enzymes and yeast were fermented for 5 days in an 11 m^3 fermenter, which resulted in an ethanol concentration of around 5–6%. This fibre beer was distilled in a traditional distillation column, with modified trays in the stripper section. The column has a capacity of 1000 kg fibre beer per hour, and is operated under vacuum at around 0.1 bar. The Inbicon Process is well described in a recent paper [22].

The first fraction was the ''fibre beer'', which is 5–6% ethanol in a mixture of water and biomass residues. The other two fractions where taken from different parts of the distillation process. Fractions 2 and 3, with greatly reduced amounts of impurities, had an ethanol concentration of 42 and 72 vol%, respectively. All fractions have been analyzed by GC-MS (Agilent 6850 GC equipped with a capillary HP-5MS column an FID detector and Agilent 5975C MSD) and GC (Agilent 6890 N equipped with a capillary HP-5 column and FID detector), the beer was also analyzed by HPLC (Dionex Ultimate 3000 HPLC equipped with a Phenomenex Rezex RHM-Monosaccharide H^+ 8% Column) to determine the composition of each.

2.2. *Catalyst synthesis*

A 10 wt% Ni/$MgAl_2O_4$ and a 1 wt% K doped 10 wt% Ni/$MgAl_2O_4$ catalyst were prepared by the incipient wetness impregnation technique. An industrial high surface area spinel ($MgAl_2O_4$) with a pore volume of 427 mL kg^{-1} and a specific surface area of 72 $m^2\,g^{-1}$ received from Haldor Topsøe A/S was used as support material. The spinel tablets were crushed to a size fraction of 300–710 μm and dried for 1 h at 100 °C. The solution for the impregnation was prepared by dissolving the desired amount of the different metal compounds, as nitrate salts, in water under moderate heating. After impregnation, the catalysts were dried at 100 °C for 2 h and finally

Table 1 – Composition of the catalysts studied

Sample	Composition
Ni	10 wt% $Ni/MgAl_2O_4$
K/Ni	1 wt% K–10 wt% $Ni/MgAl_2O_4$
Ru	2 wt% $Ru/MgAl_2O_4$

calcined at 500 °C for 4 h. A 2 wt% $Ru/MgAl_2O_4$ catalyst was prepared similarly from a nitrosyl nitrate aqueous solution [$Ru(NO)(NO_3)_3$], leaving out the calcination step to prevent any formation of the volatile and hazardous RuO4 as well as to avoid a decrease in reactivity of the catalyst due to metal sintering. The different catalysts investigated in this study are listed in Table 1.

2.3. Catalyst characterization

All catalysts were characterized by BET surface area measurements and hydrogen pulse chemisorptions to determine the total surface area, metallic surface area, metal dispersion and metal particle size. The results are summarized in Table 2. The hydrogen pulse chemisorptions were made at 50 °C for the nickel-based catalysts and at 150 °C for the ruthenium catalyst. Before the actual pulse chemisorptions, the catalysts were reduced and activated in situ according to the catalytic experiments described in the next paragraph. After the reduction, the catalyst was kept at the temperature for 1 h in a nitrogen flow of 50 mL min^{-1} to remove adsorbed hydrogen.

2.4. Catalytic measurements

The experimental setup used in the catalytic investigation is shown in Fig. 1. Catalytic experiments were performed in a tubular fixed bed quartz reactor with an inner diameter of 6 mm. For each test, 200 mg of catalyst material was loaded into the reactor and secured by quartz wool. The reactor was placed in an electrically heated oven. Before each run, the loaded catalyst was reduced and activated by heating at 5 °C min^{-1} to 500 °C for 2 h in a gas flow of 100 mL min^{-1} of Formier gas (10% hydrogen in nitrogen) (the Ru catalyst was reduced at 600 °C). SR experiments, at 400, 450, 500 and 600 °C, were conducted with a helium gas flow of 80 mL min^{-1} and an ethanol/water liquid flow of 0.04 mL min^{-1}. The liquid was pumped by a Knauer K-120 HPLC pump and vaporized by heating tape at 150–200 °C. The bioethanol (fraction 3) was diluted to approximately 25 vol% ethanol, which gave a total molar gas flow ratio to the catalyst bed of ethanol–water–helium of about 1:10:20. An Agilent GC 6890 N equipped with a CP Poraplot Q-HT capillary column to the FID detector and an advanced packed column system consisting of Porapak N column and a Molsieve column to the TCD detector was used for analyzing the reaction stream. Furthermore, a Rosemount BINOS 100 was continuously measuring the CO and CO2 contents in the exit gas after condensation of any liquids in an ice bath. The condensate was mainly water and occasionally minor amounts of unreacted ethanol and trace amounts of other liquid species.

2.5. Temperature programmed oxidation (TPO)

The experimental setup used for activity measurements was also used for analyzing the amount of carbon formed on the catalysts during SR. The TPO experiments were carried out by heating the oven to 600 °C at 10 °C min^{-1} in a gas flow of 20 mL min^{-1} consisting of a mixture of 5% oxygen in helium. By this method, the carbon deposits was completely oxidized to CO and CO_2, thus facilitating accurate measurements with the BINOS detector.

3. Results and discussion

3.1. Technical bioethanol

The unpurified fibre beer fraction is a dark mixture of many different compounds (cf. Table 3) and some sort of purification is needed before it can be used in any process. If the solids are disregarded, the main contaminants are different sugars and higher alcohols. Several methods were investigated for cleaning the broth with the best results obtained by using activated carbon under reflux at 80 °C for 16 h. After filtration, a clear ethanol solution was obtained but it still contained considerable amounts of sugars, which caramelize as soon as vaporization of the solution is attempted. No easy and inexpensive method was found for removing these sugars except distillation. Hence, this fraction was not studied further in the steam reforming reaction.

Although the different sugars in the beer have to be removed, there is no need to distill to fuel grade ethanol; for SR purposes, a simple flash distillation will probably be sufficient. This will remove the parts of the feed that are not easily vaporized, whereas most of the fusel oils and other low boiling contaminants will remain in the ethanol solution. It has been shown elsewhere [5] that this should not necessarily pose a problem since these contaminants can also be steam reformed and only cause an apparent higher yield of H_2 from the reaction. However, Akande et al. [5] used 1st generation bioethanol available from fermentation of crops with mainly lactic acid and glycerol as contaminants, which are very different than those from our study, cf. Table 3. Glycerol has previously been proven reformable [23–25] however the

Table 2 – Catalyst characterization by BET and hydrogen pulse chemisorption

Catalyst	BET surface area ($m^2 g^{-1}$)	Metal surface area ($m^2 g^{-1}$ metal)	Metal dispersion (%)	Metal particle size (nm)
10% $Ni/MgAl_2O_4$	72	66	9.9	10
1% K–10% $Ni/MgAl_2O_4$	74	40	6.0	17
2% $Ru/MgAl_2O_4$	92	265	84	1.9

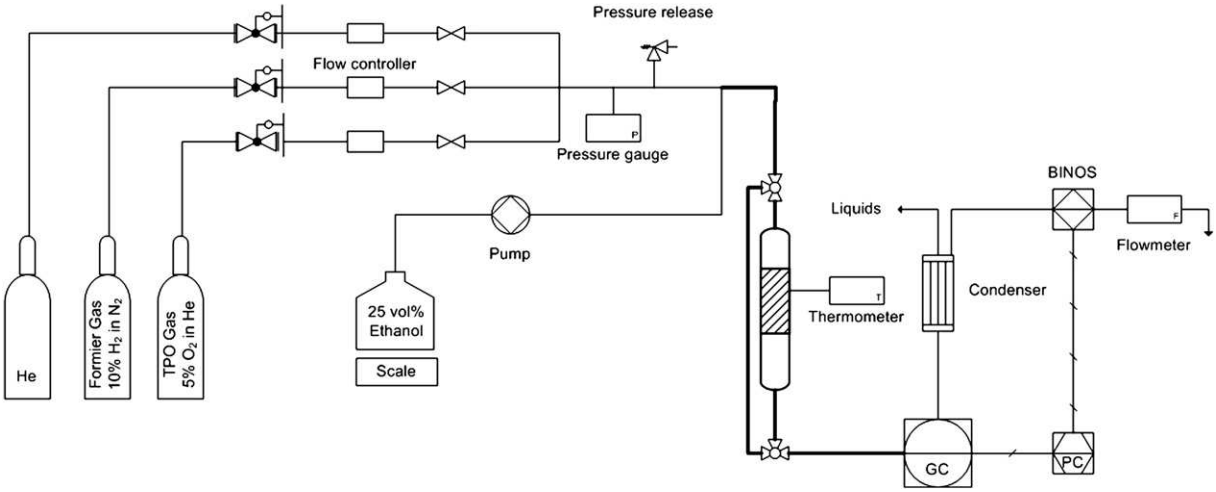

Fig. 1 – Schematic drawing of the experimental setup for the catalytic measurements.

requirements of the equipment are considerably different. The composition of contaminants in various grades of bioethanol is dependent on the feedstocks used and the different refinery processes in 1st and 2nd generation plants.

To make the ethanol SR process as economically feasible as possible, it is required that the purification of the feedstock is kept at a minimum. Therefore, this paper investigates the steam reforming reaction using technical bioethanol of different purities. As seen in Table 3, the main contaminants found in fractions 2 and 3 are various higher alcohols, which are not expected to be detrimental for the reaction. By this reasoning, the fraction with lower concentration of ethanol (fraction 2) should be the preferred feedstock for steam reforming, or perhaps a distillation fraction that matches the overall stoichiometry of the reaction with an ethanol to water molar ratio of 1:3, cf. reaction (1). The use of this fraction would allow a reduction in the cost of the feedstock, but the question still remains as to whether this fraction of bioethanol will perform comparably to using a pure ethanol/water mixture.

3.2. *Catalyst synthesis and characterization*

The catalysts used in this paper were chosen due to the industrial importance of Ni/MgAl2O4 catalyst for the SR reactions [26,27]. The spinel support has a good stability at high water pressures and temperatures, and it does not contain acidic sites, which are known to increase the carbon formation rate [28–30]. The potassium doped catalyst was expected to have a lower carbon formation rate due to the potassium covering the most active step-sites on the nickel crystals [31] as well as increasing the steam adsorption on the catalyst [26]. The ruthenium catalyst was included in this study according to recent promising results in the literature with this metal [29].

From Table 2, it is seen that the BET surface area of the spinel (72 $m^2 g^{-1}$) does not change when impregnating with Ni and K/Ni. A minor increase in surface area is observed upon impregnation with Ru, which might be attributed to the high acidity of the nitrosyl nitrate solution used to impregnate the support. The metal particle size of Ni and Ru of 10 and 1.9 nm, respectively, is very well in agreement with previously observed results from TEM experiments performed on the same catalysts in a previous study [16]. Also the relatively large average diameter of 17 nm for the K/Ni catalyst can be explained by earlier TEM analysis of this catalyst, which showed that the particles were typically around 10 nm like the undoped Ni catalyst but with several very large metal particles of up to 100 nm among them [16]. This will obviously

Table 3 – Constituents in the different fractions of bioethanol as determined by HPLC (fraction 1) and GC-MS (fractions 2 and fraction 3)

	Fraction 1	Vol%	Fraction 2	Mol%	Fraction 3	Mol%
Major constituents	Ethanol	5.7	Ethanol	18	Ethanol	44
	Xylose	1.2	3-Methyl-1-butanol	0.7	Ethyl acetate	0.5
	Glucose	1.1	2-Methyl-1-propanol	0.3	1,1-Diethoxyethane	0.2
	Lactate	0.5	2-Methyl-1-butanol	0.3		
	Acetate	0.5	Propanol	0.1		
	Glycerol	0.4	Cyclopentanone	0.05		
Trace constituents	Ethyl acetate		Furfural		Propanol	
	Acetic acid		4-Hexen-1-ol		2-Methyl-1-propanol	
			1,1-Diethoxyethane		3-Methyl-1-butanol	
					2-Methyl-1-butanol	
					Cyclopentanone	

result in a higher average diameter and a lower metal dispersion.

Ru catalysts are known to be rather difficult to analyze with chemisorption techniques [32]. Here, a TPD experiment was performed to analyze at which temperature the Ru starts to release adsorbed hydrogen. This happens at around 200 °C and therefore a slightly lower temperature of 150 °C was chosen for the hydrogen pulse experiment. On the other hand, a standard hydrogen pulse chemisorption procedure at 50 °C was chosen for the Ni-based catalysts.

3.3. SR experiments

Steam reforming of ethanol is thought to proceed through two separate routes; either by dehydrogenation to acetaldehyde (Eq. (2)) or by dehydration forming ethylene (Eq. (3)).

$$CH_3CH_2OH \rightarrow CH_3CHO + H_2 \quad (2)$$

$$CH_3CH_2OH \rightarrow C_2H_4 + H_2O \quad (3)$$

These two intermediate products can then be decomposed and steam reformed to an equilibrium mixture of methane, carbon dioxide, carbon monoxide, hydrogen and water (Eqs. (4)–(6)). Fig. 2 shows the theoretical equilibrium composition, under the experimental conditions given in the experimental section. At equilibrium the ethanol conversion is 100%, and selectivities in Fig. 2 are in complete agreement with the actual results for all the catalysts in the investigated temperature interval of 400–600 °C, as long as no deactivation is observed. Furthermore, ethylene is known to polymerize into pyrolytic coke on metal surfaces (Eq. (7)) [27], and it is assumed that it is mostly ethylene that is responsible for the carbon formation on the catalyst in this reaction although other carbon-forming reactions (Eqs. (8) and (9)) can also be important [27]. The final two reactions for achieving equilibrium among the gasses are the methane SR reaction (10) and the water gas shift (WGS) reaction (11).

$$CH_3CHO \rightarrow CH_4 + CO \quad (4)$$

$$CH_3CHO + H_2O \rightarrow 3H_2 + 2CO \quad (5)$$

$$C_2H_4 + 2H_2O \rightarrow 4H_2 + 2CO \quad (6)$$

$$C_2H_4 \rightarrow \text{coke} \quad (7)$$

$$CH_4 \rightarrow 2H_2 + C \quad (8)$$

$$2CO \rightarrow CO_2 + C \quad (9)$$

$$CH_4 + H_2O \rightarrow 3H_2 + CO \quad (10)$$

$$CO + H_2O \rightarrow CO_2 + H_2 \quad (11)$$

For an accurate comparison between the technical bioethanol and the commonly used ethanol/water mixtures, the same catalysts (Ni, K/Ni and Ru cf. Table 1) as those previously

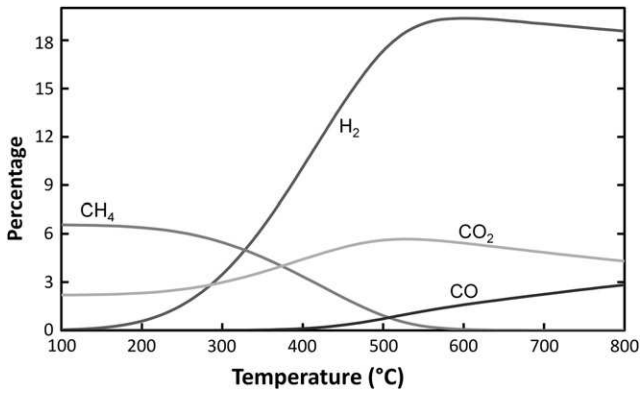

Fig. 2 – Gas composition at equilibrium, at full ethanol conversion, as a function of the temperature for the ethanol steam reforming reaction with a start composition of ethanol/water/helium of 1:10:20. Water has been withdrawn from the calculations since it is being physically condensed out and is not present at the BINOS inlet. The calculations were performed with the equilibrium calculator in *HSC Chemistry* 5.1 by Outokumpo Research Oy, Finland.

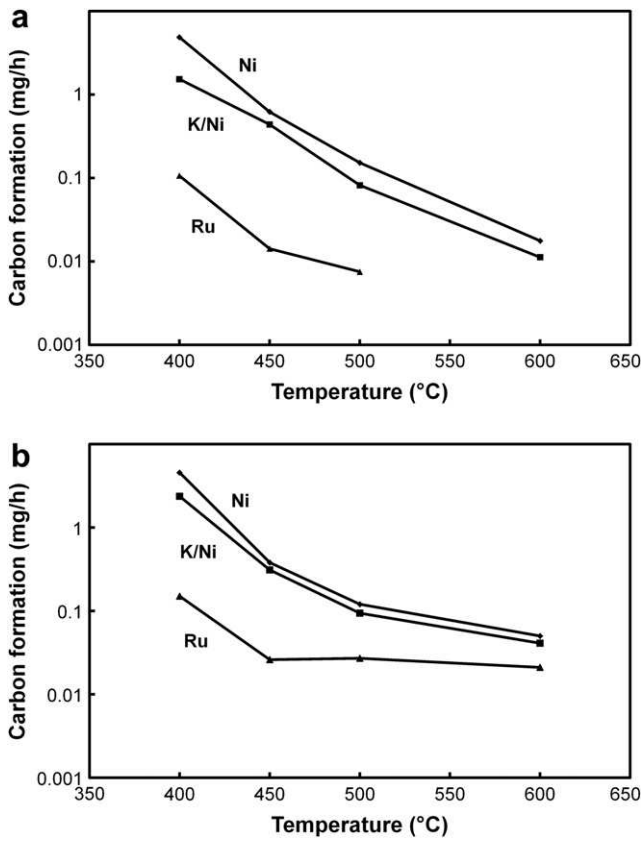

Fig. 3 – Carbon formation rate on the different catalysts as a function of reaction temperature using a: 25 vol% ethanol in water and b: bioethanol (Fraction 3 diluted to 25 vol% ethanol) as feedstock. Composition of catalysts according to Table 1.

Table 4 – Carbon formation rate in accordance to Fig. 3

Temperature (°C)	Ni (mg h^{-1})	K/Ni (mg h^{-1})	Ru (mg h^{-1})	Ni-bio (mg h^{-1})	K/Ni-bio (mg h^{-1})	Ru-bio (mg h^{-1})
400	4.86	1.53	0.11	4.55	2.37	0.15
450	0.62	0.44	0.014	0.38	0.31	0.026
500	0.15	0.082	0.008	0.12	0.094	0.027
600	0.02	0.011		0.05	0.041	0.021

investigated in our group were used [16]. In our previous investigation, it was seen that most experiments showed equilibrium composition in the exit gas, which means that all ethanol was converted to a mixture of H_2, CO_2, CO, CH_4 and H_2O. Furthermore, the experiments showed that carbon formation was highly affected by the operating temperature and the choice of catalyst. Only small amounts of carbon were deposited on any of the catalysts at 600 °C. At 400 °C, it was only the Ru catalyst, which had a full ethanol conversion and a low rate of carbon formation, cf. Fig. 3a [16]. For the current experiments, the bioethanol of fraction 3 was diluted to approximately 25 vol% ethanol to facilitate the comparison with previous results. From Fig. 3b and Table 4, it can be seen that the rate of carbon formation shows the same apparent order and trends in the runs with technical bioethanol as in the previous ones with a pure ethanol/water mixture. However, the rate of carbon formation is generally slightly higher for fraction 3 than for the pure ethanol/water mixture, which can be explained by the slightly higher concentration of carbon-containing compounds in the feed from the contaminants in fraction 3 compared to the pure ethanol/water mixtures. It is also evident, as in the investigation with pure ethanol/water mixtures that an increased temperature of the reaction slows down the rate of carbon formation. This behavior can most likely be explained by diffusion limitations [16]. Consequently, the concentration of ethanol at the catalyst surface will be low and therefore the rate of carbon formation will also be lower. Another observation from the comparison between Fig. 3a and b is the apparent significantly lower rate of carbon formation on the nickel-based catalysts with pure ethanol/water at 600 °C. These runs were maintained over a week compared to 16–18 hours for the experiments with technical bioethanol. It is anticipated that the rate of carbon formation is highest in the start of the reaction and therefore the apparent rate of carbon formation will be slightly lower for these two long runs.

Since the Ru catalyst had higher activity and longer lifetime at the lower temperatures, compared to the Ni-based catalysts, this catalyst was also used in a comparative study with the more contaminated bioethanol of fraction 2. This fraction was also diluted to 25 vol% and used as feed in the reaction at 400 °C and 500 °C. The exit gas composition as measured on the BINOS at 400 °C is shown in Fig. 4. From this it can be seen that the yield of CO_2 decreases whereas the yield of CO increases after approximately 12 h for fraction 2. For the run using fraction 3 as feedstock neither the CO nor the CO_2 concentration changes during the duration of the run (approximately 18 h). For the run at higher temperature, 500 °C, no deactivation is seen for any of the fractions during the duration of the run. It is also apparent that the CO_2 concentration at equilibrium is higher for fraction 2. Both of these observations make sense when the total concentration of steam reformable material is considered. The increased carbon concentration from the contaminants at the catalyst surface will give a higher rate of carbon formation, resulting in an earlier decrease in catalyst performance. The increased amount of steam reformable material is also responsible for the higher concentration of CO_2 in the exit gas; a calculation of the gas composition to the catalyst bed from fraction 2 and 3 shows that the extra contaminants in fraction 2 correspond to about a 10 mol% increase in the carbon content, in good agreement with the results in Fig. 4. On the other hand, it seems like the larger alcohols and other contaminants in fraction 2 also contribute to the faster deactivation of the catalyst. Through GC-analysis it is evident for all the experiments that full conversion of ethanol leads to the equilibrium gas-mixture as shown in Fig. 2. Moreover all the contaminants in fraction 2 and 3 are also reformed as they do not appear in the GC-analysis. First when the catalysts deactivate; ethanol, acetaldehyde, ethylene, ethane and traces of the contaminants start to appear in the exit gas. This is observed simultaneously with a decrease in methane and CO_2 and an increase in the CO concentration, and is occurring with all of the used ethanol/water mixtures.

The larger alcohols, as present in fraction 2, could cause severe difficulties through catalyst deactivation at low SR temperatures of technical bioethanol. One possible alternative to decrease carbon formation rates could be to use autothermal reforming instead of SR, this would negate some of

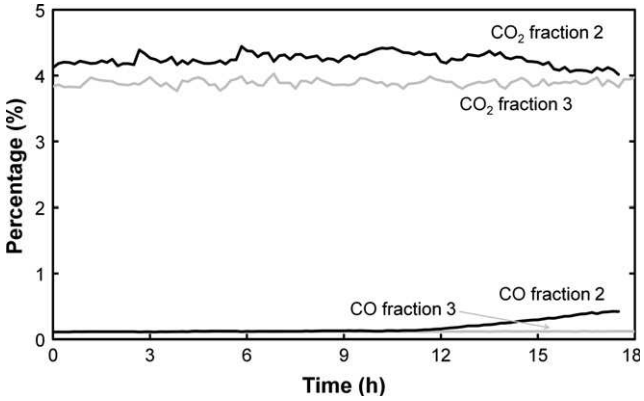

Fig. 4 – Exit gas composition over time at 400 °C for the Ru/$MgAl_2O_3$ catalyst using fraction 2 and fraction 3 as feedstock.

the problems with carbon formation but at the expense of a lower H_2 yield [33].

4. Conclusions

Here, it is shown how steam reforming of bioethanol for hydrogen production can be effectively carried out over different heterogeneous catalysts. Moreover, we have indicated some of the challenges for implementing this process into industrial applications.

Bioethanol is becoming more and more important as a fuel or fuel additive to gasoline. Yet, a conversion of ethanol to hydrogen could increase the energy-efficiency of the fuel significantly by utilizing the hydrogen in fuel cells with much higher energy efficiencies than in conventional combustion engines. One possible way to convert bioethanol to biohydrogen is by steam reforming, whereby an optimal six hydrogen molecules are formed from every molecule of ethanol (Eq. (1)).

Some industrially important heterogeneous catalysts based on ruthenium and nickel shows interesting potential as catalyst for the SR of technical bioethanol, though some challenges still remain, e.g. in reducing carbon depositions on the catalysts. A major factor in limiting carbon formations is the operating temperature. Higher temperatures decrease the carbon formation significantly. Since the activities of the catalysts are high at the temperatures used in SR, the most important parameter to optimize is the catalyst lifetime. When using technical bioethanol of lower purity the lifetime of the catalyst decreases as a consequence of the increased amount and nature of the carbon-containing compounds; this deactivation must be addressed in the design of the process. As long as the deactivation issues are accounted for, it is apparent that the use of fuel grade ethanol is not required; a simple flash distillation of the fibre beer to remove the sugars and other non-volatile substances from the feedstock seems to be sufficient. Therefore, the economics in a biorefinery can be improved by minimizing the process heat (steam) for the energy-intensive distillation along with the capital costs for the distillation equipment.

REFERENCES

[1] Haryanto A, Fernando S, Murali N, Adhikari S. Current status of hydrogen production techniques by steam reforming of ethanol: a review. Energy Fuels 2005;19:2098–106.

[2] Ni M, Leung DYC, Leung MKH. A review on reforming bio-ethanol for hydrogen production. Int J Hydrogen Energy 2007; 32:3238–47.

[3] Vaidya PD, Rodrigues AE. Insight into steam reforming of ethanol to produce hydrogen for fuel cells. Chem Eng J 2006; 117:39–49.

[4] Vargas JC, Libs S, Roger A-C, Kiennemann A. Study of Ce–Zr–Co fluorite-type oxide as catalysts for hydrogen production by steam reforming of bioethanol. Catal Today 2005;107–108: 417–25.

[5] Akande AJ, Idem RO, Dalai AK. Synthesis, characterization and performance evaluation of Ni/Al_2O_3 catalysts for reforming of crude ethanol for hydrogen production. Appl Catal A Gen 2005;287:159–75.

[6] Akande A, Aboudheir A, Idem R, Dalai A. Kinetic modeling of hydrogen production by the catalytic reforming of crude ethanol over a co-precipitated $Ni–Al_2O_3$ catalyst in a packed bed tubular reactor. Int J Hydrogen Energy 2006; 31:1707–15.

[7] Klass DL. Biomass for renewable energy, fuels, and chemicals. San Diego: Academic Press; 1998.

[8] Dale BE, Pimentel D. Two views on whether corn ethanol and, eventually, ethanol from cellulosic biomass will efficiently deliver national energy security. Chem Eng News 2007;85(51):12–6.

[9] Farrell AE, Plevin RJ, Turner BT, Jones AD, O'Hare M, Kammen DM. Ethanol can contribute to energy and environmental goals. Science 2006;311:506–8.

[10] Solomon BD, Barnes JR, Halvorsen KE. Grain and cellulosic ethanol: history, economics, and energy policy. Biomass Bioenergy 2007;31:416–25.

[11] Ritter SK. Biofuel bonanza. Chem Eng News 2007;85(26):15–24.

[12] Rass-Hansen J, Falsig H, Jørgensen B, Christensen CH. Bioethanol: fuel or feedstock? J Chem Technol Biotechnol 2007;82:329–33.

[13] Schlapbach L, Züttel A. Hydrogen-storage materials for mobile applications. Nature 2001;414:353–8.

[14] Chorkendorf I, Niemantsverdriet JW. Concepts of modern catalysis and kinetics. Weinheim: Wiley-VCH; 2003.

[15] Rostrup-Nielsen JR. Conversion of hydrocarbons and alcohols for fuel cells. Phys Chem Chem Phys 2001;3:283–8.

[16] Rass-Hansen J, Christensen CH, Sehested J, Helveg S, Rostrup-Nielsen JR, Dahl S. Renewable hydrogen: carbon formation on Ni and Ru catalysts during ethanol steam reforming. Green Chem 2007;9:1016–21.

[17] Bohlmann GM. Process economic considerations for production of ethanol from biomass feedstocks. Ind Biotechnol 2006;2(1):14–20.

[18] Pimentel D. Ethanol fuels: energy balance, economics, and environmental impacts are negative. Nat Resour Res 2003; 12(2):127–34.

[19] Seemann F. Energy reduction in distillation for bioethanol plants. Int Sugar J 2003;105:420–3.

[20] Pimentel D, Patzek T. Ethanol production: energy and economic issues related to U.S. and Brazilian sugarcane. Nat Resour Res 2007;16(3):235–42.

[21] Shapouri H, Duffield JA, Wang M. The energy balance of corn ethanol: an update. United States Department of Agriculture. Report Number 814, July 2002.

[22] Larsen J, Petersen MØ, Thirup L, Li HW, Iversen FK. The IBUS process – lignocellulosic bioethanol close to a commercial reality. Chem Eng Technol 2008;31:1–9.

[23] Adhikari S, Fernando SD, Haryanto A. Hydrogen production from glycerin by steam reforming over Ni catalysts. Renew Energy 2008;33:1097–100.

[24] Zhang BC, Tang XL, Li Y, Xu YD, Shen WJ. Hydrogen production from steam reforming of ethanol and glycerol over ceria- supported metal catalysts. Int J Hydrogen Energy 2007;32:2367–73.

[25] Simonetti DA, Rass-Hansen J, Kunkes EL, Soares RR, Dumesic JA. Coupling of glycerol processing with Fischer–Tropsch synthesis for production of liquid fuels. Green Chem 2007;9:1073–83.

[26] Rostrup-Nielsen JR. Steam reforming catalysts. Copenhagen: Danish Technical Press; 1975.

[27] Rostrup-Nielsen JR, Sehested J, Nørskov JK. Hydrogen and syngas by steam reforming. Adv Catal 2002;47:65–139.

[28] Frustreri F, Freni S, Chiodo V, Spadaro L, Blasi OD, Bonura G, et al. Steam reforming of bio-ethanol on alkali-doped Ni/MgO

catalysts: hydrogen production for MC fuel cell. Appl Catal A Gen 2004;270:1–7.
[29] Liguras DK, Kondarides DI, Verykios XE. Production of hydrogen for fuel cells by steam reforming of ethanol over supported noble metal catalysts. Appl Catal, B 2003;43:345–54.
[30] Vizcaino AJ, Carriero A, Calles JA. Hydrogen production by ethanol steam reforming over Cu–Ni supported catalysts. Int J Hydrogen Energy 2007;32:1451–61.
[31] Bengaard HS, Nørskov JK, Sehested J, Clausen BS, Nielsen LP, Molenbroeck AM, et al. Steam reforming and graphite formation on Ni catalysts. J Catal 2002;209: 365–84.
[32] Fastrup B. On the interaction of N_2 and H_2 with Ru catalyst surfaces. Catal Lett 1997;48:111–9.
[33] Deluga GA, Salge JR, Schmidt LD, Verykios XE. Renewable hydrogen from ethanol by autothermal reforming. Science 2004;303:993–7.

Green Chemistry

Cutting-edge research for a greener sustainable future

www.rsc.org/greenchem

Volume 9 | Number 10 | October 2007 | Pages 1029–1144

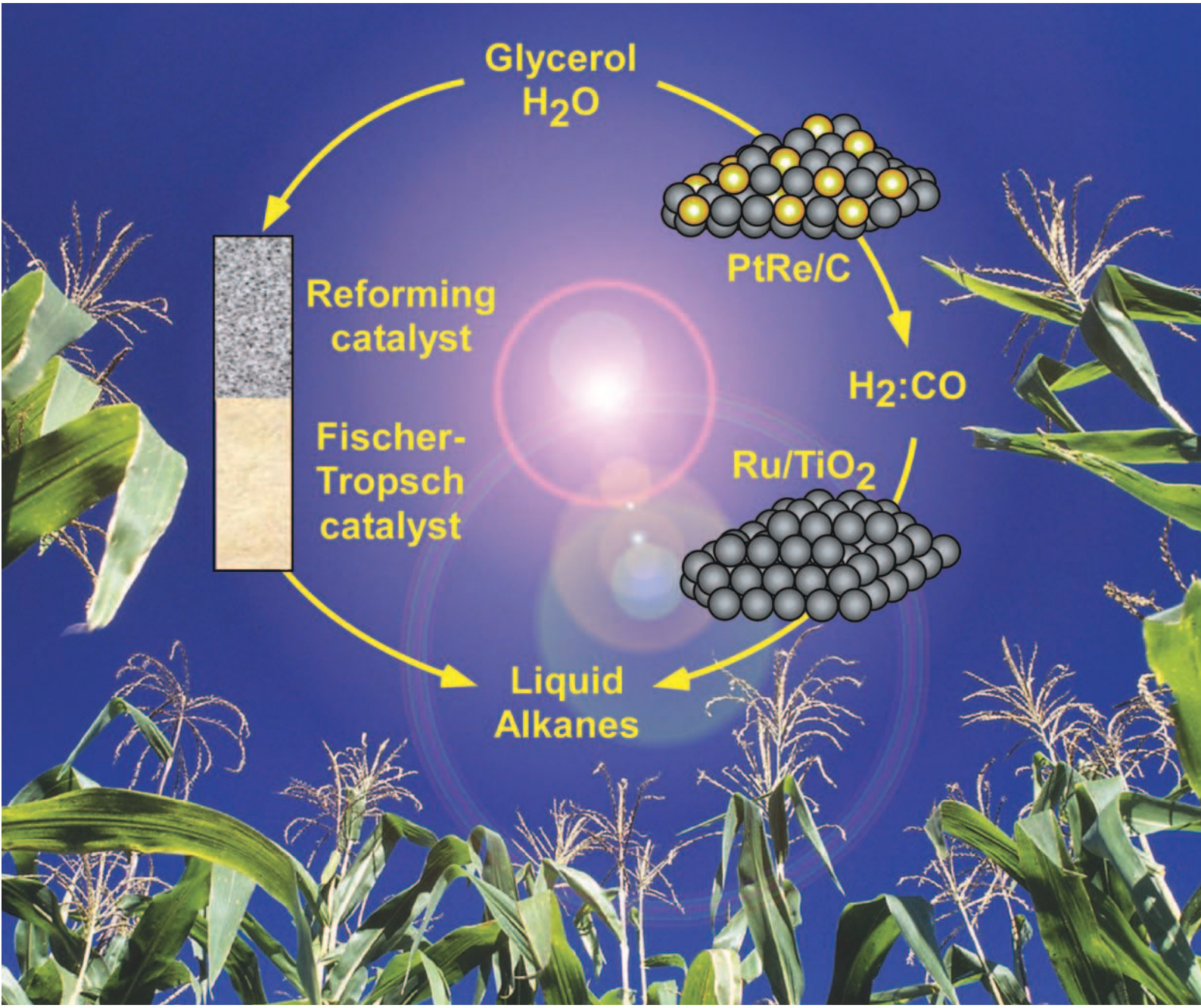

ISSN 1463-9262

RSC Publishing

1463-9262(2007)9:10;1-T

Coupling of glycerol processing with Fischer–Tropsch synthesis for production of liquid fuels

Dante A. Simonetti,[a] Jeppe Rass-Hansen,[ab] Edward L. Kunkes,[a] Ricardo R. Soares[ac] and James A. Dumesic*[a]

Received 23rd March 2007, Accepted 4th June 2007
First published as an Advance Article on the web 22nd June 2007
DOI: 10.1039/b704476c

Liquid alkanes can be produced directly from glycerol by an integrated process involving catalytic conversion to H_2/CO gas mixtures (synthesis gas) combined with Fischer–Tropsch synthesis. Synthesis gas can be produced at high rates and selectivities suitable for Fischer–Tropsch synthesis (H_2/CO between 1.0 and 1.6) from concentrated glycerol feed solutions at low temperatures (548 K) and high pressures (1–17 bar) over a 10 wt% Pt–Re/C catalyst with an atomic Pt : Re ratio of 1 : 1. The primary oxygenated hydrocarbon intermediates formed during conversion of glycerol to synthesis gas are ethanol, acetone, and acetol. Fischer–Tropsch synthesis experiments at 548 K and 5 bar over a Ru-based catalyst reveal that water, ethanol, and acetone in the synthesis gas feed have only small effects, whereas acetol can participate in Fischer–Tropsch chain growth, forming pentanones, hexanones, and heptanones in the liquid organic effluent stream and increasing the selectivity to C_{5+} alkanes by a factor of 2 (from 0.30 to 0.60). Catalytic conversion of glycerol and Fischer–Tropsch synthesis were coupled in a two-bed reactor system consisting of a Pt–Re/C catalyst bed followed by a Ru/TiO_2 catalyst bed. This combined process produced liquid alkanes with S_{C5+} between 0.63 and 0.75 at 548 K and pressures between 5 and 17 bar, with more than 40% of the carbon in the products contained in the organic liquid phase at 17 bar. The aqueous liquid effluent from the integrated process contains between 5 and 15 wt% methanol, ethanol, and acetone, which can be separated from the water by distillation and used in the chemical industry or recycled for conversion to gaseous products. This integrated process has the potential to improve the economics of ''green'' Fischer–Tropsch synthesis by reducing capital costs and increasing thermal efficiency. Importantly, the coupling between glycerol conversion to synthesis gas and Fischer–Tropsch synthesis leads to synergies in the operations of these processes, such as (i) avoiding the highly endothermic and exothermic steps that would result from the separate operation of these processes and (ii) eliminating the need to condense water and oxygenated hydrocarbon byproducts between the catalyst beds.

Introduction

Petroleum currently provides a significant fraction ($\sim$37%) of the world's energy.[1] In the United States, the total consumption of petroleum corresponds to about 7.5 billion barrels of oil equivalent each year (43×10^{15} BTU), and almost 70% of this petroleum is consumed by the transportation sector. Indeed, more than 95% of the energy used by the transportation sector is provided by petroleum.[2] Because the proven reserves of petroleum are projected to be exhausted within the next half-century,[2] it is becoming important to develop alternative sources of transportation fuels. Biomass is an intriguing candidate in this respect because it is renewable, and the processing of biomass is CO_2 neutral.[3] Importantly, the amount of biomass grown annually in the U.S. is sufficient to provide energy for approximately 70% of the transportation sector, provided that this biomass can be converted to clean-burning fuels having high energy densities, such as currently provided by petroleum. In particular, it is estimated that the U.S. could produce 1.3 billion dry tons of biomass per year without major changes in agricultural practices and still meet its food, feed, and export demands;[4] and this amount of biomass corresponds to approximately 3.5×10^9 barrels of oil equivalent each year.

Biomass is comprised primarily of carbohydrates (*e.g.*, starch and cellulose),[3] and one method to convert these compounds to liquid fuels is by fermentation to produce liquid alcohols, such as ethanol and butanol. The technology to convert grain-derived starches to ethanol by the combination of hydrolysis, fermentation, and distillation is well established,[5,6] and advances are being made in the cost-effective conversion of lignocellulosics to ethanol (*e.g.*, through the development of new enzymes for cellulose hydrolysis).[7–10] The advantages of ethanol as a transportation fuel are that it is a liquid and it has a high octane number (*i.e.*, research octane number of 130);[11] however, ethanol has the following disadvantages as a fuel: (i) it has a lower energy density compared

[a]*Department of Chemical and Biological Engineering, University of Wisconsin, 1415 Engineering Drive, Madison, WI 53706, USA. E-mail: dumesic@engr.wisc.edu; Fax: +1 608 262 5434*
[b]*Center for Sustainable and Green Chemistry, Technical University of Denmark, Department of Chemistry, DK-2800, Lyngby, Denmark*
[c]*Faculdade de Engenharia Química, Universidade Federal de Uberlândia, Av. João Naves de Ávila 2121, Uberlândia, MG 38408-100, Brasil*

to petroleum (*i.e.*, approximately 20×10^3 BTU l^{-1} for ethanol versus 30×10^3 BTU l^{-1} for petroleum),[12] (ii) it is completely miscible with water, leading to significant absorption of water into the fuel, and (iii) it has a relatively low boiling point (346 K), leading to excessive evaporation at elevated temperatures. Importantly, the fermentation process used to produce bio-ethanol from carbohydrates leads to an aqueous solution containing only 5–10 wt% ethanol, and significant expenditure of energy is required to produce fuel-grade ethanol by distillation of this rather dilute aqueous solution.[6,13] Indeed, the overall energy balance for production of bio-ethanol is not very favorable, and it has been estimated that the amount of energy required to produce bio-ethanol is approximately equal to (or greater than) the energy-content of the ethanol produced.[5,6,14,15]

Long-chain alkanes comprise the vast majority of components in transportation fuels from petroleum (branched for gasoline and linear for diesel), and the conversion of renewable biomass resources to liquid alkanes thus represents an attractive processing option. For example, the liquid alkanes from such a conversion (i) can be distributed using infrastructure already employed for petroleum products, (ii) can be added to the existing petroleum pool for further processing, and (iii) can be combusted without alterations in existing engines. The production of liquid alkanes from biomass typically occurs by gasification of biomass to produce synthesis gas (H_2/CO) followed by Fischer–Tropsch synthesis.[16,17] However, both conventional Fischer–Tropsch synthesis (*i.e.*, using coal or natural gas) and "green" Fischer–Tropsch synthesis (using biomass) have similar economic disadvantages, specifically, high capital and operating costs, of which greater than 50% stems from synthesis gas generation.[18,19] Also, Fischer–Tropsch synthesis processes suffer from low thermal efficiency.[18,19] Because of these limitations, liquid alkane production by Fischer–Tropsch synthesis becomes economically viable only at large scales.[16–19] Indeed, improvements in synthesis gas generation and thermal efficiency are necessary to improve the economics of Fischer–Tropsch synthesis processes.[16,17,19]

We have recently reported that glycerol can be converted to synthesis gas at high rates and selectivities at temperatures from 498 to 620 K according to eqn (1).[20]

$$C_3O_3H_8 \rightarrow 3CO + 4H_2 \quad (1)$$

This glycerol can be derived from fermentation of glucose,[21] from hydrogenolysis of sorbitol,[22] or as a waste product from the transesterification of plant oils and animal fats.[23] Operation at low temperatures provides the opportunity to couple this endothermic glycerol conversion with exothermic Fischer–Tropsch synthesis to produce liquid transportation fuels *via* the following integrated process:[20]

$$C_3O_3H_8 \rightarrow \frac{7}{25}C_8H_{18} + \frac{19}{25}CO_2 + \frac{37}{25}H_2O \quad (2)$$

This integrated process can potentially improve the economics of "green" Fischer–Tropsch synthesis by reducing costs associated with synthesis gas production, for example, by eliminating the need for an O_2-blown auto-thermal reformer or biomass gasifier.[16–20] Also, our process presents the opportunity for reducing the size of the Fischer–Tropsch synthesis reactor by producing an undiluted synthesis gas stream and for eliminating subsequent cleaning steps required for synthesis gas produced from biomass gasification.[16–18,20] A reduction in capital costs may result in reduced operation and maintenance costs as well.[17] Accordingly, our integrated process potentially allows for smaller scale Fischer–Tropsch synthesis plants to produce liquid fuels from biomass, which is an advantage for distributed biomass resources. In addition, the low temperature of our glycerol conversion process allows for potential thermal coupling with the Fischer–Tropsch synthesis reaction, thereby increasing thermal efficiency.[20] Furthermore, the coupling between these processes may lead to chemical synergies related to the presence of chemical species from both reactions in the same reactor. For example, the intermediates produced from glycerol conversion (*e.g.*, acetol) can enter the growing hydrocarbon chain on the Fischer–Tropsch catalyst sites. Fig. 1 shows a process schematic which illustrates this integrated process as well as potential end-uses for each of the three product phases. The gaseous product stream consisting of light alkanes can be combusted to produce heat and electricity while the oxygenated hydrocarbons in the aqueous phase effluent can be separated by distillation for use in the chemical industry. Importantly, the oil phase containing liquid alkanes can be upgraded to gasoline and diesel fuel.

In this study, we demonstrate the formation of liquid fuels by the integration of glycerol conversion with Fischer–Tropsch synthesis. We conduct reaction kinetics studies at different pressures and glycerol feed concentrations to demonstrate that glycerol conversion produces synthesis gas suitable for Fischer–Tropsch synthesis at moderate pressures (*e.g.*, 17 bar) and using concentrated glycerol feeds (*e.g.*, 80 wt%). Furthermore, we conduct Fischer–Tropsch synthesis studies to investigate the effects of water and oxygenated hydrocarbons on the selectivity and activity of an Ru-based Fischer–Tropsch synthesis catalyst. Finally, we show that liquid alkanes can be produced directly from glycerol by conversion to synthesis gas combined with Fischer–Tropsch synthesis in a two-bed reactor system.

Experimental

Catalyst preparation and characterization

Glycerol conversion studies were carried out using a Pt–Re/C catalyst that was prepared by incipient wetness impregnation of carbon black (Vulcan XC-72) with an aqueous solution of $H_2PtCl_6 \cdot 6H_2O$ (Sigma–Aldrich) and $HReO_4$ (Strem Chemicals) to yield a catalyst with loadings of 5.1 wt% Pt and 4.9 wt% Re (atomic Pt : Re ratio of 1 : 1). The support was dried in air for 12 h at 373 K prior to impregnation, and 1.7 g of solution was used per gram of support. The catalyst was dried at 403 K for 12 h in air prior to activation. Several Ru/TiO_2 catalysts (1.0 wt% and 2.9 wt%) were prepared for Fischer–Tropsch synthesis according to the methods described by Iglesia *et al.*[24]

Prior to reaction kinetics studies or gas adsorption measurements (*i.e.*, CO and O_2 chemisorption), the Pt–Re/C catalyst was reduced at 723 K (ramp rate of 0.5 K min^{-1}) for 2 h in flowing H_2 (140 cm^3(NTP) min^{-1}). The Ru/TiO_2

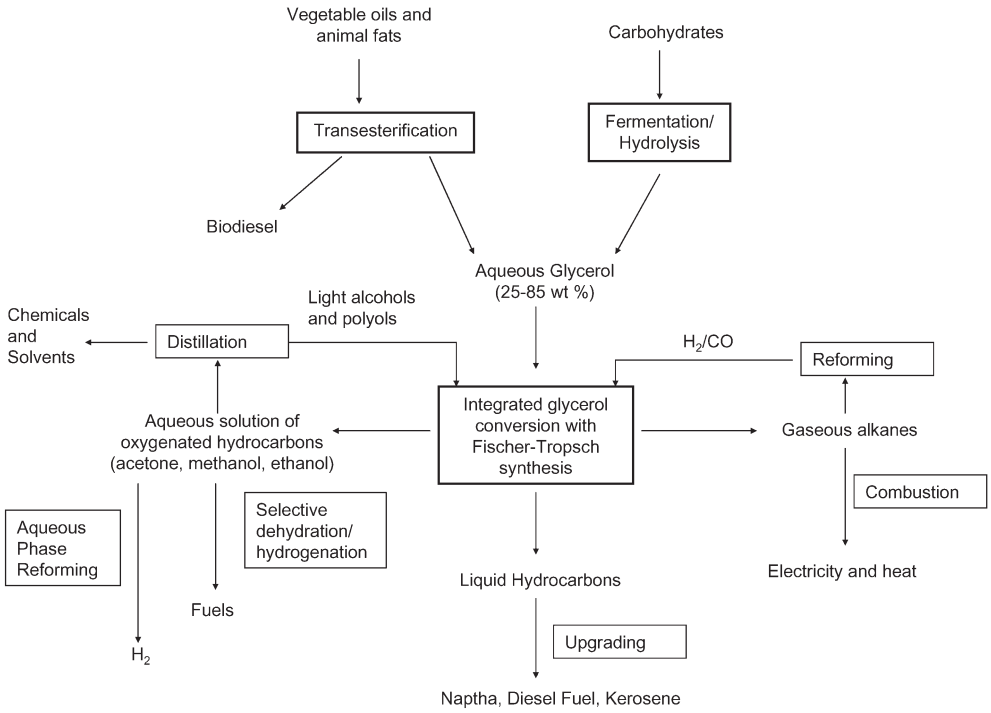

Fig. 1 Process pathway for production of liquid fuels from biomass by integrated glycerol conversion to synthesis gas and Fischer–Tropsch synthesis.

catalysts were reduced *in-situ* before reaction kinetics studies and gas adsorption measurements. The gas hourly space velocity (GHSV) was calculated for Fischer–Tropsch synthesis experiments using the total volumetric flowrate of gas (at standard conditions) to the reactor and a bed density of 0.175 g cm^{-3} (g catalyst per total bed volume) for Ru/TiO_2 catalyst diluted with an equal volume of crushed SiO_2 granules. The weight hourly space velocity (WHSV) was calculated for glycerol conversion experiments using the mass flowrate of glycerol into the reactor and the total mass of catalyst. The irreversible CO uptake of Pt–Re/C at 300 K was taken to be the number of catalytic sites (150 μmol g^{-1}) and was measured using a standard gas adsorption apparatus described elsewhere.[25] This number of sites corresponds to a dispersion (molar CO : total metal ratio) of 29%. The dispersions of the Ru/TiO_2 catalysts were determined by chemisorption of O_2 at 195 K in a static chemisorption system.[26] Table 1 shows the properties of the Ru/TiO_2 catalysts, and these results are in agreement with similar catalysts studied by Iglesia *et al.*[27]

Reaction kinetics measurements

The apparatus used to conduct reaction kinetics measurements for Pt–Re/C is described elsewhere.[20] Fresh catalyst was loaded into a 12.7 mm (0.5 inch) outer diameter tubular stainless steel reactor with a wall thickness of 0.71 mm (0.028 inch). The catalyst bed was contained between an end plug of quartz wool (Alltech) and fused SiO_2 granules (−4 + 16 mesh; Sigma–Aldrich) which aid in vaporization of the liquid feed. The Pt–Re/C catalyst powder was mixed with an equal volume of SiO_2 granules to decrease the pressure drop across the catalyst bed. For experiments that combined glycerol conversion with Fischer–Tropsch synthesis, a bed of 1.0 wt% Ru/TiO_2 was mixed with an equal volume of crushed SiO_2 granules, and this bed was loaded downstream of the Pt–Re/C bed. The reactor was heated with a furnace consisting of a close fitting aluminum block heated externally by a well-insulated furnace (1450 W/115 V, Applied Test Systems series 3210). Type-K thermocouples (Omega) were attached to the outside of the reactor to measure reactor temperature, which was controlled with a series 16A type temperature controller (Dwyer Instruments). Fresh catalyst was reduced in flowing H_2, as described previously. Mass-flow controllers (5850 Brooks Instruments) were used to control the flowrate of H_2. An HPLC pump (Model 301, Alltech) was used to introduce the aqueous feed solution into a 6 inch needle with a point 5 style tip (Hamilton) soldered into a section of 3.2 mm (0.125 inch) outer diameter, stainless steel tubing, and this

Table 1 Properties of Fischer–Tropsch catalysts

Ru loading (wt%)	BET surface area/m^2 g^{-1}	Dispersion (O : Ru ratio)	Ru site density/10^{16} m^{-2}	Average pellet radius/10^{-4} m	Average pore radius[a] /10^{-10} m	χ/10^{16} m^{-1}[b]
1.0	15	0.55	217	0.63	210	40
2.9	30	0.36	208	0.63	165	50

[a] Estimated from BET surface area measurement and values for similar catalysts studied by Iglesia, *et al.*[27] [b] Calculated as in ref. 27.

needle was positioned upstream of the Pt–Re/C catalyst bed. The liquid effluent was condensed in a gas-liquid separator and drained periodically for gas-chromatograph (GC) analysis (Agilent 6890 with a flame ionization detector (FID) and HP-Innowax column or Shimadzu GC-2010 with an FID detector and Rtx-5 column) and total organic carbon analysis (Shimadzu TOC-V CSH). Each effluent was tested for the presence of glycerol and other liquid byproducts. For runs that combined glycerol conversion with Fischer–Tropsch synthesis, the downstream system lines were heated to 373 K.

The effluent gas stream passed through a back-pressure regulator (GO Regulator, Model BP-60) which controlled the system pressure. The effluent gas was analyzed by gas chromatography: H_2 with a Carle GC (series 8700) using a thermal conductivity detector (TCD), CO and CH_4 using an HP 5890 GC with TCD and washed molecular sieve 5A 80/100 column (Alltech), and CO_2 and light alkanes (C_2–C_3) using an HP 5890 GC with TCD and a Porapak QS 100/120 column (Alltech). All feed solutions were prepared by mixing glycerol (99.5%, ACS reagent, Sigma-Aldrich) with deionized water.

The apparatus used to conduct Fischer–Tropsch synthesis experiments is similar to the system used for reaction kinetics measurements of glycerol conversion over Pt–Re/C, except that the downstream lines from the reactor were heated to 373 K. The 2.9 wt% Ru/TiO_2 catalyst was mixed with an equal volume of crushed SiO_2 granules to help dissipate the heat generated by the exothermic Fischer–Tropsch reaction and loaded into a 12.7 mm (0.5 inch) outer diameter, stainless steel tubular reactor. The liquid phase products were collected in a gas-liquid separator and analyzed by GC (Shimadzu GC-2010 with an FID detector and Rtx-5 column). The effluent gas stream was analyzed for C_1–C_{10} hydrocarbons with a Varian GC-MS (Saturn 3) using an FID detector and GS-Q capillary column. H_2, CO, and CO_2 were analyzed using an HP 5890 GC with TCD and a Porapak QS 100/120 column (Alltech). Ultra-high purity CO and H_2 (Linde) gases were mixed to give a synthesis gas feed with $H_2 : CO \approx 2$, and aqueous solutions of acetone, acetol, and ethanol were introduced into the reactor in a similar way as described above for glycerol conversion experiments.

Results and discussion

Glycerol conversion to synthesis gas

Fischer–Tropsch synthesis is typically operated at pressures between 5 and 20 bar,[18] and it is advantageous to carry out the conversion of glycerol to synthesis gas at these higher pressures to reduce compression costs. Accordingly, while our previous work investigated the performance of Pt–Re/C at atmospheric pressure,[20] in the present work we studied the production of synthesis gas at a pressure of 8.3 bar at 548 K over 10 wt% Pt–Re (atomic ratio 1 : 1)/C using a feed solution containing 30 wt% glycerol in water. Fig. 2 shows the conversion to gas phase products and the CO/CO_2 and H_2/CO molar ratios for glycerol conditions at this elevated pressure. The total inlet flowrate of carbon (as glycerol) for this experiment was 833 μmol min^{-1} (feed flowrate of 0.08 cm^3 min^{-1}), and the total conversion of glycerol was 90% (57% to gas phase products and 33% to liquid phase products). After a period of

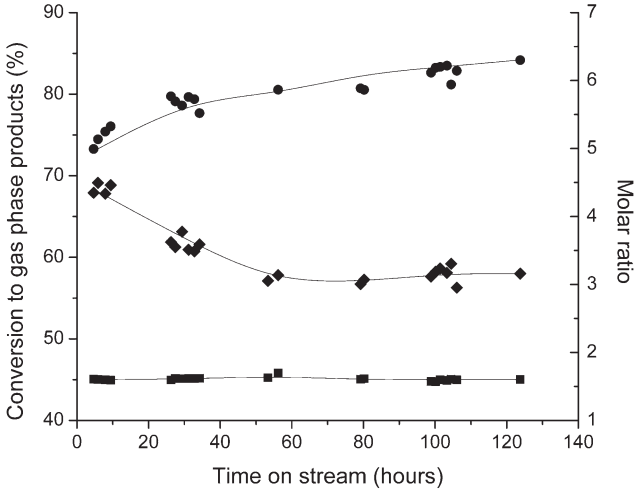

Fig. 2 Conversion to gas phase products (◆), CO/CO_2 molar ratio (●), and H_2/CO molar ratio (■) for gas-phase processing of 30 wt% aqueous-glycerol feed at 548 K and 8.3 bar. Conversion to gas phase is calculated as (carbon atoms in gas phase product stream/total carbon into reactor as feed) × 100. Reaction carried out using 0.08 cm^3 min^{-1} of feed solution over 520 mg of catalyst (WHSV = 3.0 h^{-1}).

60 h, during which the conversion of glycerol to gas-phase products decreased from 68% to 57%, the catalyst showed excellent stability for an additional 60 h time on stream. The gas-phase effluent is comprised of synthesis gas with a $H_2 : CO$ ratio equal to 1.6, which can be adjusted, if necessary, *via* the water-gas shift reaction to reach the stoichiometric 2 : 1 ratio appropriate for Fischer–Tropsch synthesis.[20] The balance of the gaseous products consists of CO_2 (CO/CO_2 molar ratio of 6) and light alkanes (C_1–C_3, with a CO/alkanes carbon ratio of 10). At 548 K and 5 bar, the gas-phase product distribution and catalytic stability were similar, and the conversion to gas-phase products was 80%. The aqueous liquid effluent contained 15 wt% of oxygenated hydrocarbons (methanol, ethanol, *n*-propanol, ethylene glycol, 1,2 propanediol, acetone, and acetol), and the carbon balance closed to within 10% for this experiment.

To couple the conversion of glycerol to synthesis gas with Fischer–Tropsch synthesis in a two-bed reactor system, it is necessary to expose the down-stream Fischer–Tropsch catalyst to water vapor from the aqueous glycerol feed. Iglesia *et al.* report that small amounts of water can, in fact, improve the performance of Co-based Fischer–Tropsch catalysts.[28] However, the highest water partial pressure in their study (P_{H_2O}/P_{CO} = 3) was lower than that which results from conversion of a 30 wt% glycerol feed (P_{H_2O}/P_{CO} = 8). Also, the studies by Iglesia *et al.* were conducted at higher total pressure (20 bar).[28] Therefore, it is advantageous to decrease the concentration of water in our system. Thus, we tested the Pt–Re/C catalyst for conversion of 50 wt% and 80 wt% glycerol solutions at pressures between 1 and 11 bar, and Table 2 shows the conversion to gas phase products as well as the H_2/CO and CO/CO_2 molar ratios for these experiments. The conversion to gas phase products increases with decreasing concentration of glycerol in the feed at constant pressure and decreases with increasing pressure at constant feed

Table 2 Performance of Pt–Re/C for conversion of concentrated solutions of glycerol in water to synthesis gas at various pressures. Reaction carried out over 1.0 g of catalyst at 548 K using ~0.04 cm^3 min^{-1} of feed (WHSV between 1.4 and 1.7 h^{-1}). Conversion to gas phase products calculated as in Fig. 2

Feed concentration (wt%)	Pressure/bar	H_2/CO	CO/CO_2	Conversion to gas phase products (%)
80	1	1.4	23	86
50	1	1.6	11	96
80	5	1.2	13	56
50	5	1.5	7.8	76
80	11	1.0	5.0	44
50	11	1.4	2.7	55

concentration. The water gas shift activity increases at higher pressures and/or lower feed concentrations because of the increased partial pressure of H_2O, as evidenced by the decrease in the CO : CO_2 ratio. These experiments were carried out at 548 K and pressures above the dew point for 50 wt% and 80 wt% glycerol feed solutions. Each condition tested showed stable operation for approximately 20 h time on stream, and there was only a 6% loss in activity after operation at 11 bar with 80 wt% glycerol feed. The liquid phase contained oxygenated hydrocarbon products similar to those for the conversion of a 30 wt% glycerol feed. Table 3 shows the carbon distributions for the conditions in Table 2. The primary gaseous carbon product is CO, while the aqueous liquid phase contains between 6 and 30 wt% oxygenated hydrocarbons when the conversion to gas phase products is less than 90%. The total conversion of glycerol was 100% for each condition.

The selectivity for production of C_{5+} alkanes by Fischer–Tropsch synthesis typically increases at higher pressures. Therefore, we studied the conversion of glycerol to synthesis gas at 548 K for 11 and 17 bar, to test whether the Pt–Re/C catalyst would show good stability and selectivity at higher pressures with incomplete vaporization of the liquid feed. Fig. 3 shows the conversion to gas phase products and the H_2/CO and CO/CO_2 molar ratios for 48 h time on stream. Lower CO/CO_2 ratios are observed at these higher pressures (as compared to glycerol conversion at 5 bar), indicating increased conversion of CO to CO_2 *via* water-gas shift. Furthermore, the conversion to gas phase products decreases (from 56% to 40%) when pressure increases to 11 or 17 bar. Thus, the Fischer–Tropsch catalyst in a two-bed system operating at 11 bar or

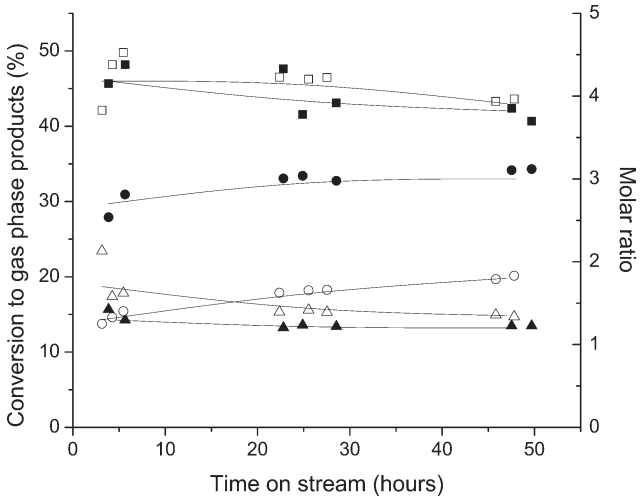

Fig. 3 Conversion to gas phase products (squares), CO/CO_2 molar ratio (circles), and H_2/CO molar ratio (triangles) for gas-phase processing of 80 wt% aqueous-glycerol feed at 548 K and 11 bar (closed symbols) and 17 bar (open symbols). Conversion to gas phase products calculated as in Fig. 2.

17 bar would be exposed to a large amount of oxygenated hydrocarbons from the aqueous-liquid effluent of the Pt–Re/C bed (*e.g.*, more than half of the carbon fed to the Pt–Re/C bed as glycerol). We note that the catalyst remains stable during this period of time at both pressures. The liquid phase product distributions at 11 and 17 bar contained 25 wt% and 29 wt% oxygenated hydrocarbons (methanol, ethanol, propanol, acetone, acetol, and propanediols), respectively.

The product distributions for the conversion of aqueous glycerol solutions at various pressures are consistent with the reaction scheme proposed by Cortright *et al.* for aqueous phase reforming of polyols, which consists of glycerol adsorption–dehydrogenation, C–C bond cleavage, and desorption of CO and H_2.[29] Water-gas shift of adsorbed CO leads to CO_2 production, and cleavage of C–O as opposed to C–C bonds results in the formation of alkanes and alcohols.[29] We note that the methanol, ethanol, and acetone components in the aqueous effluent stream from the processing of glycerol are similar in concentration (5–30 wt%) to the aqueous ethanol stream produced by fermentation of glucose (*e.g.*, 5 wt%).[6] Thus, it may be advantageous to separate these valuable components from the effluent aqueous stream for use in the chemical industry (*e.g.*, as fuels or solvents).[29]

Table 3 Carbon distribution for conversion of 50 wt% and 80 wt% solutions of glycerol in water to synthesis gas over Pt–Re/C at 548 K and various pressures. Reaction conditions as in Table 2

Feed concentration (wt%)	Pressure/bar	Total C_{in}/ μmol min^{-1}	Total C_{out} gas/μmol min^{-1}	Mol% CO in gas products[a]	Total C_{out} liquid[b] / μmol min^{-1}	wt% oxygenates in aqueous effluent[c]	Error in C balance (%)
80	1	946	816	89	52	6.6	8
50	1	737	708	87	23	2.3	0.8
80	5	914	515	80	431	24	4
50	5	700	533	80	128	6.3	6
80	11	946	417	67	552	30	2
50	11	663	368	58	352	17	9

[a] Calculated as $F_{CO}/F_{total} \times 100$, where F_{CO} is the molar flowrate of carbon as CO and F_{total} is the total molar flowrate of carbon in gas products. [b] Determined by total organic carbon analysis of liquid effluent. [c] Calculated as total mass of methanol, ethanol, acetone, acetol, and propanediols per total mass of aqueous effluent.

Table 4 Results of Fischer–Tropsch synthesis over 4 g of 2.9 wt% Ru/TiO_2 at 548 K. Reaction carried out using $\sim$150 cm^3 min^{-1} synthesis gas (H_2 : CO = 2)

Oxygenated feed molecule	P_{CO}/bar	P_{H_2}/bar	P_{H_2O}/bar	$P_{oxygenate}$/bar	Total P/bar	GHSV[a] /h^{-1}	X_{CO}[b] (%)	Site time yield[c] /min^{-1}	S_{C5+}[d,e]	S_{CH_4}	S_{C2-C4}	α_{C3-C10}[f]	$\alpha_{C11-C30}$[g]
—	1.7	3.3	—	—	5	410	53	2.7	0.30	0.39	0.29	0.61	0.85
Water	1.7	3.5	2.9	—	8.1	630	55	2.8	0.32	0.41	0.29	0.61	0.84
Acetol–Water	1.8	3.5	2.6	0.2	8.1	630	30	1.5	0.60	0.24	0.17	0.80	0.79
Ethanol–Water	1.9	3.7	2.2	0.3	8.1	590	32	1.7	0.38	0.39	0.23	0.68	0.82
Acetone–Water	1.9	3.8	2.1	0.3	8.1	570	26	1.4	0.37	0.41	0.23	0.65	0.85

[a] Calculated as total volumetric flowrate into the reactor divided by total volume of the catalyst bed.[27] [b] Conversion of CO is calculated as $[(F_{CO})_{In} - (F_{CO})_{Out}/(F_{CO})_{In}] \times 100$, where F is the molar flowrate. [c] Defined as in ref. 27. [d] Selectivities calculated as $S_{C_nH_x} = nF_{C_nH_x}/F_{total}$, where n is the number of carbons in the hydrocarbon product C_nH_x, $F_{C_nH_x}$ is the molar flowrate of product C_nH_x, and F_{total} is the total molar flowrate of carbon in all Fischer–Tropsch hydrocarbon products. [e] Selectivities calculated on a CO_2 and oxygenated hydrocarbon free basis. [f] ASF chain growth probability for alkanes in the C_3–C_{10} range. [g] ASF chain growth probability for alkanes in the C_{11}–C_{30} range.

Fischer–Tropsch synthesis

To achieve energy integration between the endothermic conversion of glycerol to synthesis gas and the exothermic conversion of synthesis gas to liquid alkanes, the temperature for the Fischer–Tropsch synthesis step must be comparable to (or higher than) that employed in the glycerol conversion step.[20] Also, the pressures at which both reactions are conducted must be similar to minimize compression costs. Furthermore, if the synthesis gas from the glycerol conversion step is fed directly to the Fischer–Tropsch catalyst, then this catalyst will be exposed to water and oxygenated hydrocarbon byproducts. Therefore, we conducted Fischer–Tropsch synthesis experiments at 548 K and a pressure of synthesis gas (H_2 : CO = 2) equal to 5 bar over 4 g of 2.9 wt% Ru/TiO_2 catalyst. In these experiments, the feed to the reactor was 150 cm^3 min^{-1} of dry synthesis gas with co-feeds of water or aqueous solutions of acetol, ethanol, or acetone (the most abundant liquid phase products from glycerol conversion) to simulate the conditions of a two-bed reactor system processing an 80 wt% glycerol feed at 5 bar. We used a Ru-based Fischer–Tropsch catalyst, because a Co-based catalyst showed low activity during initial experiments, and Ru is a more active Fischer–Tropsch catalyst.[30] Additionally, the formation of inactive oxides at high partial pressures of water can cause Co-based Fischer–Tropsch catalysts to deactivate.[18]

Table 4 lists the conversion of CO, activity (as defined by the site time yield), and selectivities to CH_4, C_2–C_4, and C_{5+} hydrocarbons for these Fischer–Tropsch synthesis experiments. The conversion of CO is about 50% for Fischer–Tropsch synthesis with dry synthesis gas. The addition of water to the synthesis gas feed has a negligible effect. In particular, the conversion of CO, the activity, and the selectivities are similar to the values measured for the experiment using dry synthesis gas. The CO conversion and the catalytic activity both decrease with the addition of oxygenated hydrocarbons to the synthesis gas. It is possible that adsorbed species from these molecules inhibit the Fischer–Tropsch reaction by blocking Ru sites for CO and H_2 adsorption. The selectivity to C_{5+} hydrocarbons increases slightly (from 0.30 to 0.38) with the addition of ethanol and acetone to the synthesis gas, while the value of S_{CH_4} remains unchanged and the value of S_{C2-C4} decreases slightly. However, upon the addition of acetol to the synthesis gas, the C_{5+} selectivity increases by a factor of two. This result indicates that acetol participates in Fischer–Tropsch chain growth. Indeed, acetol was the only oxygenated feed molecule to react upon addition to the synthesis gas stream during Fischer–Tropsch reaction. Specifically, while more than 90% of the ethanol and acetone feed molecules were recovered in the gaseous and aqueous liquid effluents, all of the acetol feed was converted to products, with 30% being converted to acetone, methanol, and ethanol in the aqueous product phase and 20% being converted to oxygenated species in the organic product phase (acetone, pentanones, hexanones, and heptanones). Another 10% of the acetol feed was converted to gaseous acetone. Therefore, 40% of the carbon fed to the reactor as acetol possibly entered into Fischer–Tropsch chain growth and was converted into liquid hydrocarbons.

The total carbon selectivities (Table 5) for these Fischer–Tropsch synthesis experiments exhibit similar trends as the Fischer–Tropsch selectivities in Table 4. The selectivities in Table 5 are based on the total amount of carbon in all of the products (*i.e.*, Fischer–Tropsch products as well as CO_2 and oxygenated hydrocarbons in the organic and aqueous liquid effluents). The addition of water to the synthesis gas feed increases the selectivity to CO_2 at the expense of

Table 5 Total carbon selectivities for experiments in Table 4. Selectivities calculated as $S_i = F_i/F_{total}$, where F_i is the total flowrate of carbon in product i, and F_{total} is the total flowrate of carbon in all of the products

Oxygenated feed molecule	S_{CH_4}	S_{C2-C4}	S_{C5+}	S_{CO_2}	S_{oxy} aqueous[a]	S_{oxy} organic[b]
—	0.35	0.27	0.29	0.09	—	—
Water	0.32	0.23	0.23	0.23	—	—
Acetol–Water[c]	0.16	0.11	0.40	0.05	0.16	0.06
Ethanol–Water	0.35	0.21	0.34	0.10	—	—
Acetone–Water	0.35	0.20	0.32	0.11	0.02	0.01

[a] Oxygenated hydrocarbon products (acetone, ethanol, and methanol) in aqueous liquid effluent. [b] Oxygenated hydrocarbon products (acetone, butanones, pentanones, hexanones, and heptanones) in organic liquid effluent. [c] $S_{gaseous\ acetone}$ is 0.06.

Fischer–Tropsch alkanes (C_1–C_{5+}), most likely by an increase in the rate of water-gas shift. We note that the CO_2 selectivity for aqueous co-feeds of oxygenated molecules is similar to the value observed for the dry synthesis gas feed, even though the partial pressure of water is similar to that when water alone is co-fed. This result is possibly due to the lower activity of Ru/TiO_2 caused by site blocking, as explained previously. The selectivities in Table 5 show that the addition of aqueous solutions of ethanol or acetone to synthesis gas has a negligible effect on the product distribution, in agreement with the Fischer–Tropsch selectivities in Table 4. There is a slight increase in the value of S_{C5+} and a corresponding decrease in the value of S_{C2-C4}, while S_{CH_4} is unchanged with the addition of ethanol and acetone to the synthesis gas feed. However, these total carbon selectivities confirm that the addition of acetol to the synthesis gas leads to a shift from light alkane products to heavier products. Light alkanes (C_1–C_4) account for more than 50% of the total carbon in the products for the dry synthesis gas experiment as well as experiments with water, ethanol, and acetone co-feeds. However, about 50% of the carbon in the products from the acetol co-feed experiment was contained in the C_{5+} hydrocarbons and oxygenated hydrocarbons in the organic liquid effluent. This increase in heavier products is accompanied by a more than two-fold decrease in selectivity to light alkanes. We note that the aqueous effluent from the acetol co-feed experiment is 6 wt% acetone, ethanol, and methanol, a solution suitable for further distillation.

In general, the product distribution of Fischer–Tropsch synthesis can be described by the Anderson–Schulz–Flory (ASF) chain growth model:

$$\frac{W_n}{n} = \alpha^{n-1}(1-\alpha)^2 \quad (3)$$

where n is the hydrocarbon chain length, W_n is the weight fraction of hydrocarbon products of length n, and α is the chain growth probability.[18,31] Eqn (3) assumes that chain growth probability is independent of n, and a semi-log plot of eqn (3) gives a straight line with a slope of α.[18,31] However, the selectivity (and activity) of Fischer–Tropsch catalysts can be affected by transport limitations within the catalyst pellets, such that α becomes dependent on chain length.[27,28,31] An increase in Ru site density or pellet radius leads to an increase in the C_{5+} selectivity caused by diffusion-enhanced readsorption of α-olefins, which inhibits chain termination.[31] However, these diffusional limitations can become sufficiently severe that they inhibit CO diffusion within the pellet, resulting in a decrease in C_{5+} selectivity.[31] Iglesia *et al.* define a structural parameter (χ) to indicate the extent of these diffusion restrictions within a catalyst, and this parameter is dependent on catalyst pellet radius, pore size distribution, and the volumetric density of surface Ru atoms.[31]

For the 2.9 wt% Ru/TiO_2 catalyst used in this paper, the value of χ is estimated to be 50×10^{16} m^{-1}. This value is in agreement with values determined by Iglesia *et al.* for TiO_2-supported Ru catalysts,[27] and it lies in the intermediate range, suggesting that transport limitations promote readsorption of α-olefins but do not slow the diffusion of reactants into the catalyst pellets.[31] Indeed, catalysts with intermediate values of χ lead to optimum C_{5+} selectivity.[27,28,31] Furthermore, readsorption of olefins leads to deviation from ASF chain growth kinetics. As a hydrocarbon chain increases in length, diffusion through the catalyst pores becomes more difficult and the possibility for readsorption increases.[27,28,31] This effect increases the chain growth probability for longer hydrocarbon chains and results in curvature in the semi-log plot of the molecular weight distribution.[27,28,31] Fig. 4 shows semi-log plots for the five Fischer–Tropsch runs in Table 4, and these distributions begin to deviate from ASF kinetics at C_{10}–C_{15}, in agreement with studies by Iglesia *et al.*[27,28,31] The deviation in the molecular weight distribution in the C_6–C_{12} range for the experiment employing acetol co-feed is caused by increased formation of C_6–C_{12} hydrocarbons from acetol entering into Fischer–Tropsch chain growth. Table 4 also shows values of α for the C_3–C_{10} and C_{11}–C_{30} hydrocarbon ranges. The values of α for C_{11}–C_{30} are larger than those for C_3–C_{10} for the dry synthesis gas experiment and the experiments with water, ethanol, and acetone co-feeds. Conversely, the two α values for the acetol co-feed experiment are similar, resulting from an increase in the formation of C_6–C_{12} alkanes during this run. We note that the olefin to paraffin ratios were low, consistent with the long bed residence times used in these studies (6–9 s).[27]

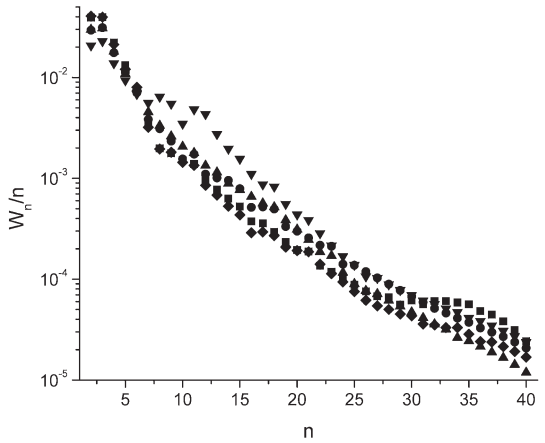

Fig. 4 Molecular weight distributions for dry synthesis gas (■), and water (◆), acetone (●), ethanol (▲), and acetol (▼) co-feeds. Experimental conditions as in Table 4.

Glycerol conversion combined with Fischer–Tropsch synthesis

Following our studies of glycerol conversion to synthesis gas and our studies of Fischer–Tropsch synthesis using synthesis gas streams containing water and oxygenated hydrocarbons (ethanol, acetone, acetol), we investigated the formation of liquid alkanes by the integration of glycerol conversion with Fischer–Tropsch synthesis. These experiments employed a two-bed catalyst system using 1.0 g of 10 wt% Pt–Re (1 : 1)/C followed by 1.7 g of 1.0 wt% Ru/TiO_2, with an 80 wt% glycerol feed at 548 K and total pressures between 5 and 17 bar.

Table 6(A) shows the selectivities to C_{5+}, CH_4, and C_2–C_4 alkanes for each of the combined experiments based solely on the alkane products from Fischer–Tropsch synthesis (*i.e.*, with the C_1–C_3 alkanes produced by the Pt–Re/C catalyst excluded). The selectivity for production of C_{5+} alkanes by Fischer–Tropsch synthesis typically increases at higher

Table 6 Results from experiments for glycerol conversion combined with Fischer–Tropsch synthesis. (A) Selectivities to C_{5+}, CH_4, and C_2–C_4 hydrocarbons over Ru/TiO_2, calculated as in Table 4. (B) Total carbon selectivities, calculated as $S_i = F_i/F_{total} \times 100$, where F_i is the total flowrate of carbon in product i, and F_{total} is the total flowrate of carbon in all of the products. Reactions carried out at 548 K using $\sim$0.04 cm^3 min^{-1} of 80 wt% glycerol feed (WHSV of glycerol over Pt–Re/C = 1.7 h^{-1})

(A)	P_{tot}/bar	S_{C5+}	S_{CH_4}	S_{C2-C4}	α_{C3-C10}[a]	$\alpha_{C11-C30}$[b]
	5	0.63	0.15	0.21	0.85	0.75
	11	0.75	0.10	0.15	0.92	0.75
	17	0.70	0.12	0.18	0.92	0.71

(B)	P_{tot}/bar	$S_{Alkanes}$ (%)	S_{CO_2} (%)	S_{CO}[c] (%)	$S_{org-oxy}$[d] (%)	$S_{aqu-oxy}$[e] (%)
	5	31.9	15.2	37.3	1.7	13.9
	11	44.1	16.5	17.5	7.4	14.6
	17	55.2	23.1	1.3	9.1	11.2

[a] ASF chain growth probability for alkanes in the C_3–C_{10} range. [b] ASF chain growth probability for alkanes in the C_{11}–C_{30} range. [c] CO from glycerol. [d] Oxygenated hydrocarbon products (acetone, butanones, pentanones, hexanones, and heptanones) in organic liquid effluent. [e] Oxygenated hydrocarbon products (acetone, ethanol, and methanol) in aqueous liquid effluent.

pressures, and the results for the two-bed reactor system obey this trend. An increase in pressure from 5 to 11 bar results in an increase in the selectivity to C_{5+} hydrocarbons from 0.63 to 0.75; however, a further increase in pressure to 17 bar produces only a slight decrease in S_{C5+} to 0.70. Importantly, the selectivity to C_{5+} hydrocarbons is almost three times higher than the total selectivity to CH_4 and C_2–C_4 at 11 and 17 bar. Furthermore, the value of S_{C5+} for the combined run at 5 bar is similar to the Fischer–Tropsch experiment with an acetol co-feed. This result indicates the participation of acetol in Fischer–Tropsch chain growth, thus increasing the selectivity to longer-chain hydrocarbons. Based on the production of CO from the glycerol conversion experiments discussed previously, the average conversion of CO across the Ru/TiO_2 bed was 28% and 42% for 5 and 11 bar, respectively, and the site time yield was 1.3 min^{-1} at both pressures. An increase in pressure to 17 bar results in an increase in the activity of the Fischer–Tropsch catalyst indicated by a higher average site-time yield (2.5 min^{-1}) and average conversion of CO (94%).

Table 6(B) shows the total carbon selectivities based on the total amount of carbon in all of the products. At 5 bar, the primary product from glycerol conversion was CO, with only 32% of the carbon being converted to alkanes; however, increasing the pressure to 11 and 17 bar shifts the carbon distribution toward C_1–C_{5+} alkanes (*i.e.*, $S_{Alkanes}$ increases to 42% and 51% at 11 bar and 17 bar, respectively). Also, the amount of carbon as oxygenates in the organic liquid effluent (acetone, pentanones, hexanones, and heptanones) increases by a factor of 5 with increasing pressure. This appearance of oxygenates in the organic liquid is similar to the Fischer–Tropsch experiment with an acetol co-feed described previously, and it further indicates the synergistic effects of acetol in the Fischer–Tropsch reaction. At 17 bar, the amount of carbon leaving the reactor as CO decreases by more than an order of magnitude, and the selectivity to alkanes increases compared to the run at 11 bar. However, the selectivity to C_{5+} alkanes slightly decreases. This behavior results from both increased water-gas shift activity (indicated by higher S_{CO_2}) as well as an increase in the rate of Fischer–Tropsch synthesis at higher pressures (as mentioned previously). The carbon distribution is shifted toward lighter alkane products (*i.e.*, increase in $S_{Alkanes}$ without a corresponding increase in S_{C5+}).

Table 7 Percentage of carbon contained in each product phase for experiments in Table 6 of glycerol conversion combined with Fischer–Tropsch synthesis

P_{tot}/bar	Gaseous[a]	Organic liquid[b]	Aqueous liquid[c]
5	71.6	14.6	13.9
11	54.3	31.1	14.6
17	50.5	38.2	11.2

[a] CO, CO_2, and C_1–C_9 alkanes. [b] C_{5+} alkanes, acetone, butanones, pentanones, hexanones, and heptanones. [c] Methanol, ethanol, acetone, and *n*-propanol.

Table 7 shows the percentage of carbon contained in the three products phases: gaseous (CO, CO_2, and C_1–C_9 alkanes), organic liquid (C_{5+} alkanes, acetone, pentanones, hexanones, and heptanones), and aqueous liquid (acetone, methanol, and ethanol). We note that the percentage of carbon in the organic liquid-phase product was 43% at 17 bar, 35% at 11 bar, and 15% at 5 bar, with the percentage of carbon in gaseous products decreasing from 71% at 5 bar to approximately 50% at 11 and 17 bar. At 5 and 11 bar, 14% of the carbon is contained as oxygenated species in the aqueous effluent, and at 17 bar, this value slightly decreases to 10%. These aqueous liquid effluents contain between 5 wt% and 15 wt% methanol, ethanol, and acetone and are suitable for further distillation.

The value of χ for the 1.0 wt% Ru/TiO_2 catalyst used in all the combined experiments was 40 $\times$ 10^{16} m^{-1}, in agreement with results from Iglesia *et al.*[27] Fig. 5 shows the product molecular weight distributions for these experiments that combined glycerol conversion with Fischer–Tropsch synthesis, and these distributions exhibit similar deviations from ASF kinetics as the Fischer–Tropsch experiments described in the previous section, indicating α-olefin readsorption effects. The intermediate value of χ for this Ru/TiO_2 catalyst allows for optimum C_{5+} selectivity. Values of α for the C_3–C_{10} and

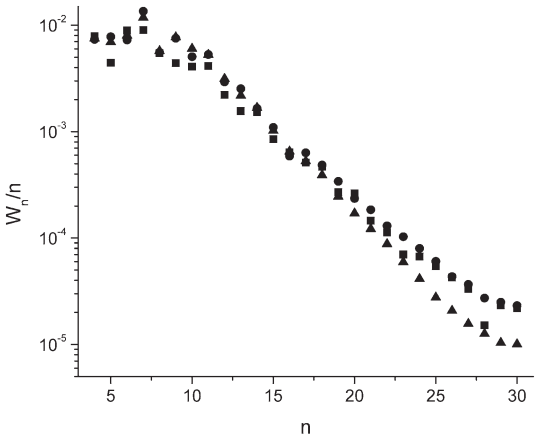

Fig. 5 Molecular weight distributions for combined glycerol conversion with Fischer–Tropsch synthesis experiments at 548 K and 5 bar (■), 11 bar (●), and 17 bar (▲). Experimental conditions as in Table 6.

C_{11}–C_{30} hydrocarbon ranges are also shown in Table 6A. The values in the C_3–C_{10} range are high, most likely caused by the participation of oxygenates (acetol) in Fischer–Tropsch chain growth, increasing the production of C_6–C_{12} species. This result is similar to the acetol co-feed experiment in Table 4.

The C_{5+} selectivity, selectivity to pentanones, hexanones, and heptanones in the organic liquid, and the conversion of CO for combined glycerol conversion with Fischer–Tropsch synthesis at 11 and 17 bar are all higher than those at 5 bar, despite the fact that synthesis gas production from glycerol is decreased at these elevated pressures. These results indicate that the more favorable Fischer–Tropsch conditions (*i.e.*, higher pressure) are more important to the integrated process than the synthesis gas production rate. Also, the H_2/CO ratio varies between 1.0 and 1.5 for the conversion of glycerol to synthesis gas at pressures between 5 and 17 bar. However, the integrated runs at these pressures show good selectivities to C_{5+} hydrocarbons. These results show that synthesis gas with a stoichiometric H_2/CO ratio of 2 : 1 is not essential to the production of liquid alkanes *via* our integrated process. Furthermore, the Ru/TiO_2 catalyst is exposed to increasing amounts of oxygenated hydrocarbon byproducts at 11 and 17 bar; however, the selectivity to oxygenates in the aqueous liquid effluent at these pressures is similar to or lower than that of the aqueous effluent at 5 bar. This result indicates that the oxygenated hydrocarbon byproducts from glycerol react over the Ru/TiO_2 bed, most likely by entering into Fischer–Tropsch chain growth. Because the aqueous product distribution contains a wide array of oxygenated species, it is likely that other byproducts with similar functionality as acetol (*e.g.*, polyols, secondary alcohols, and hydroxyl-ketones) have a similar synergistic effect on Fischer–Tropsch synthesis. Importantly, these experiments demonstrate that liquid alkanes can be produced directly from glycerol in a two-bed reactor system using an integrated process.

Potential industrial application

The integrated process presented in this paper has the potential to improve the economics of ''green'' Fischer–Tropsch synthesis. For example, previous studies investigating the optimum design of large scale ''green'' Fischer–Tropsch plants conclude that synthesis gas production and cleanup are critical steps in the entire process and have significant effects on the economics of producing liquid alkanes from biomass.[16,17] Studies by Hamelinck *et al.* and Tijmensen *et al.* show that capital costs account for more than 50% of the total costs of producing liquid alkanes from ''green'' Fischer–Tropsch synthesis, and of these capital costs nearly 50% result from biomass gasification (18–25%), oxygen production (12–15%) and synthesis gas processing and cleaning (10–18%).[16,17]

Typical gasifiers suitable for conventional ''green'' Fischer-Trospch processes are circulated fluidized bed designs that can operate over a wide range of conditions.[16,17] For example, these gasifiers operate from atmospheric pressure to 30 bar using air or O_2 with exit temperatures of 1100–1240 K.[17] The major disadvantage of an air-blown gasifier operating at atmospheric pressure is the increased cost for larger downstream equipment necessary to handle the synthesis gas diluted with N_2.[16,17] Furthermore, dilution of synthesis gas with N_2 has negative effects on the C_{5+} selectivity.[17] Pressurized gasifiers are more costly at small scale and are more difficult to maintain,[17] and the air separation plant required for O_2-blown gasifiers is expensive, especially at small scales.[16,17] Another disadvantage of conventional biomass gasifiers is that the synthesis gas stream often contains contaminants (*e.g.*, HCN, NH_3, H_2S, COS, and HCl among others)[17] that must be removed to concentrations lower than 10–20 ppb each, with some requiring complete removal.[17] Typically, gas cleaning trains are comprised of five to seven different cleaning steps (*e.g.*, tar cracker, cyclone separator, bag filters, wet and/or dry scrubbers, and ZnO guard beds).[16,17] The integrated process presented in the present paper is advantageous over these conventional synthesis gas production methods in that our process produces an undiluted synthesis stream at the temperature, pressure, and purity appropriate for Fischer–Tropsch synthesis. In addition, our integrated process is advantageous over conventional gasifiers in that our process can produce synthesis gas with varying H_2/CO compositions, thus eliminating the need for a water-gas shift reactor and allowing for the use of Fischer–Trospch catalysts that operate at different H_2/CO ratios.[32–34] Thus, capital costs and operating expenses can be reduced (by close to 50%) by eliminating the need for a biomass gasifier, large downstream equipment, and synthesis gas cleaning steps.

In addition to potential economic improvements, the different product streams of our integrated process each have potential end-uses, as illustrated in Fig. 1. In an industrial application, the gaseous product stream would contain primarily gaseous alkanes in the C_1–C_2 range; however, some process studies show that recovering the C_3–C_4 fractions from the gas stream is energy consuming and not economical.[16] Also, the gaseous products would contain unconverted H_2 and CO with some CO_2. The most likely use for the gas alkanes in our process would be combustion to produce process heat and electricity (Fig. 1) with some of the unconverted H_2 and CO being recycled to the Fischer–Tropsch bed. However, these gaseous alkanes could be reformed to synthesis gas and recycled to the Fischer–Tropsch bed as well.[16] The organic liquid phase product contains primarily liquid hydrocarbons with a small amount of oxygenates (acetone, butanone, pentanone, hexanone, and heptanone). In some applications, the oxygenates could be hydrogenated to alcohols, which are excellent fuel additives. Alternatively, the oxygenates in the organic liquid could undergo hydrodeoxygenation to remove the oxygen and form saturated hydrocarbons.[35] If diesel fuel is the desired product, the C_5–C_9 fraction would be separated, and the waxy C_{10+} fraction would be hydrocracked to naptha, kerosene, and diesel.[16,17] The aqueous liquid product stream contains oxygenated hydrocarbons (*e.g.*, ethanol, methanol, and acetone) at concentrations between 5–15 wt%. This aqueous solution is suitable for distillation with the oxygenated hydrocarbons either being recycled for further conversion to synthesis gas or being used as intermediates or solvents in the chemical industry. However, this aqueous solution could be converted to H_2 by aqueous phase

reforming[29] or upgraded to transportation fuels *via* selective dehydration/hydrogenation.[36,37]

Conclusions

The production of synthesis gas from glycerol coupled with the conversion of synthesis gas to produce liquid fuels by Fischer–Tropsch synthesis is a net exothermic process with a heat of reaction that is 4% of the lower heating value of glycerol.[20] We show that conversion of glycerol over a Pt–Re/C catalyst produces a synthesis gas stream that is suitable for Fischer–Tropsch synthesis over a wide range of glycerol feed concentrations and at pressures up to 17 bar where incomplete vaporization of the glycerol feed occurs. Also, we have demonstrated that the oxygenated hydrocarbon byproducts in the synthesis gas stream from glycerol conversion (*e.g.*, ethanol, acetone, acetol) have positive effects on the Fischer–Tropsch synthesis step. In particular, water, ethanol and acetone have slightly positive effects, such as slightly increasing the selectivity to C_{5+} hydrocarbons (S_{C5+}); and, acetol can participate in Fischer–Tropsch chain growth, forming pentanones, hexanones, and heptanones in the liquid organic effluent stream. This synergistic participation of acetol (and, possibly, other oxygenates) in Fischer–Tropsch chain growth has beneficial effects with respect to integration of glycerol conversion with Fischer–Tropsch synthesis in a two-bed system, such as (i) eliminating the need to condense water and oxygenated hydrocarbon byproducts between the catalyst beds, (ii) allowing for operation at higher pressures (*i.e.*, 17 bar) where synthesis gas production over Pt–Re/C is decreased and the production of liquid byproducts is increased, and (iii) causing an increase in the selectivity to C_{5+} hydrocarbons. Accordingly, glycerol conversion and Fischer–Tropsch synthesis can be carried out effectively (and perhaps synergistically) at the same conditions and in a two-bed reactor system, allowing the coupling between glycerol conversion and Fischer–Tropsch synthesis to be used for the production of liquid fuels from aqueous-glycerol solutions.

The integrated process presented in this paper is a simple, two step catalytic process that can be carried out at low temperature and moderate pressure and can effectively harness the energy from a renewable resource. Importantly, our process minimizes the amount of waste byproducts since each product phase is useful (Fig. 1). Therefore, this ''green'' process represents an energy efficient alternative for producing liquid transportation fuels from petroleum. Furthermore, it presents the opportunity for improving the economic viability of ''green'' Fischer–Tropsch synthesis by reducing costs associated with synthesis gas production and by improving the thermal efficiency of Fischer–Tropsch processes.

Acknowledgements

This work was supported by the U.S. Department of Energy (DOE), Office of Basic Energy Sciences. R. R. Soares acknowledges a post-doctoral grant from CAPES. We thank Randy Cortright and Manos Mavrikakis for valuable discussions and collaborations throughout this project. We also thank Jennifer Ross for assistance in collecting reaction kinetics data.

References

1 G. Alexander and G. Boyle, Introducing Renewable Energy, in *Renewable Energy*, ed. G. Boyle, Oxford University Press, New York, 2004.
2 Energy Information Administration, U. S. Department of Energy, http://www.eia.doe.gov/.
3 D. L. Klass, *Biomass for Renewable Energy, Fuels, and Chemicals*, Academic Press, San Diego, 1998.
4 R. D. Perlack, L. L. Wright, A. F. Turhollow, R. L. Graham, B. J. Stokes and D. C. Erbach, *Biomass as Feedstock for a Bioenergy and Bioproducts Industry: The Technical Feasibility of a Billion-Ton Annual Supply*, United States Department of Energy, Oak Ridge National Laboratory, DOE/GO-102005-2135, 2005, 1–78.
5 A. E. Farrell, R. J. Plevin, B. T. Turner, A. D. Jones, M. O'Hare and D. M. Kammen, Ethanol can contribute to energy and environmental goals, *Science*, 2006, **311**, 506–508.
6 H. Shapouri, J. A. Duffield and M. Wang, *The Energy Balance of Corn Ethanol: An Update*, United States Department of Agriculture, Agricultural Economic Report No. 814, 2002, 1–15.
7 K. L. Kadam and J. D. McMillan, Availability of corn stover as a sustainable feedstock for bioethanol production, *Bioresour. Technol.*, 2003, **88**, 17–25.
8 J. D. McMillan, Bioethanol Production: Status and Prospects, *Renew. Energ.*, 1997, **10**, 295–302.
9 V. Senthilkumar and P. Gunasekaran, Bioethanol production from cellulosic substrates: engineered bacteria and process integration challenges, *J. Sci. Ind. Res. India*, 2005, **64**, 845–853.
10 P. O. Ward and A. Singh, Microbial technology for bioethanol production from agricultural and forestry wastes, in *Microbial Biotechnology in Agriculture and Aquaculture*, ed. R. C. Ramesh, Science Publishers, Inc., Enfield, NH, USA, 2005.
11 The European Fuel Oxygenates Association, http://www.efoa.org/oxygen.html.
12 Energy Efficiency and Renewable Energy, U.S. Department of Energy, http://www.eere.energy.gov/.
13 T. W. Patzek, Thermodynamics of the Corn-Ethanol Biofuel Cycle, *Crit. Rev. Plant Sci.*, 2004, **23**, 519–567.
14 T. Patzek and D. Pimentel, Thermodynamics of Energy Production from Biomass, *Crit. Rev. Plant Sci.*, 2005, **24**, 327–364.
15 D. Pimentel and T. W. Patzek, Ethanol Production Using Corn, Switchgrass, and Wood; Biodiesel Production Using Soybean and Sunflower, *Nat. Resour. Res.*, 2005, **14**, 65–76.
16 C. N. Hamelinck, A. P. C. Faaij, H. den Uil and H. Boerrigter, Production of FT transportation fuels from biomass; technical options, process analysis and optimisation, and development potential, *Energy*, 2004, **29**, 1743–1771.
17 M. J. A. Tijmensen, A. P. C. Faaij, C. N. Hamelinck and M. R. M. van Hardeveld, Exploration of the possibilities for production of Fischer Tropsch liquids and power via biomass gasification, *Biomass Bioenerg.*, 2002, **23**, 129–152.
18 C. H. Bartholomew and R. J. Farrauto, *Fundamentals of Industrial Catalytic Processes*, Wiley, Hoboken, NJ, USA, 2006.
19 P. L. Spath and D. C. Dayton, *Preliminary Screening–Technical and Economic Assessment of Synthesis Gas to Fuels and Chemicals with Emphasis on the Potential for Biomass-Derived Syngas*, United States Department of Energy, National Renewable Energy Laboratory, NREL/TP-510-34929, 2003, 1–142.
20 R. R. Soares, D. A. Simonetti and J. A. Dumesic, Glycerol as a Source for Fuels and Chemicals by Low-Temperature Catalytic Processing, *Angew. Chem., Int. Ed.*, 2006, **45**, 3982–3985.
21 C. S. Gong, J. X. Du, N. J. Cao and G. T. Tsao, Co-production of ethanol and glycerol, *Appl. Biochem. Biotechnol.*, 2000, **84–86**, 543–559.
22 T. A. Werpy, J. G. Frye, A. H. Zacher and D. J. Miller, PCT, Hydrogenolysis of 6-carbon sugars and other organic compounds, *World Pat.* WO 03/035582 A1, 2003.
23 J. Van Gerpen, Biodiesel processing and production, *Fuel Process. Technol.*, 2006, **86**, 1097–1107.
24 E. Iglesia, S. L. Soled and R. A. Fiato, Fischer–Tropsch Synthesis on Cobalt and Ruthenium – Metal Dispersion and Support Effects on Reaction-Rate and Selectivity, *J. Catal.*, 1992, **137**, 212–224.
25 B. E. Spiewak, J. Shen and J. A. Dumesic, Microcalorimetric Studies of CO and H_2 Adsorption on Nickel Powders Promoted with Potassium and Cesium, *J. Phys. Chem.*, 1995, **99**, 17640.

26 K. C. Taylor, Determination of Ruthenium Surface-Areas by Hydrogen and Oxygen Chemisorption, *J. Catal.*, 1975, **38**, 299–306.
27 E. Iglesia, S. C. Reyes and R. J. Madon, Transport-Enhanced Alpha-Olefin Readsorption Pathways in Ru-Catalyzed Hydrocarbon Synthesis, *J. Catal.*, 1991, **129**, 238–256.
28 E. Iglesia, Design, synthesis, and use of cobalt-based Fischer–Tropsch synthesis catalysts, *Appl. Catal. A*, 1997, **161**, 59–78.
29 R. D. Cortright, R. R. Davda and J. A. Dumesic, Hydrogen from catalytic reforming of biomass-derived hydrocarbons in liquid water, *Nature*, 2002, **418**, 964–967.
30 M. A. Vannice, The catalytic synthesis of hydrocarbons from H_2/CO mixtures over the group VIII metals: I. The specific activities and product distributions of supported metals, *J. Catal.*, 1975, **37**, 449–461.
31 E. Iglesia, S. C. Reyes, R. J. Madon and S. L. Soled, Selectivity Control and Catalyst Design in the Fischer–Tropsch Synthesis – Sites, Pellets, and Reactors, *Adv. Catal.*, 1993, **39**, 221–302.
32 M. E. Dry, Chemical concepts used for engineering purposes, *Stud. Surf. Sci. Catal.*, 2004, **152**, 196–257.
33 M. E. Dry, FT catalysts, *Stud. Surf. Sci. Catal.*, 2004, **152**, 533–600.
34 M. E. Dry and A. P. Steynberg, Commercial FT process applications, *Stud. Surf. Sci. Catal.*, 2004, **152**, 406–481.
35 G. W. Huber, S. Iborra and A. Corma, Synthesis of transportation fuels from biomass: chemistry, catalysts, and engineering, *Chem. Rev.*, 2006, **106**, 4044–4098.
36 C. D. Chang, Hydrocarbons from methanol, *Catal. Rev. Sci. Eng.*, 1983, **25**, 1–118.
37 R. J. J. Nel and A. de Klerk, Fischer-Tropsch aqueous phase refining by catalytic alcohol dehydration, *Ind. Eng. Chem. Res.*, 2007, **46**, 3558–3565.

Sustainable Chemistry

DOI: 10.1002/anie.200601180

Formation of Acetic Acid by Aqueous-Phase Oxidation of Ethanol with Air in the Presence of a Heterogeneous Gold Catalyst**

Claus H. Christensen, Betina Jørgensen, Jeppe Rass-Hansen, Kresten Egeblad, Robert Madsen, Søren K. Klitgaard, Stine M. Hansen, Mike R. Hansen, Hans C. Andersen, and Anders Riisager*

Bioethanol is produced by fermentation of biomass in increasing amounts to meet the growing demands for CO_2-neutral transportation fuels and to eventually remove the dependence on fossil fuels. However, bioethanol could also find use as a versatile, sustainable chemical feedstock. Herein, it is shown that it is possible to selectively oxidize ethanol into acetic acid in aqueous solution using air as the oxidant with a heterogeneous gold catalyst at temperatures of about 423 K and O_2 pressures of 0.6 MPa. This reaction proceeds readily in aqueous acidic media and yields of up to 90% are achieved, with CO_2 as the only major by-product. Thus, it constitutes a very simple, green route to acetic acid.

The oxidation of ethanol by air into acetic acid over platinum was among the first heterogeneously catalyzed reactions to be reported. The initial discovery was made by Döbereiner about two centuries ago, even before the term catalysis was coined.[1] So far, the reaction has not been used for large-scale production of acetic acid. Instead, three other routes to acetic acid have found industrial application: fermentation (vinegar), catalytic liquid-phase oxidation of butane, naphtha, or acetaldehyde, and the carbonylation of methanol, which has recently become the most important.[2]

In the most widely used industrial processes today, the feedstock is almost exclusively derived from fossil fuels. Thus, the production of acetic acid consumes fossil fuels and therefore contributes slightly to increasing CO_2 levels in the atmosphere, and, more importantly, the cost of acetic acid is strongly dependent on the price of the fossil fuels. Therefore, it is interesting that the cost of renewable feedstocks has decreased dramatically relative to fossil fuel feedstocks over the last four decades. Specifically, the cost of corn relative to oil has decreased fivefold from 1950 to 2005. Today, bioethanol is mostly produced by fermentation of starch-containing crops, such as corn or sugar cane, but it seems likely that cellulose-rich agricultural waste will gain importance as a feedstock in the future.[3] Therefore, and also because of the continuing technological improvements of the production process, the cost of bioethanol is expected to decrease.[4] Thus, with increasing fossil fuel prices, the production of acetic acid from bioethanol will become increasingly favorable compared to current fossil fuel-based methods. Clearly, this development requires that an active and selective catalyst for oxidation of ethanol with dioxygen to form acetic acid [Eq. (1)] is available.

$$CH_3CH_2OH + O_2 \rightarrow CH_3COOH + H_2O \quad (1)$$

So far, primarily palladium and platinum catalysts have received attention as catalysts for ethanol oxidation.[5] However, with these catalysts it has proven difficult to reach sufficient selectivities at high conversions.

Here, it is reported for the first time that gold catalysts are both very active and selective catalysts for aqueous-phase oxidation of ethanol with air into acetic acid at 373–473 K with O_2 pressures of 0.5–1 MPa. Interestingly, metallic gold was for many years considered too unreactive to be useful as a catalyst.[6] However, this view was challenged in the seminal studies of Haruta and co-workers,[7,8] who showed that gold very efficiently catalyzed the room-temperature oxidation of CO with O_2 to form CO_2, and by Hutchings, who studied acetylene hydrochlorination with gold catalysts.[9] Since then, numerous reports of different gold-catalyzed reactions have appeared and the field has recently been reviewed and highlighted.[10–12]

[*] Prof. C. H. Christensen, B. Jørgensen, J. Rass-Hansen, K. Egeblad, Prof. R. Madsen, S. K. Klitgaard, S. M. Hansen, M. R. Hansen, H. C. Andersen, Prof. A. Riisager
Center for Sustainable and Green Chemistry
Department of Chemistry
Technical University of Denmark
Kemitorvet building 207, 2800 Kgs. Lyngby (Denmark)
Fax: (+45) 4525-2235
E-mail: chc@kemi.dtu.dk

[**] The Center for Sustainable and Green Chemistry is sponsored by the Danish National Research Foundation. Financial support from the Danish Research Agency (grant 2104-04-0003) is acknowledged.

The catalytic oxidation of alcohols with air has also attracted significant attention as a "green" reaction.[13] Among the heterogeneous catalysts, mainly Pd and Pt have shown promising result.[14,15] Rossi and co-workers were the first to show that alcohols, specifically diols and sugars, can be oxidized to the corresponding acids with gold catalysts but only when a base is present.[16,17] Later, the oxidation of glycerol to glycerate using Au/C was similarly demonstrated.[18] Recently, it was shown that heterogeneous ceria-supported gold catalysts are able to oxidize several higher alcohols into the corresponding carboxylic acids using air as oxidant.[19] In these experiments, the support played an active role in the catalytic cycle. However, it has also been shown that solvent-free oxidations of primary alcohols can selectively yield aldehydes.[20] Thus, it is noteworthy that the gold-catalyzed aqueous-phase oxidation of ethanol with air into acetic acid reported here proceeds readily in acidic aqueous solution.

Bioethanol is typically produced in a series of steps, namely fermentation in a batch process (yielding 3–15 vol% aqueous ethanol), distillation to obtain the azeotrope (containing 96 vol% ethanol), and further distillation to achieve the anhydrous ethanol that is required as a fuel additive.[21] Therefore, we decided to study the oxidation of ethanol in a batch process with ethanol concentrations corresponding to those obtained during fermentation, as this is expected to represent the easiest scheme for acetic acid production from bioethanol. All catalysts were prepared on a porous support of $MgAl_2O_4$ (65 $m^2 g^{-1}$) using $HAuCl_4 \cdot 3H_2O$, $PtCl_4$, and $PdCl_2$ as metal precursors. The catalytic experiments were conducted in stirred reactors (50 mL, Parr Autoclaves, stainless steel). Liquid samples were drawn from the reactor periodically using the sampling system and analyzed by gas chromatography (GC). Similarly, gas samples were also analyzed by GC. No reaction was observed in the absence of catalyst or when using the pure supports without gold. The metal content of all catalysts was analyzed by atomic absorption spectroscopy (AAS). The gold catalysts were also characterized by transmission electron microscopy (TEM) before and after testing. Typically, 20 images were recorded for each catalyst sample.

Initially, we studied whether gold could catalyze the selective oxidation of ethanol into acetic acid with air in aqueous solution, and how such a catalyst would compare with previously reported systems based on platinum and palladium. Table 1 compares the performance of Au, Pt, and Pd catalysts on a $MgAl_2O_4$ support. Previously, the nature of the support has been shown to be critically important for gold catalysts.[19,22] $MgAl_2O_4$ was chosen as the support material here since it is stable at high water pressures and because it can be considered completely inactive in redox processes. Thus, the observed activity can be attributed solely to the metal nanoparticles, and no synergistic effect with the support is expected. Other supports might be found to affect the catalytic performance.

Remarkably, the gold catalyst not only exhibits similar or higher catalytic activity than palladium or platinum but, in particular, a significantly higher selectivity towards acetic acid than both of these well-known catalysts. The major by-product for the gold catalyst is CO_2, whereas the Pd and Pt catalysts also produce significant amounts of acetaldehyde. Thus, we decided to further investigate the performance of gold catalysts for ethanol oxidation to gain a more detailed insight into this reaction and to identify suitable reaction conditions.

Figure 1 shows representative TEM images of the 1 wt% $Au/MgAl_2O_4$ catalyst used in this study. Generally, gold particle sizes of 3–6 nm are observed both before and after testing, with no sign of sintering. Figure 1 also illustrates how the ethanol conversion and the acetic acid yield depend on the reaction time. The reaction is conducted with only a slight excess of oxygen and therefore the reaction rate does not obey pseudo-first-order kinetics.

Table 1: Comparison of $MgAl_2O_4$-supported Au, Pt, and Pd catalysts for oxidation of aqueous ethanol to acetic acid with air.[a]

Cat.	T [K]	p [MPa]	t [h]	Conv. [%]	Yield [%]	STY[b] [mol h^{-1} L^{-1}]
Au[c]	453	3	4	97	83	0.21
Pt	453	3	4	82	16	0.047
Pd	453	3	4	93	60	0.15

[a] Conditions: 150 mg catalyst, 1 wt% of metal, 10 mL of 5 wt% aqueous ethanol, [b] Space-time yield. [c] Corresponding to 0.07 mol% Au.

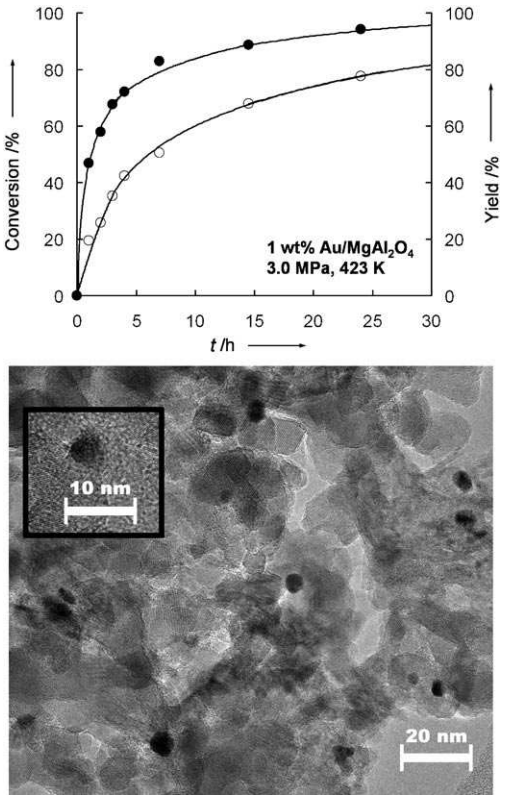

Figure 1. Top: Performance of 150 mg of 1 wt% $Au/MgAl_2O_4$ catalyst in the oxidation of 10 mL of aqueous 5 wt% ethanol with air at 423 K and 3.0 MPa (● ethanol conversion, ○ acetic acid yield). Bottom: TEM images of the 1 wt% $Au/MgAl_2O_4$ catalyst used for ethanol oxidation. The inset shows a high-resolution image of a gold particle with a diameter of about 5 nm.

Figure 2 shows how the performance of the catalyst depends on temperature and pressure. It is noteworthy that yields above 80% are obtained without any special effort to optimize the reaction conditions or catalyst composition. It can also be seen that the reaction rate and selectivity are only slightly influenced by the total pressure when oxygen is present in excess.

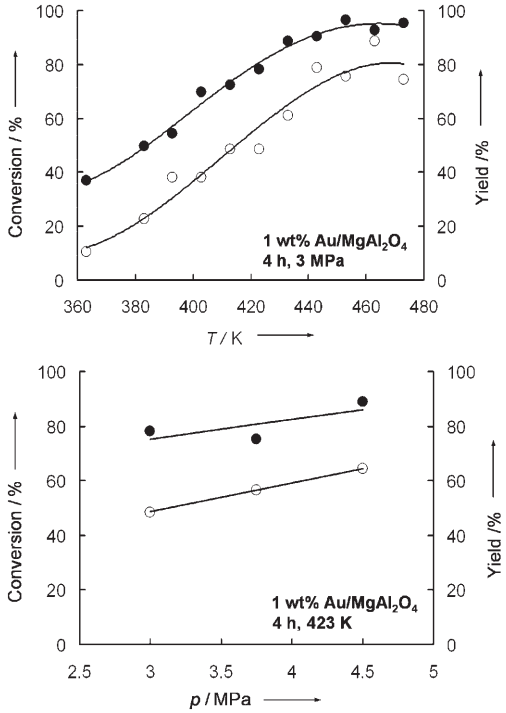

Figure 2. Ethanol conversion (●) and acetic acid yield (○) with 10 mL of 5 wt% aqueous ethanol after 4 h in the presence of 150 mg of 1 wt% $Au/MgAl_2O_4$ catalyst. Top: temperatures of 363–473 K and an air pressure of 3 MPa. Bottom: pressures of 3–4.5 MPa and a temperature of 423 K.

As the reaction progresses, the solution becomes more and more acidic, but this does not influence the catalyst's performance. By more careful selection of reaction conditions, for example by increasing the reaction time at 423 K or at 453 K and 3.5 MPa, it is possible to achieve acetic acid yields of over 90% (e.g., 92% yield after 8 h at 453 K and 3.5 MPa). The spinel is found to be quite stable under the present reaction conditions. After a typical reaction run, less than 1% is lost according to ICP-MS. Additionally, only phase-pure spinel is found by powder X-ray diffraction. This is in agreement with the previous finding that magnesium aluminum hydroxide (Al/Mg = 2) transforms into spinel under hydrothermal conditions.[23]

Thus, it is seen that gold catalysts are indeed able to selectively oxidize ethanol to acetic acid in air at moderate temperatures and dioxygen pressures with very high yields. This suggests that it might prove viable to produce aqueous acetic acid in a gold-catalyzed process using aqueous bioethanol as the feedstock. Acetic acid can also be obtained directly by fermentation, however this also represents a challenge since the bacteria do not thrive under the highly acidic reaction conditions.[2] Here, the very high stability of the gold-on-$MgAl_2O_4$ catalyst allows the use of high temperatures and pressures, which results in high rates. Recently, bioethanol has also received attention as a feedstock for renewable dihydrogen by steam-reforming[24] or autothermal reforming.[25] Figure 3 illustrates some proven possibilities for using bioethanol, including both fuel and feedstock applications.

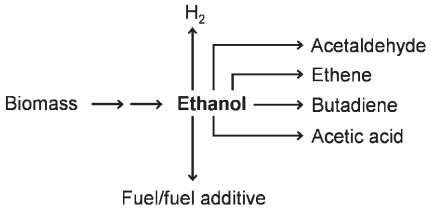

Figure 3. Possible uses of bioethanol as a fuel or as a feedstock for important bulk chemicals.[26]

A future challenge for chemists could be to find efficient routes from bioethanol to fuels and chemicals. Such processes will also compete with other new processes that allow direct conversion of carbohydrates into, for example, dihydrogen[27,28] or synfuels,[28,29] which are currently being explored. Here, we have focused on synthesizing acetic acid from ethanol in a simple, green process since acetic acid has a significantly higher value than fuels (including dihydrogen) and also than ethene, acetaldehyde, and butadiene, for example. Therefore, this might represent the currently most efficient use of part of the available bioethanol.

Experimental Section

The gold catalysts were prepared by deposition-precipitation[30] of $HAuCl_4 \cdot 3H_2O$ (supplied by Aldrich) on $MgAl_2O_4$. Stoichiometric $MgAl_2O_4$, calcined at 1000 °C,[31] was tabletized, crushed, and sieved to a particle size of 100–250 μm prior to use. For comparative purposes, Pd and Pt catalysts supported on $MgAl_2O_4$ were prepared by incipient-wetness impregnation of hydrochloric acid solutions of $PdCl_2$ and $PtCl_4$, respectively. The resulting catalyst precursors were dried at 120 °C for 6 h and calcined at 773 K for 2 h. The pure, stoichiometric, and calcined spinel used here is neutral and causes essentially no change of pH (less than ±0.05) when suspended in water or treated hydrothermally in water.

The reactor (total free volume of 55 mL) was charged with 5 wt% aqueous ethanol (10 mL), and the catalyst (150 mg) was added. After closing the autoclave, it was charged with technical air (80 vol% N_2, 20 vol% O_2) at the required pressure (2.5–5.0 MPa) and sealed. No dioxygen was added to replace that consumed by the reaction and consequently only a limited excess of oxygen is present after reaction. The reactor was then heated to a reaction temperature between 373 and 473 K where it was kept for the desired time period (4 to 45 h). The time required to reach the reaction temperature varied slightly. The pressure was monitored during the reaction and the pH was determined in the product. After the reaction, the autoclave was cooled to about 278 K. After each run, the reactor and internal components were cleaned by polishing and washing with water. The catalyst was separated by ultrafiltration and used up to three times. At this point it had lost most of its activity, which corresponds to TONs of more than 10000. The content of Al, Mg, and Au in solution after each run was measured by ICP-MS. In a separate experiment, pure spinel was treated under hydrothermal conditions (150 °C, 3.0 MPa)

with 5 wt% acetic acid. No acetic acid was found to be lost onto the support.

The GC apparatus was equipped with both FID and TCD detectors to allow identification of all liquid and gaseous products present in amounts above about 1 vol%. Product compositions and concentrations were determined using standard solutions. In some cases, the entire reaction mixture was also titrated with aqueous sodium hydroxide after the reaction run to validate the GC results. In all cases, the analyses gave identical results within the experimental uncertainties.

Received: March 24, 2006
Published online: June 22, 2006

Keywords: acetic acid · bioethanol · gold · heterogeneous catalysis · oxidation

[1] J. W. Döbereiner, *Ann. Phys.* **1822**, *72*, 193.
[2] H. Cheung, R. S. Tanke, G. P. Torrence, *Ullmann's Encyclopedia of Industrial Chemistry*, Wiley-VCH, Weinheim, **2005**.
[3] S. Kim, B. E. Dale, *Biomass Bioenergy* **2004**, *26*, 361.
[4] R. Wooley, M. Ruth, D. Glassner, J. Sheehan, *Biotechnol. Prog.* **1999**, *15*, 794.
[5] Y. Obana, H. Uchida, K.-i. Sano, US Patent 6,867,164, **2005**.
[6] J. Schwank, *Gold Bull.* **1983**, *16*, 103.
[7] M. Haruta, T. Kobayashi, H. Sano, N. Yamada, *Chem. Lett.* **1987**, 405.
[8] M. Haruta, N. Yamada, T. Kobayashi, S. Iilima, *J. Catal.* **1989**, *115*, 301.
[9] G. J. Hutchings, *J. Catal.* **1985**, *96*, 292.
[10] T. Mallat, A. Baiker, *Catal. Today* **1994**, *19*, 247.
[11] G. J. Hutchings, M. Haruta, *Appl. Catal. A* **2005**, *291*, 2.
[12] G. J. Hutchings, *Catal. Today* **2005**, *100*, 55.
[13] G.-J. ten Brink, I. W. C. E. Arends, R. A. Sheldon, *Science* **2000**, *287*, 1636.
[14] K. Mori, T. Hara, T. Mizugaki, K. Ebitani, K. Kaneda, *J. Am. Chem. Soc.* **2004**, *126*, 10657.
[15] T. Nishimura, N. Kakiuchi, M. Inoue, S. Uemura, *Chem. Commun.* **2000**, 1245.
[16] L. Prati, M. Rossi, *J. Catal.* **1998**, *176*, 552.
[17] C. Bianchi, F. Porta, L. Prati, M. Rossi, *Top. Catal.* **2000**, *13*, 231.
[18] S. Carretin, P. McMorn, P. Johnston, K. Griffin, C. J. Kiely, G. J. Hutchings, *Chem. Commun.* **2002**, 696.
[19] A. Abad, P. Concepción, A. Corma, H. Garcia, *Angew. Chem.* **2005**, *117*, 4134; *Angew. Chem. Int. Ed.* **2005**, *44*, 4066.
[20] D. I. Enache, D. W. Knight, G. J. Hutchings, *Catal. Lett.* **2005**, *103*, 43.
[21] G. Soboèan, P. Glaviè, *Appl. Therm. Eng.* **2000**, *20*, 529.
[22] M. S. Chen, D. W. Goodman, *Science* **2004**, *306*, 252.
[23] G. Fornasari, R. Glöckler, M. Livi, A. Vaccari, *Appl. Clay Sci.* **2005**, *20*, 258.
[24] A. Haryanto, S. Fernando, N. Murali, S. Adhikari, *Energy Fuels* **2005**, *19*, 2098.
[25] G. A. Deluga, J. R. Salge, L. Schmidt, X. E. Verykios, *Science* **2004**, *303*, 993.
[26] Bioethanol, acetaldehyde, ethene, butadiene, acetic acid, and gasoline are currently produced in quantities of about 30, 1.4, 120, 7.5, 8.5, and 1100 million tonnes per year, respectively.
[27] R. D. Cortright, R. R. Davda, J. A. Dumesic, *Nature* **2002**, *418*, 964.
[28] J. R. Rostrup-Nielsen, *Science* **2005**, *308*, 1421.
[29] G. W. Huber, J. N. Cheeda, C. J. Barrett, J. A. Dumesic, *Science* **2005**, *308*, 1446.
[30] M. Haruta, *Catal. Today* **1997**, *36*, 153.
[31] J. Dohrup, C. J. H. Jacobsen, C. Olsen, US Patent 6,416,731, **2002**.

The Hydrocarbon Pool in Ethanol-to-Gasoline over HZSM-5 Catalysts.

Journal:	*Catalysis Letters*
Manuscript ID:	draft
Manuscript Type:	Original Manuscript
Date Submitted by the Author:	n/a
Complete List of Authors:	Johansson, Roger; Technical University of Denmark, Center for Sustainable and Green Chemistry Hruby, Sarah; Iowa State University, Department of Chemical and Biological Engineering Rass-Hansen, Jeppe; Technical University of Denmark, Center for Sustainable and Green Chemistry Christensen, Claus; Haldor Topsøe A/S; Technical University of Denmark, Center for Sustainable and Green Chemistry
Keywords:	ethanol-to-gasoline, hydrocarbon pool, H-ZSM-5

The Hydrocarbon Pool in Ethanol-to-Gasoline over HZSM-5 Catalysts.

Roger Johansson,[a] Sarah L. Hruby,[b] Jeppe Rass-Hansen,[a] Claus H. Christensen[a,c]

[a)] Center for Sustainable and Green Chemistry, Department of Chemistry, Technical University of Denmark, Building 206, DK-2800 Lyngby, Denmark, [b)] Department of Chemical and Biological Engineering, Iowa State University, Ames, IA 50011, USA [c)] Haldor Topsøe A/S, Nymøllevej 55, DK-2800 Lyngby, Denmark
email: chc@topsoe.dk

Keywords: ethanol-to-gasoline, hydrocarbon pool, ZSM-5

With the current development of new large methanol plants, including a 5000 ton/day plant recently opened in Saudi Arabia[1] and a 1500 ton/day plant under construction in Russia[2], the subsequent expected increases in available methanol and the cost competitiveness due to economics of scale are generating significant potential for the methanol to hydrocarbon (MTH) reaction to become an important industrial process in the coming years. Some existing plants are currently utilizing this route to produce olefins; one of the largest belongs to Viva Methanol Ltd. in Nigeria.[3] MTH or, depending on process conditions, methanol to gasoline (MTG) or methanol to olefins (MTO) can be used to produce liquid fuels for the automotive sector or to make olefins suitable for polymerization. The production of liquid fuels from natural gas via methanol was first commercialized by Mobil in the 1980s with a plant operating in New Zealand with a planned production of 600,000 tons annually. However, at that time the economy for the process was unfavorable due to low fossil fuel costs; consequently, the MTG part of the operation was discontinued in the 1990s. Today, the increasing prices of fossil feedstocks could once again make the MTG process a viable option. The MTG reaction was first discovered by Silvestri and Chang in the 1970s and it is catalyzed by acidic zeolites at temperatures up to 400°C giving a variety of lower aliphatic hydrocarbons, olefins and aromatics.[4] The product distribution in MTG depends on several factors where, in particular, the topology of

the catalyst is of paramount importance. Since its discovery, MTG has been extensively studied and a plausible reaction mechanism has been suggested through the work of several research groups.[5,6] The basic premise for the proposed mechanism is the hydrocarbon pool model, which suggests that the actual catalytic sites in the zeolite are organic-inorganic hybrids consisting of cyclic organic species contained within the zeolitic framework. These organic species act as the hydrocarbon pool from which the products in the exit gas stem via cracking as shown in a simplified reaction scheme in Scheme 1. The MTG process has been extensively studied by Kolboe et al., who studied the nature and amount of retained material within the catalysts H-beta,[7,8,9] SAPO-34 [10,11] and H-ZSM-5. [12,13] These authors gained considerable insight into the mechanism by determination of retained material in the used catalyst and many aspects of the hydrocarbon pool model stem from their work. The MTG process has a counterpart in the ethanol to gasoline (ETG) process, which gives an almost identical product distribution as the MTG process.[14,15,16] Since MTG and ETG most likely proceed through similar routes, the study of retained material in the ETG reaction could also provide interesting insight into MTG.

The amount of ethanol currently produced has increased significantly in recent years due to the rising demand for domestic, biorenewable alternatives to petroleum-based fuels and chemicals. There are many potential reactions utilizing ethanol to produce important chemical feedstocks[17] such as steam reforming to hydrogen,[18,19,20] dehydration to ethylene,[21] oxidation to acetaldehyde,[22] oxidation to acetic acid[23,24]and oxidation followed by condensation to butadiene.[25] Some of these aforementioned reactions, namely the processes leading to ethylene and butadiene, have been demonstrated on an industrial scale but have not retained their importance when routes starting from fossil fuels have been implemented instead. The other processes

mentioned above have mostly received attention in the last decade but have not found industrial applications yet. One of the important drawbacks of the production of ethanol from biomass is the energy input required for distillation, which usually comes from fossil fuels. Consequently, when developing new reactions aqueous ethanol would be the preferred feedstock to achieve a more favorable energy balance by reducing the required extent of distillation. As a result, processes that do not require fuel-grade ethanol such as the dehydration of ethanol to ethylene and steam reforming to hydrogen are attracting interest.[26,18] Other researchers have investigated the use of the ethanol to gasoline reaction as an alternative to fuel grade distillation of ethanol.[27] One challenge with the ETG process that can be envisioned when using ethanol as feed is a more rapid catalyst deactivation due to the formation of ethylene, which is a known coke precursor on H-ZSM-5.[28] This deactivation could perhaps be inhibited by addition of water to the feed,[28,29] Using lightly distilled bio-ethanol as the feed would add additional water to the reaction and slow down deactivation and lower the ethanol feed concentration. Our first effort towards this is to study the mechanism behind ETG through the analysis of retained material in the catalyst after the ethanol to gasoline reaction. This has been done previously for the MTG reaction but to our knowledge no such information exists for the ETG reaction. We are also comparing the ETG and MTG reaction with the same process parameters to further our understanding of these reactions.

The catalyst used in this study was H-ZSM-5 (Si/Al = 11.5), supplied by Zeolyst International. The experiments for determining retained material were performed in a continuous flow fixed bed quartz tubular reactor with an inner diameter of 6 mm; the catalyst bed was heated in an oven, the temperature monitored with a thermocouple

situated immediately below the catalyst bed. The ethanol was added through a HPLC pump and then evaporated by heating tapes and carried through the catalyst bed with a flow of helium. The stream was then brought to an Agilent 6890 GC equipped with a Varian PoraPlot Q-HT column and a FID where the product distribution was analyzed. The experiments comparing ETG with MTG were performed on a similar setup but using a stainless steel reactor fitted with a condenser to separate gaseous products from condensable products before analysis on a Agilent 6890 GC equipped with a J&W Scientific GS-Gaspro column and a FID where the gaseous products were analyzed.

Experiments were carried out at 450 °C or 400 ˚C with a WHSV of 9 h^{-1} or 6 h^{-1} respectively. For the retained material study the reactor was heated to 450 ˚C and after 15, 60 or 120 minutes, the reactor was immediately moved to another oven where the catalyst was flushed with helium for 5 minutes at 55 °C to remove small molecules not trapped inside the zeolite pores.

For determining the retained material in the methanol to olefin process we have replicated the method employed by Guisnet et al.[30] in order to gain insight into the ethanol to gasoline reaction. In a closed Teflon vial 100 mg of spent catalyst was dissolved in 3 ml of 20 % wt. hydrofluoric acid. The mixture was shaken and allowed to stand overnight. When the zeolite was completely dissolved, the retained material was extracted with 1 ml of dichloromethane with added chlorobenzene as an internal standard. The organic phase was filtered and most of the dichloromethane was allowed to evaporate; Arstad et al.[10] have shown that this should not have an effect on the product distribution in the sample. The concentrated samples were then analyzed on an Agilent 6850 GC fitted with a quadruple mass spectrometer detector 5975C.

As it was stated previously, the products achieved from the MTG and the ETG processes are very similar; specifically the gaseous products are the same in both processes as can be seen in Figure 1. Additionally the condensable products are similar although there are subtle differences between the two processes; Figure 2 gives spectra showing the main liquid products in the ETG and MTG respectively. In the MTG there are small amounts of trimethyl benzene and tetramethyl benzene that are not seen in ETG, in ETG there are instead small amounts of ethyl methyl benzene that is not found in MTG. These differences are not discernible using FID but can be seen when analyzing the samples with mass spectrometry. The similar product distribution for both processes suggests that the same mechanism is in operation in both of these processes. If the same mechanism is in operation it would also be likely that the same material is retained within the catalyst. Figure 3 shows the most abundant retained material found in HZSM-5 for MTG and ETG respectively. When comparing the material released from the dissolved zeolite from the ETG reaction with the products in the reactor effluent it is apparent that the true retained material consists of tetraethyl benzene, triethyl methyl benzene, triethyl benzene, diethyl dimethyl benzene and diethyl methyl benzene, see Figure 3, since these compounds are not present in the reactor effluent. Many of the smaller methyl benzenes such as the xylenes are present in both reactions and are expected to lead to the same products. In the catalyst from the ETG reaction there are several mixed methyl ethyl benzenes that are similar to the methyl benzenes found in MTG but it is surprising that these mixed benzenes give the same product distribution as the hydrocarbon pool containing only methyl benzenes. A more thorough examination of the results from experiments with different reaction times revealed that the amounts of tetraethyl benzene, triethyl methyl benzene and triethyl benzene were increasing over time

whereas the amount of methyl benzenes were approximately the same throughout, as seen in Figure 4. This implies that the methyl benzenes that are common for both reactions are reacting faster than the ethyl benzenes present in the ETG reaction. Considering that the most reactive species of the hydrocarbon pool are shared between the two processes it is not so surprising that the product distribution is almost the same in both processes, the differences in product distribution should therefore come from those species that are not shared between ETG and MTG. Special attention should be given to the peaks corresponding to triethyl methyl benzene and tetraethyl benzene; these appear to be increasing more than any of the other peaks over time and it is reasonable to believe that these do not participate significantly in the reaction and could be considered as "dead ends" in the reaction network, similar to what Bjørgen et al. found for hexamethyl benzene in HZSM-5 for the MTG reaction.[12] If the triethyl methyl benzene and the tetraethyl benzene are true dead ends, as the time study suggests, they would be left unchanged by a flushing experiment at the reaction temperature, in this paper 450 ˚C. When flushing the catalyst at 450 ˚C a substantial decrease in the amount of tetraethyl benzene and triethyl methyl benzene is apparent, but at this time it is not clear why these species are decreasing. This behavior could mean that these species are indeed part of the reaction network, although at a slower rate than the smaller species in the hydrocarbon pool or they could be transformed into coke. When examining the catalysts used in reactions for longer times there are visible traces of the early stages of coke formation, which could be a logical progression from tetraethyl benzene and triethyl benzene. Whether these two species are reacting slowly or are coke precursors is inconsequential to the overall reactivity – either way the product distribution will not depend much on the larger species in the hydrocarbon pool.

The catalyst appears to deactivate faster with the formation of these compounds that potentially block the acidic sites within the zeolitic framework, thereby opening a second route towards deactivation apart from the coke formation on the surface of the zeolite crystals as has been seen by others in reactions with ZSM-5 catalysts.[31,32] When performing deactivation runs using either ethanol or methanol as the feed it was seen that the ethanol feed gives a faster deactivation than the methanol feed. The deactivation in MTG is seen as a decrease of all products and formation of dimethyl ether, for the ETG reaction the deactivation manifests itself as an increase in the amount of ethylene forming from dehydration of ethanol whereas the other products are decreasing. The faster deactivation could be a consequence of the formation of the larger species found in the retained material in addition to the coke formation due to ethylene that was mentioned previously. In conclusion it is reasonable that MTG and ETG give similar product distributions since the products mostly stem from the same retained material via the hydrocarbon pool model, the difference in product distribution seen for the liquid products can be explained by the presence of larger hydrocarbon species found in the zeolite but which are not completely retained. In essence the formation of ethyl benzenes have small effects on the products formed but it could have serious implications for catalyst activity and deactivation.

[1] Focus on Catalysts Volume 2006, Issue 11, November 2006, Page 5

[2] Chemical Week; 9/5/2007, Vol. 169 Issue 29, p22

[3] Focus on Catalysts Volume 2008, Issue 3, March 2008, Page 5

[4] C. D. Chang, A. J. Silvestri, J. Catal. 47 (1977) 249

[5] J. F. Haw, W. Song, D. M. Marcus, J. B. Nicholas Acc. Chem. Res. 36 (2003) 317

[6] U. Olsbye, M. Bjørgen, S. Svelle, KP. Lillerud, S. Kolboe Catalysis Today 106 (2005) 108

[7] M. Bjørgen, S. Kolboe Applied Catalysis A- General 225 (2002) 285

[8] Ø. Mikkelsen, S. Kolboe, Microporous And Mesoporous Materials 29 (1999) 173

[9] M. Bjørgen, U. Olsbye, D. Petersen, S. Kolboe, J. Catal. 221 (2004) 1

[10] B. Arstad, S. Kolboe, Catalysis Letters 71 (2001) 209

[11] B. Arstad, S. Kolboe, J. Am. Chem. Soc. 123 (2001) 8137

[12] M. Bjørgen, S. Svelle, F. Joensen, J. Nerlov, S. Kolboe, F. Bonino, L. Palumbo, S. Bordiga, U. Olsbye, J. Catal. 249 (2007) 195

[13] S. Svelle, F. Joensen, J. Nerlov, U. Olsbye, KP. Lillerud, S. Kolboe, M. Bjørgen, J. Am. Chem. Soc. 128 (2006) 14770

[14] E. Costa, A. Uguina, J. Aguado, P. J. Hernandez, Ind. Eng. Chem. Process Des. Dev. 24 (1985) 239

[15] A. K. Talukdar, K. G. Bhattacharyya, S. Sivasanker, Applied Catalysis A: General 148 (1997) 357

[16] J. Schulz, F. Bandermann, Chem. Eng. Technol. 17 (1994) 179

[17] J. Rass-Hansen, H. Falsig, B. Jorgensen, C.H. Christensen, J. Chem. Tech. BioTech. 82 (2007) 329

[18] A. Haryanto, S. Fernando, N. Murali, S. Adhikari, Energy Fuels 19 (2005) 2098

[19] M. Ni, DYC. Leung, MKH. Leung, Int. J. Hydrogen Energy 32 (2007) 3238

[20] J. Rass-Hansen, C.H. Christensen, J. Sehested, S. Helveg, J. R. Rostrup-Nielsen, S. Dahl, Green Chem. 9 (2007) 1016

[21] Y. C. Hu, Hydrocarbon Process. 62 (1983) 113

[22] B. Jorgensen, R. Fehrmann, C. H. Christensen, A. Riisager, Top. Catal. (2008) submitted.

[23] C.H. Christensen, B. Jorgensen, J. Rass-Hansen, K. Egeblad, R. Madsen, S.K. Klitgaard, S.M. Hansen, M.R. Hansen, H.C. Andersen, A. Riisager, Angew. Chem. International Ed. 45 (2006) 4648

[24] X. Li, E. Iglesia, Chem. Eur. J. 13 (2007) 9324

[25] W.J. Toussaint, J. T. Dunn, D.R. Jackson, Ind. Eng. Chem. 39 (1947) 120

[26] R. Le Van Mao, T. My Nguyen, G. P. Mclaughlin, Applied Catal. 48 (1989) 265

[27] D. R. Whitcraft, X. E. Verykios, R. Mutharasan. Ind. Eng. Chem. Process Des. Dev. 22 (1983) 452

[28] A.T. Aguayo, A.G. Gayubo, A. Atutxa, M. Olazar, J. Bilbao, Ind. Eng. Chem. Res. 41 (2002) 4216

[29] GZ. Qi, ZK. Xie, WM. Yang, SQ. Zhong, HX. Liu, CF. Zhang, QL. Chen, Fuel Processing Technology 88 (2007) 437

[30] P. Magnoux, P. Roger, C. Canaff, V. Fouche, N.S. Gnep, M. Guisnet, Stud. Surf. Sci. Catal. 34 (1987) 317

[31] P. Gallezot, C. Leclercq, M. Guisnet, P. Magnoux, J. Catal. 114 (1987) 100

[32] T. Behrsing, H. Jaeger, J. V. Sanders, Appl. Catal. 54 (1988) 289

Scheme 1. A simplified scheme showing the principle behind the hydrocarbon pool model in the methanol-to-gasoline reaction. Methanol reacts with hydrocarbons trapped inside the zeolite giving a charged organic-inorganic hybrid that then loses a smaller fragment giving back the same or a similar hydrocarbon.

Figure 1. Comparison of FID spectra of the gaseous products found in ethanol-to-gasoline reaction and methanol-to-gasoline run at 400 ˚C with a WHSV= 6 h^{-1}. Spectra obtained after 2 h on stream.

Figure 2. FID spectra showing the major condensable products in the ethanol-to-gasoline and the methanol-to- gasoline reactions at 400 ˚C with WHSV=6 h^{-1}. Spectra is showing the organic phase collected over the first 2 hours of reaction.

Figure 3. The major compounds of retained material found within H-ZSM-5 after reaction with either methanol (a) or ethanol (b). Reactions run at 450 ˚C with WHSV = 9 h^{-1}. The truly retained compounds are depicted in the last row in the MTG and in the lower two rows in ETG.

Figure 4. Total ion chromatogram for the retained material in HZSM-5 after addition of ethanol at 450 ˚C with a WHSV of 9 h^{-1} for (a) 15 minutes, (b) 60 minutes and (c) 120 minutes. *) oxidized form of tetraethyl benzene due to the treatment with hydrofluoric acid.

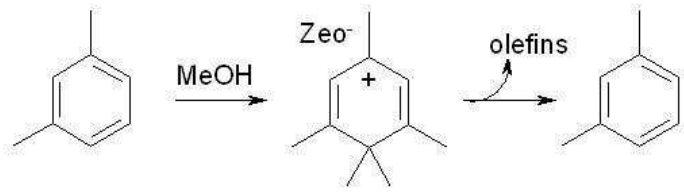

Scheme 1. A simplified scheme showing the principle behind the hydrocarbon pool model in the methanol-to-gasoline reaction. Methanol reacts with hydrocarbons trapped inside the zeolite giving a charged organic-inorganic hybrid that then loses a smaller fragment giving back the same or a similar hydrocarbon.
190x122mm (96 x 96 DPI)

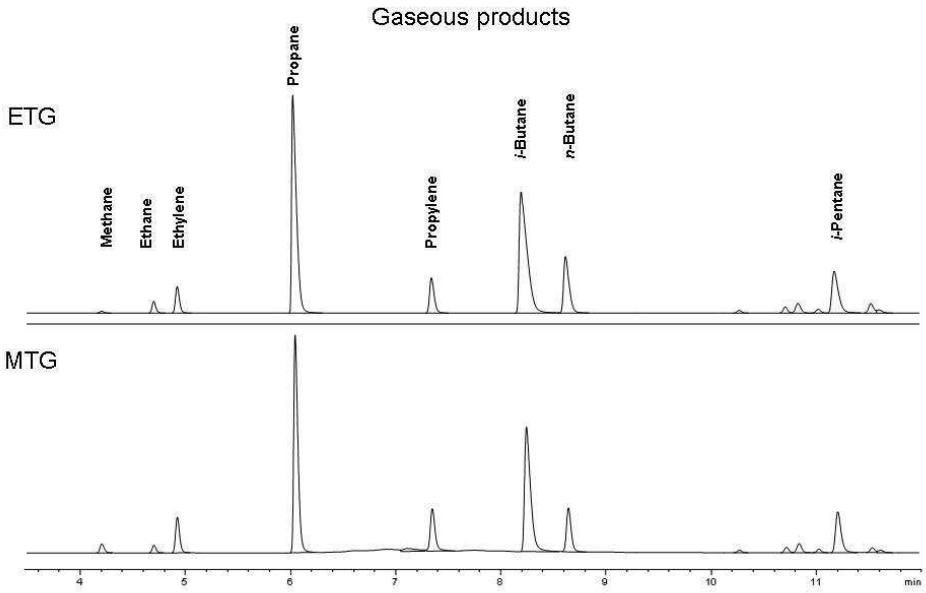

Figure 1. Comparison of FID spectra of the gaseous products found in ethanol-to-gasoline reaction and methanol-to-gasoline run at 400 ºC with a WHSV= 6 h-1. Spectra obtained after 2 h on stream.
254x190mm (96 x 96 DPI)

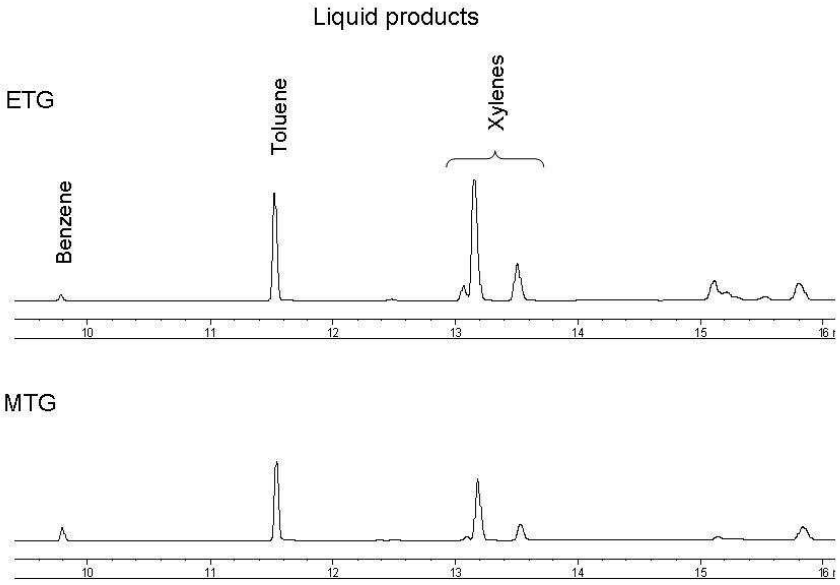

Figure 2. FID spectra showing the major condensable products in the ethanol-to-gasoline and the methanol-to- gasoline reactions at 400 °C with WHSV=6 h^{-1}Spectra is showing the organic phase collected over the first 2 hours of reaction.
254x190mm (96 x 96 DPI)

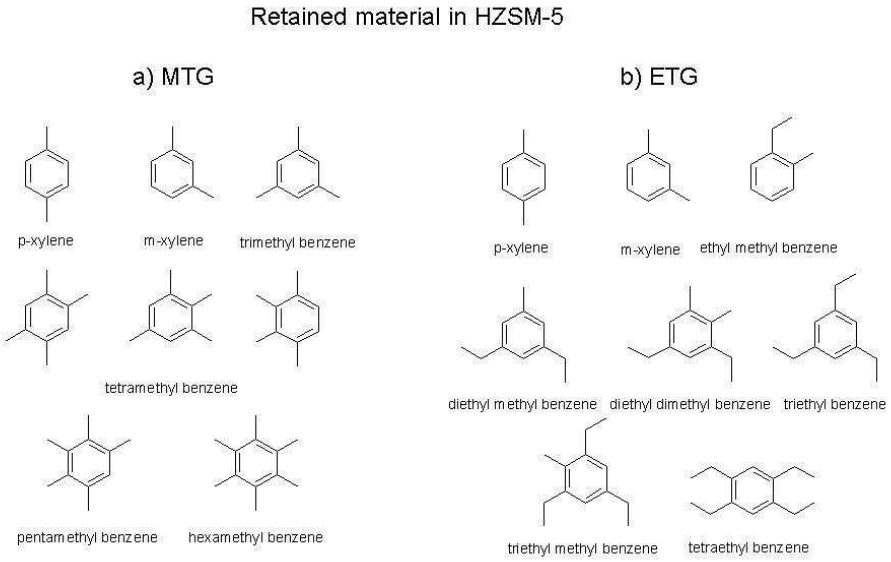

Figure 3. The major compounds of retained material found within H-ZSM-5 after reaction with either methanol (a) or ethanol (b). Reactions run at 450 ºC with WHSV = 9 $^{h-1}$. The truly retained compounds are depicted in the last row in the MTG and in the lower two rows in ETG.

254x190mm (96 x 96 DPI)

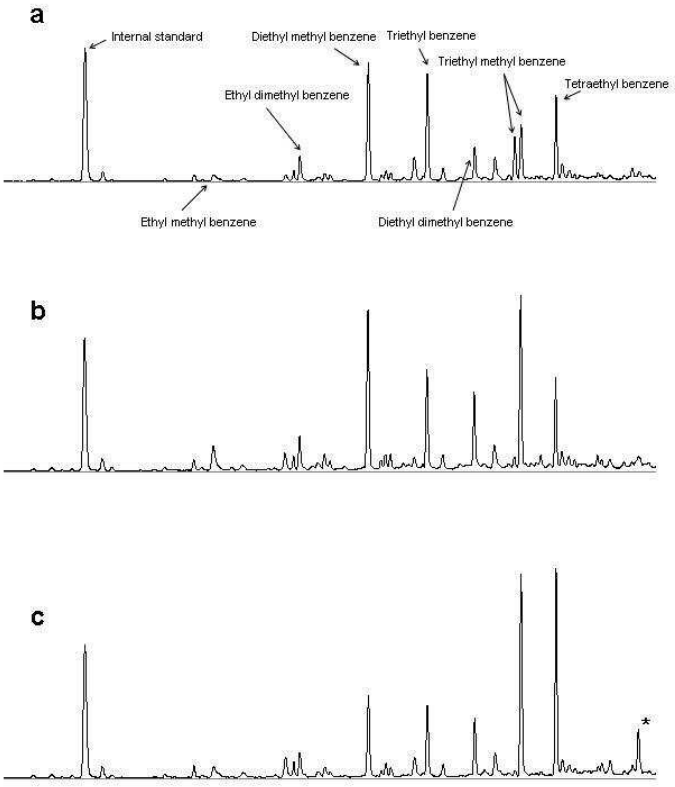

Figure 4. Total ion chromatogram for the retained material in HZSM-5 after addition of ethanol at 450 ºC with a WHSV of 9 h^{-1} for (a) 15 minutes, (b) 60 minutes and (c) 120 minutes. *) oxidized form of tetraethyl benzene due to the treatment with hydrofluoric acid.

190x275mm (96 x 96 DPI)